Physical and Material Investigation on Advanced Optoelectronics Materials and Nano/Quantum Structures

Zhe Chuan Feng

Professor, Institute of Photonics & Optoelectronics, Department of Electrical Engineering, National Taiwan University, Taipei, Taiwan

Tel: 886-2-3366-3543; E-mail: zcfeng@ntu.edu.tw; Web: http://gipo.ntu.edu.tw/

Zhe Chuan Feng's 9-books

Published ~500 papers (~200 in SCI), cited >2300

2012:

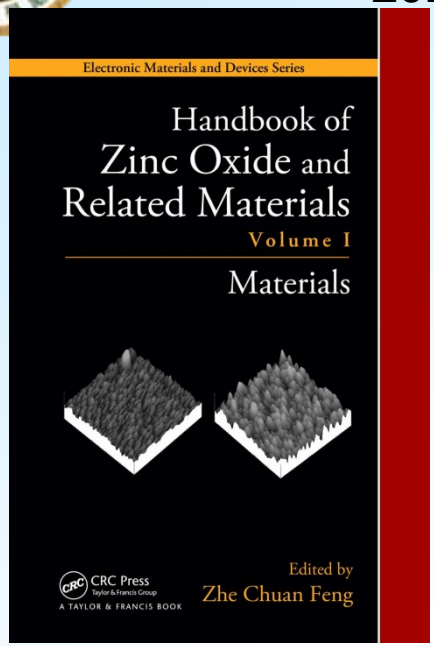

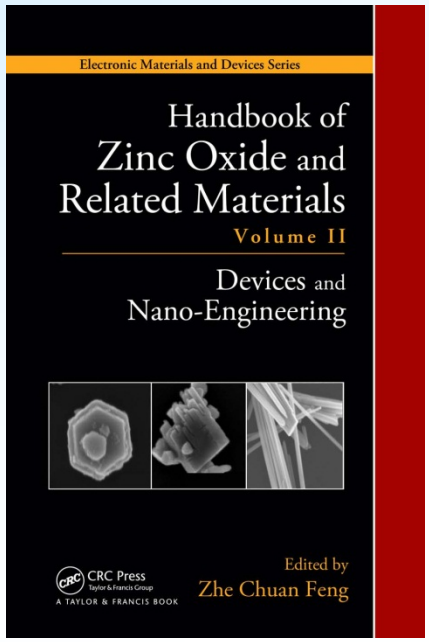

2008:

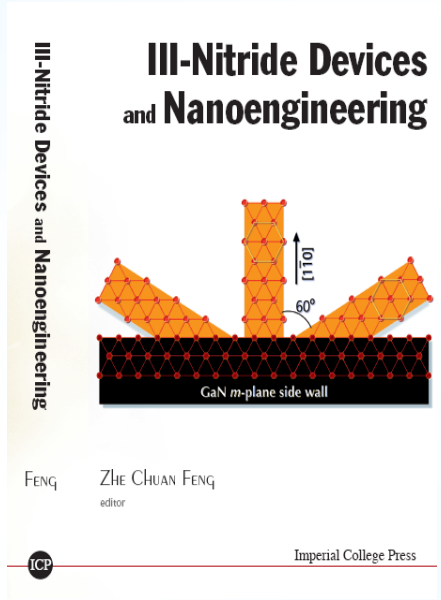

2006:

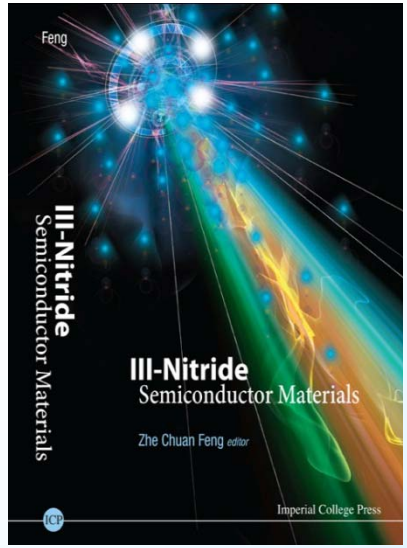

2004:

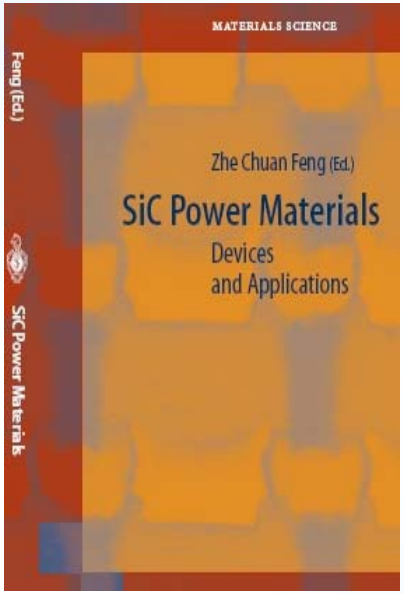

2003:

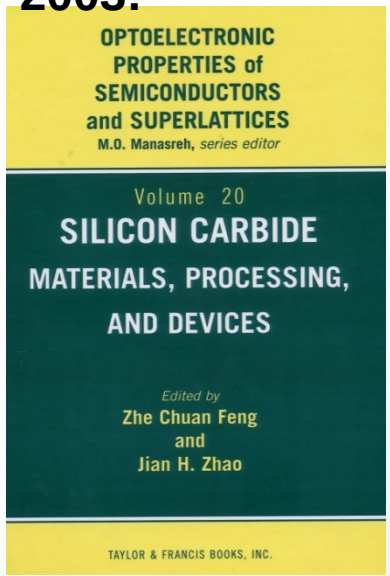

1994:

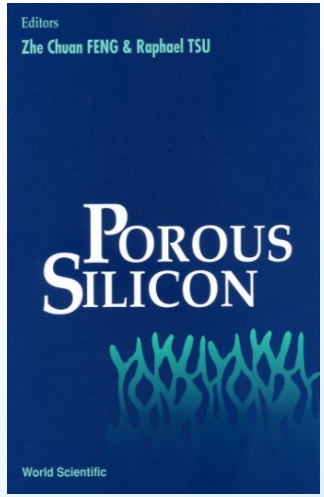

1993:

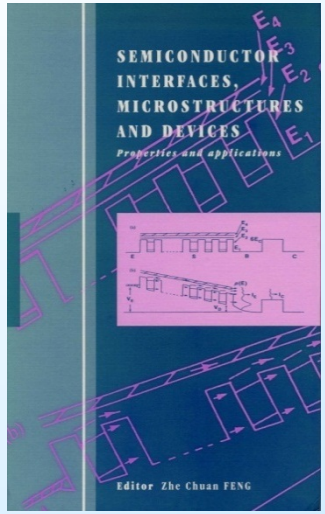

1992:

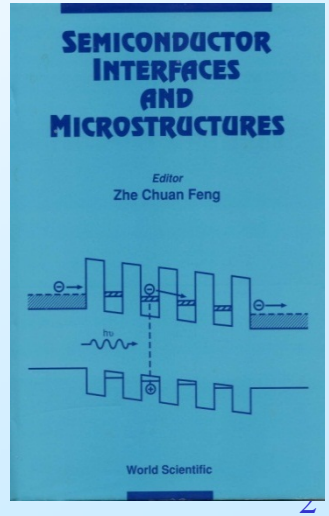

National Taiwan University, Taipei, Taiwan

國際交流

教學卓越

基礎建設

研究創新

行政精進

校園文化

學院發展

Abstract

Research and developments on advanced semiconductors, especially wide energy pap GaN, SiC and ZnO based, various oxides, related materials and quantum/nano structures are very active in recent years. Energy-efficient and environmentally friendly solid-state light sources, in particular GaN-based light emitting diodes (LEDs), and solar cells, are currently revolutionizing an increasing number of applications, and bring apparent benefits to vast areas of development, such as lighting, communications, biotechnology, imaging, energy conversion, photovoltaic, and medicine.

It is expecting that LEDs may replace the traditional light bulbs and tubes to achieve a new lighting echo. Solar cells may gradually increase their share in energy production. SiC is recognizing as the power electronic materials for the 21st century. ZnO is rapidly rising as the 3rd class of promising wide gap semiconductor. New oxides & compound semiconductors are developing amazingly, incorporated into above energy-saving devices.

This presentation reports on our physics and material science studies on these materials and structures. It emphasize on interdisciplinary studies via multi-techniques of high-resolution X-ray diffraction (HRXRD), high-resolution transmission electron microscopy (HRTEM), Raman scattering (RS), photoluminescence (PL), photoluminescence excitation (PLE), time resolved (TR) PL, Fourier transform infrared (FTIR), X-ray photoelectron spectroscopy (XPS), secondary ion mass spectroscopy (SIMS), Rutherford backscattering (RBS) and ion channeling, Synchrotron radiation (SR) XRD, X-ray absorption (XAS) and their combinations. Works and contributions in these fields from the author, students and collaborators in recent years, especially in 2011-2012 are introduced. Some challenging/unsolved scientific issues are raised. The following topics are given:

Abstract -- continued

Part-I Research Accomplishments in 2011-12

Part-II Interdisciplinary investigation on MOCVD-grown GaN-based LEDs:

HR-XRD, Reciprocal Spatial Map (RSM), HR-TEM; Temperature dependent (TD) & time-resolved (TR) photoluminescence (PL), PL excitation; Quantum confined Stark effect (QCSE), quantum dot (QD), tunneling; new designs/new processing; Luminescence mechanisms.

Part-III Optics & combined studies on advanced semiconductors and oxides:

- MgZnO on sapphire grown by MOCVD;
- MBE-grown InN/sapphire, m-GaN/m-sapphire, GaN/Si, InGaN/GaN/sapphire;
- InAlGaN - anomalous luminescence behavior, defect-related optical properties;
- Infrared and theoretical studies on II-VI CdZnTe, CdSeTe
- Nonlinear optical properties and ultrafast dynamics of bulk SiC & ZnO, GaN:Mg film.

Part-IV Synchrotron radiation (SR) X-ray absorption (XAS) & correlated studies:

GaN on sapphire and on Si; 4H-SiC and 3C-SiC; on MBE-grown CdTe/InSb; MBE-grown InPSb on GaAs; for carbon nanotube arrays.

Hope to penetrate into the fundamental concepts/properties of above issues, to explore & solve some tough problems, to promote the research in related fields, and to establish/develop the cross-strait collaboration & exchanging, for students, professors and engineers.

Outlines

- Introduction
- Nano-features & luminescnce mechanism of InGaN/GaN MQW LEDs
- New designs & development of MOCVD growth of InGaN/GaN MQW LEDs
- Attractive researches on III-Nitrides in recent years
- Synchrotron Radiation Technology, Nuclear and Surface Science Investigation
- Synchrotron Radiation X-ray absorption & Raman scattering of GaN on Si

Part-I a) Research Accomplishments in 2012

<<**Handbook of Zinc Oxides and Related Materials:** ***Volume 1) Materials, and Volume 2) Devices and Nano-Engineering***>>

Devki N. Talwar, Zhe Chuan Feng and Tzuen-Rong Yang, "Vibrational signatures of isotopic impurities and complexes in II-VI compound semiconductors", Phys. Rev. B **85**, 195203 (2012).

S.Y. Hu, Y.C. Lee, Z.C. Feng, S.H. Yang, "Investigation of defect-related optical properties in $Al_xIn_yGa_{1-x-y}N$ quaternary alloys with different Al/In ratios", Journal of Luminescence **132**, 1037–1040 (2012).

Zhe Chuan Feng, Cheng Chen, Qiang Xu, Suwan P. Mendis, Ling-Yun Jang, Chin-Che Tin, Kung-Yen Lee, Chee Wee Liu, Zhengyun Wu, and Zhi Ren Qiu, "Raman scattering and X-ray absorption from CVD grown 3C-SiC on Si", Materials Science & Forum **717-720**, 505-508 (2012).

Qiang Xu, Hua Yang Sun, Cheng Chen, Ling-Yun Jang, RUSLI, Suwan P. Mendis, Chin Che Tin, Zhi Ren Qiu, Zhengyun Wu, Chee Wee Liu, and Zhe Chuan Feng, "4H-SiC wafers studied by X-ray absorption and Raman scattering", Materials Science & Forum **717-720**, 509-512 (2012).

Z.C. Feng, T.W. Kuo, L.H. Zhu, C.Y. Wu, H.L. Tsai, B.L. Liu, and J.R. Yang, "Optical and structural studies of dual wavelength InGaN/GaN tunnel-injection light emitting diodes grown by metalorganic chemical vapor deposition", Thin Solid Films, doi: 10.1016/j.tsf.2012.05.038 (2012).

Zhe Chuan Feng, "Brief history review of research/development and basic/interdisciplinary characterization on ZnO", in *Handbook of Zinc Oxides and Related Materials: Volume 1) Materials, and Volume*, Ed. Zhe Chuan FENG, CRC press**,** Taylor & Francis Group, London/New York, www.crcpress.com, Ch. 1, pp. 3-36, (2012).

Chen-Jun Wu, Zhe Chuan Feng, Wen-Ming Chang, Chih-Chung Yang, and Hao-Hsiung Lin, "Bond lengths and lattice structure of $InP_{0.52}Sb_{0.48}$ grown on GaAs", Appl. Phys. Lett. **101**, 091902 (2012).

C. R. Ding, Z. L. Li, Z. R. Qiu, Z. C. Feng, and P. Becla, "Observation of In-related collective spontaneous emission (superfluorescence) in $Cd_{0.8}Zn_{0.2}Te$:In crystal", Appl. Phys. Lett. **101**, 091115 (2012).

L. Liu, L. Wang, D. Li, N. Liu, X. Hu , Z.C. Feng, C.Y. Wu, H.L. Tsai, Y.C. Lee and J.R. Yang, "Investigation of the light emission properties and carrier dynamics in dual-wavelength InGaN/GaN multiple-quantum well light emitting diodes", J. Appl. Phys. in press (2012).

H.C. Hsu, G.M. Hsu, Y.S. Lai, Z.C. Feng, A. Lundskog, U. Forsberg, E. Janzén, K.H. Chen, L.C. Chen,, "Polarized and diameter-dependent Raman scattering from individual AlN nanowires: the antenna and cavity effects ", J. Appl. Phys., in press.

Cheng Chen, Xiang Ping Shu, Hua Yang Sun, Zhi Ren Qiu, Ting-Wei Liang, Li-Wei Tu, and Zhe Chuan Feng, "Temperature dependence of Raman scattering in m-plane GaN with varying Ⅲ/Ⅴ ratios", Advanced Materials Research, in press.

Part-I b) Research Accomplishments in 2011

C.C. Wu, D.S. Wuu, P.R. Lin, T.N. Chen, R.H. Horng, S.L. Ou, Y.L. Tu, C.C. Wei, *Z.C. Feng*, "Characterization of MgZnO thin films grown on sapphire by metalorganic chemical vapor deposition", Thin Solid Films **519**, 1966-70 (2011).

S.Y.Hu, Y.C. Lee, *Z.C. Feng* and S.H. Yang, "Anomalous luminescence behavior in the InAlGaN thin film", J. Alloy and Compounds **509**, 2300-3 (2011).

Lei Liu, Lei Wang, Ding Li, Ningyang Liu, Lei Li, Wenyu Cao, Wei Yang, Chenghao Wan, Weihua Chen, Xiaodong Hu, and *Zhe Chuan Feng*, "Influence of Indium Composition in the Prestrained InGaN Interlayer on the Strain Relaxation of InGaN/GaN Multiple Quantum Wells in Laser Diode Structures", J. Appl. Phys. **109**, 073106-1-5 (2011).

Tzuen-Rong Yang, Sheng-Hong Jhang, Yen-Hao Shih, Wan-Ni Cheng, Fu-Chung Hou, Yu-Chang Yang, P. Becla, Der-Chi Tien, and Zhe-Chuan Feng, "Study of Optical and Transport Properties of $Cd_{1-x}Zn_xTe$ and $CdSe_xTe_{1-x}$ by Far-IR Reflectance Spectra", Chinese Journal of Physics **49**, 239-249 (2011).

Z. S. Lee**,** L. M. Kong**,** *Z. C. Feng***,** A. G. Li**,** H. L. Tsai and J. R. Yang, "Luminescence dynamics and structural investigation of InGaN/GaN multiple quantum well light emitting diodes", Advanced Materials Research **216**, 445-9 (2011).

Dongsheng Peng, Ke Jin, Ruisheng Zheng, Lei Liu and *Zhe Chuan Feng*, "Comparative Study of GaN-Based LED Grown on Different Substrates", Advanced Materials Research 194-196, 2241-4 (2011).

Z. S. Lee**,** L. M. Kong**,** *Z. C. Feng***,** A. G. Li**,** H. L. Tsai and J. R. Yang, "Luminescence dynamics and structural investigation of InGaN/GaN multiple quantum well light emitting diodes", Advanced Materials Research **216**, 445-9 (2011).

F. Cheng, TaoFa, ShudeYao, Chen-JunWu, Hao-HsiungLin, ZheChuanFeng, "Tetragonal distortion of InAsPSb film grown on InAs substrate studied by Rutherford backscattering/channeling and synchrotron X-ray diffraction", Physica B 406,3219-21 (2011).

Yee Ling Chung, Xingyu Peng, Ying Chieh Liao, Shude Yao, Li Chyong Chen, Kuei Hsien Chen, and *Zhe Chuan Feng*, "Raman scattering and Rutherford backscattering studies on InN films grown by plasma-assisted molecular beam epitaxy", Thin Solid Films, **519**, 6778–6782 (2011).

Lianshan Wang, Zhiqin Lu, Sheng Liu, and *Zhe Chuan Feng*, "Shallow–Deep InGaN Multiple-Quantum-Well System for Dual-Wavelength Emission Grown on Semipolar (112) Facet GaN", J. Electronic Mat. **40**, 1572-7 (2011).

Yu-Li Tu, Yan-Hao Huang, Lingmin Kong, Kung-Yen Lee, Ling-Yun Jang, Chin-Che Tin, Chee-Wee Liu and *Zhe Chuan Feng*, "Synchrotron Radiation X-ray Absorption and Optical Studies of Cubic SiC Films Grown on Si by Chemical Vapor Deposition", Advanced Materials Research **306-7**, 167-170 (2011).

Ting-Wei Kuo, Lingmin Kong, *Zhe Chuan Feng*, Wei Liu, Soo Jin Chua, Y.-S. Huang, and Dong-Sing Wuu, "Luminescence Properties of InGaN/GaN Multiple Quantum Well Light Emitting Diodes by Metalorganic Chemical Vapor Deposition", Advanced Materials Research **306-7**, 1133-7 (2011).

Devki N Talwar, Tzuen-Rong Yang, *Zhe Chuan Feng* and P. Becla, "Infrared reflectance and transmission spectra in II-VI alloys and superlattices", Physical Review B **84**, 174203_1-11 (2011).

Ding Bin-Beng, Pan Feng, Feng Zhe-Chuan, Fa Tao, Cheng Feng-Feng and Yao Shu-De, "Structural Analysis of InGaN/GaN MQWs by Different Experimental Methos", Chinese Phys. Lett. **28**, 078401 (2011).

Nano-structures and luminescence mechanisms of InGaN-based quantum well light emitting diodes

Professor Zhe-Chuan Feng
Graduate Institute of Photonics and Optoelectronics, National Taiwan University

Sample Structure

Sample QW8a :

Well: 3nm $In_{0.18}Ga_{0.82}N$
Barrier: 6nm GaN

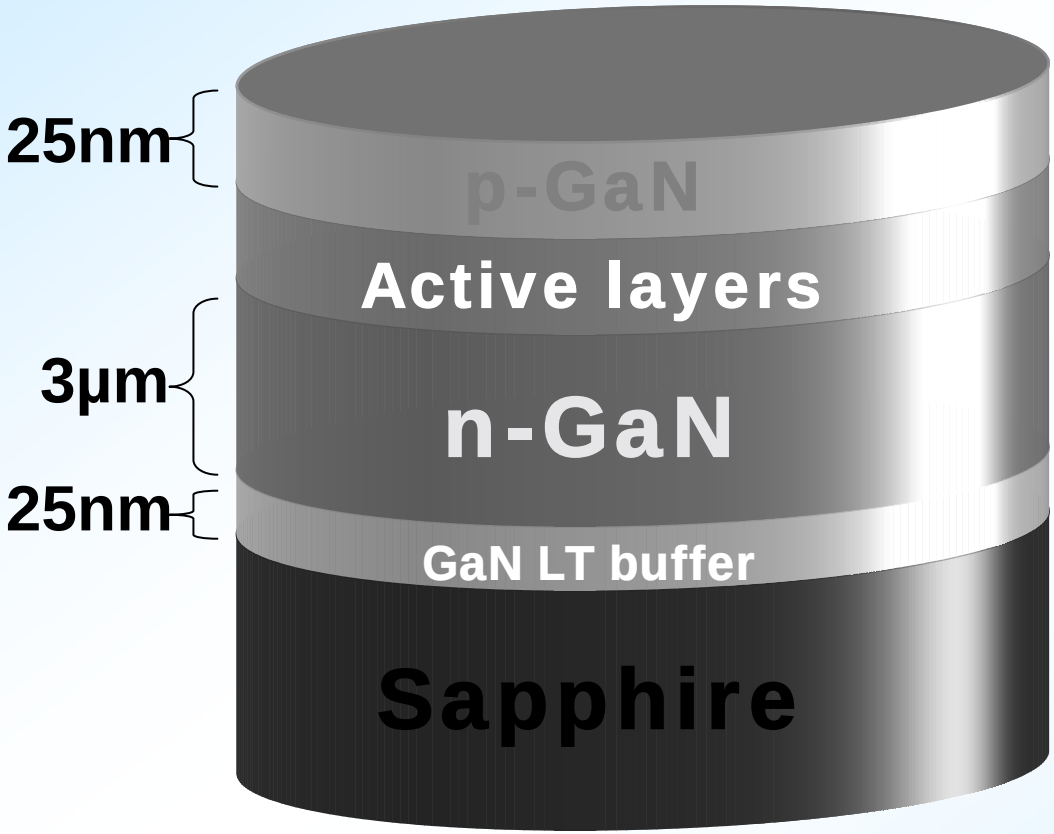

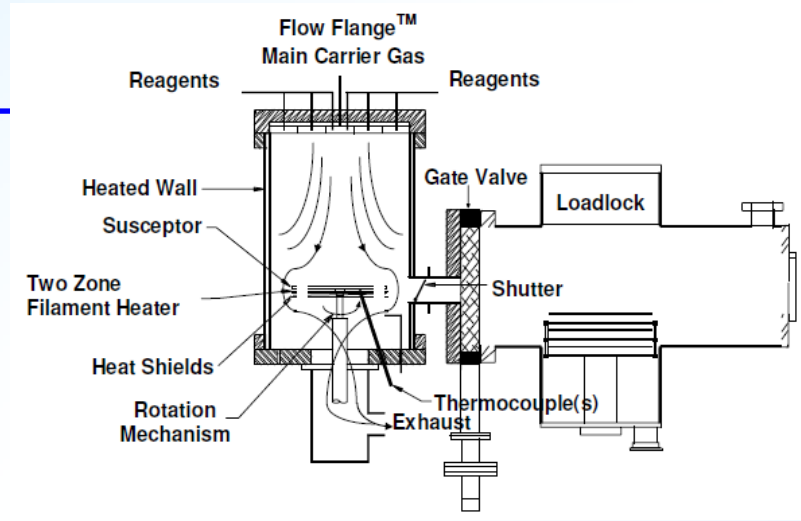

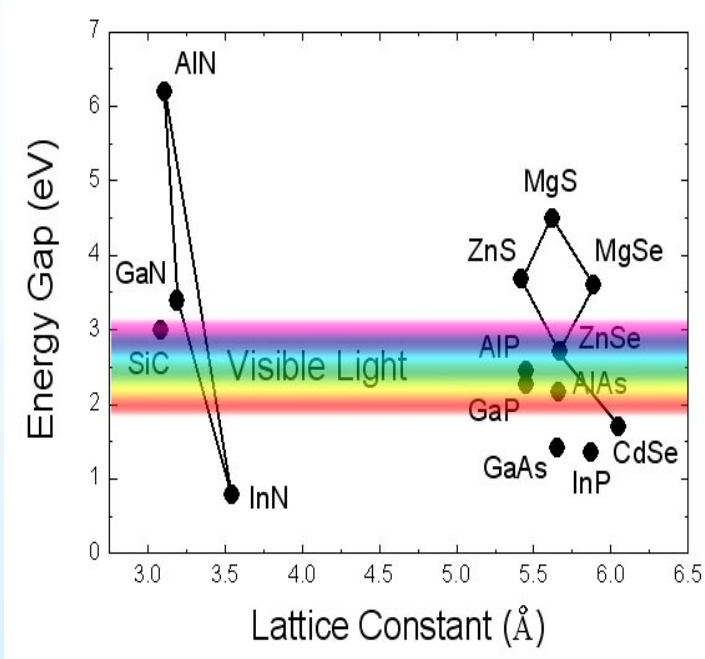

Grown by MOCVD.

Important Property Review:

Quantum-confined Stark Effect

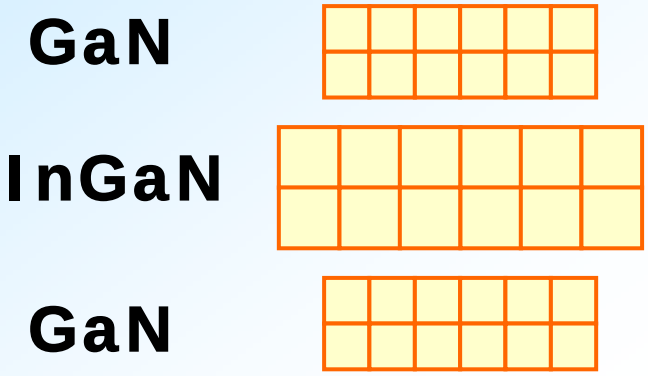

Larger lattice mismatch

→ Strain effect

→ Large electric field

→ Spatial separation of electrons and holes

→ Wavefunction overlap ↓

→ **1. Red-shift**
2. FWHM ↑
3. Intensity ↓

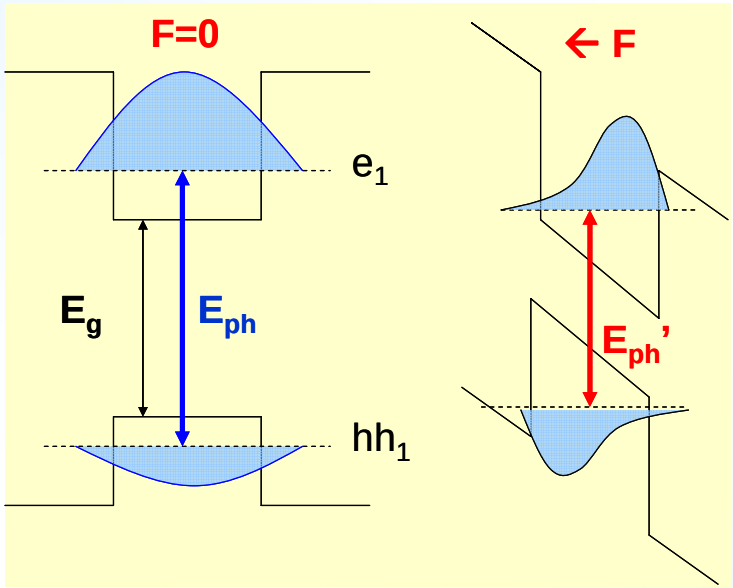

Multi-Tech studies on InGaN/GaN MQW LEDs by MOCVD

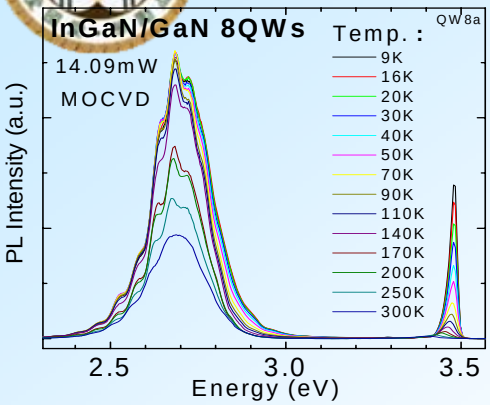

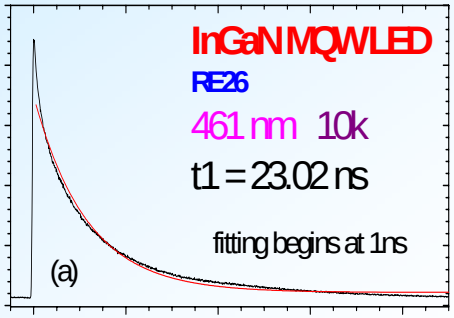

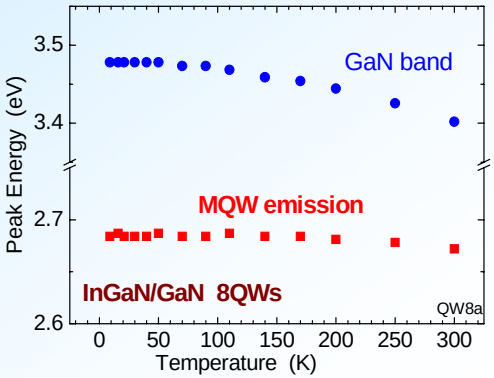

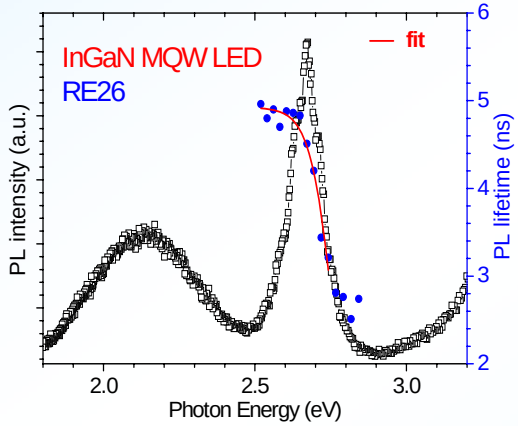

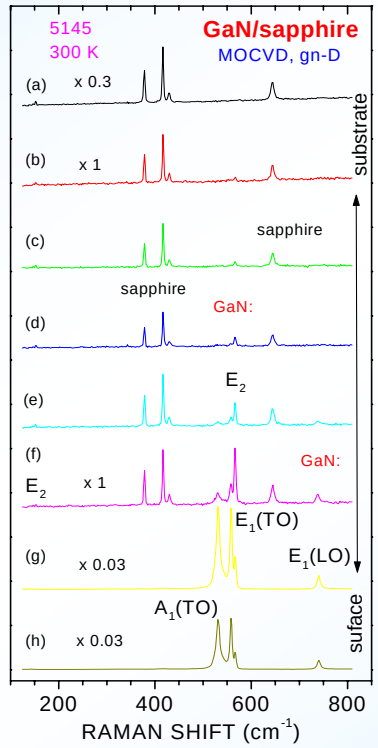

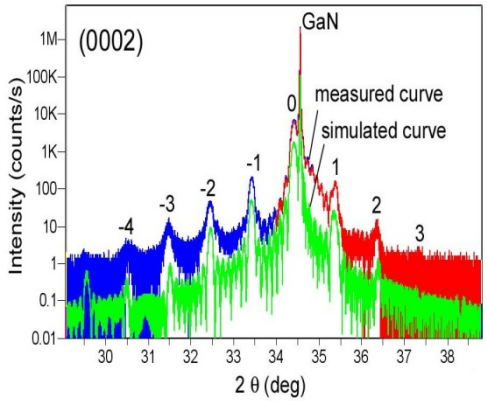

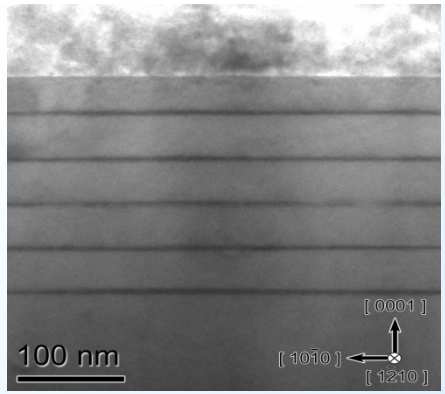

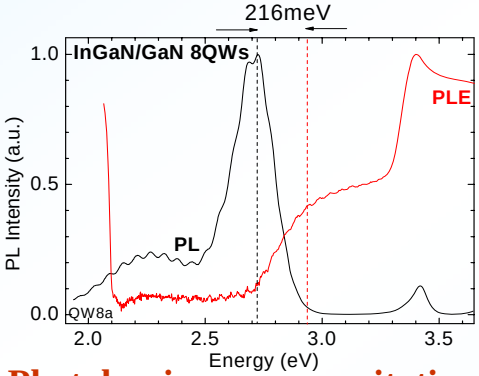

Photoluminescence excitation (PLE)

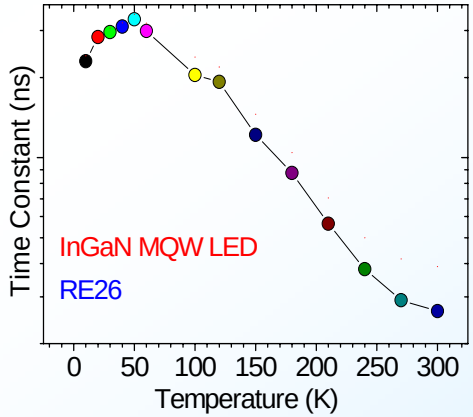

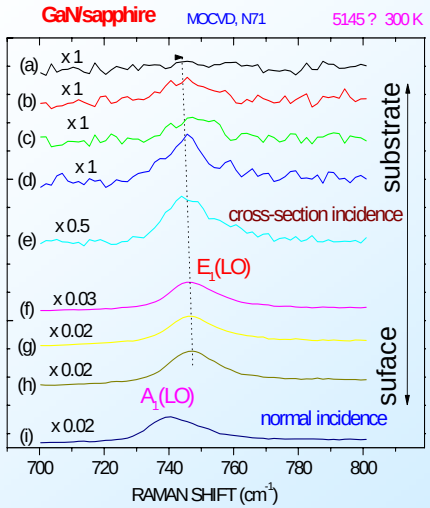

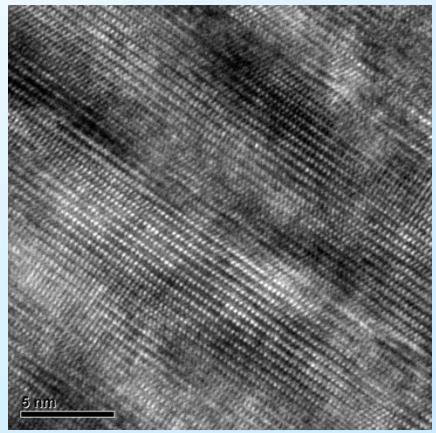

InGaN-GaN MQW: *excellent characteristic* HR-XRD

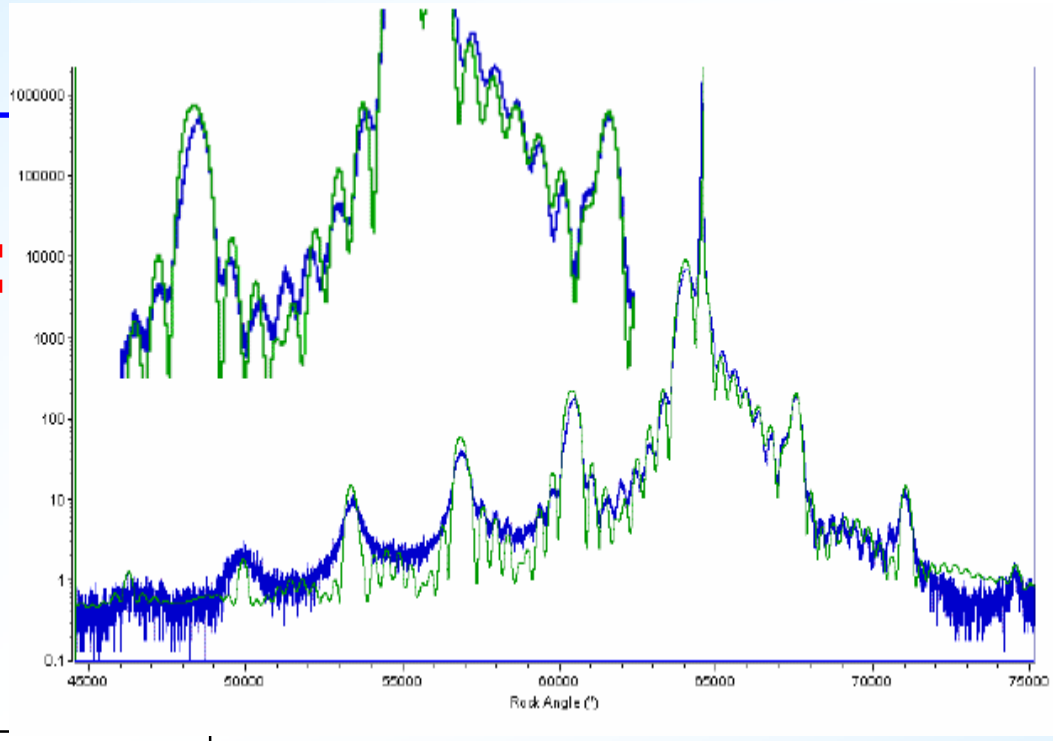

(QW8a)

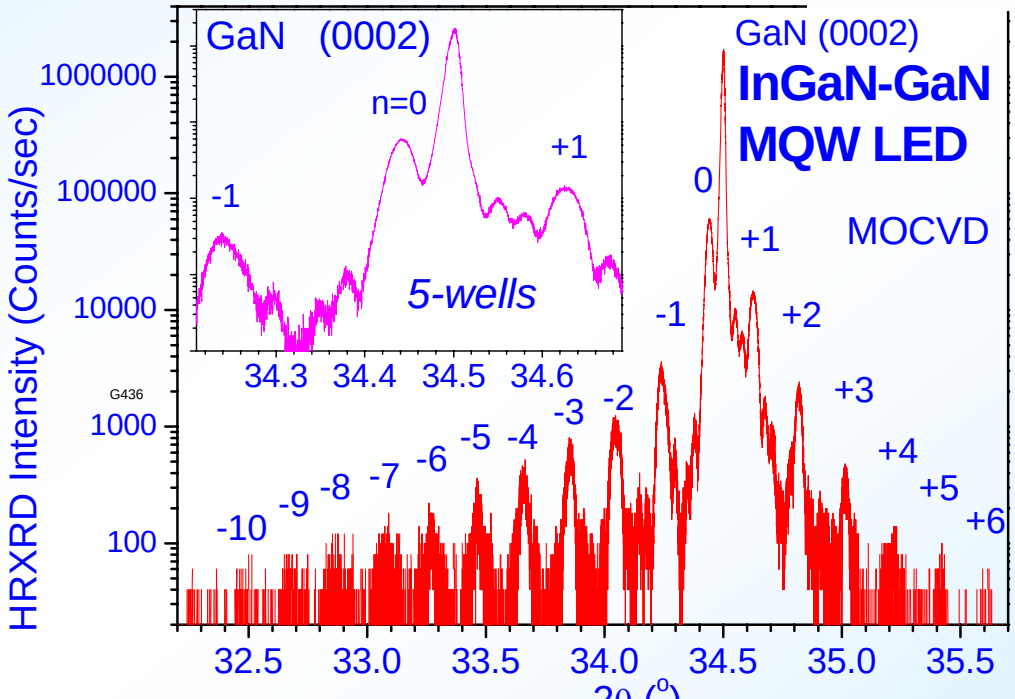

(G978)

How to achieve the MOCVD growth of InGaN-GaN MQW LED: with excellent characteristic

Temperature dependent PL

InGaN/GaN 8QWs: Temperature dependent PL

(W) 1.2nm
(B) 3nm
8-QWs
x(In)=17.8%

Left:
Emissions
- QW

Right:
Emissions
- GaN barriers

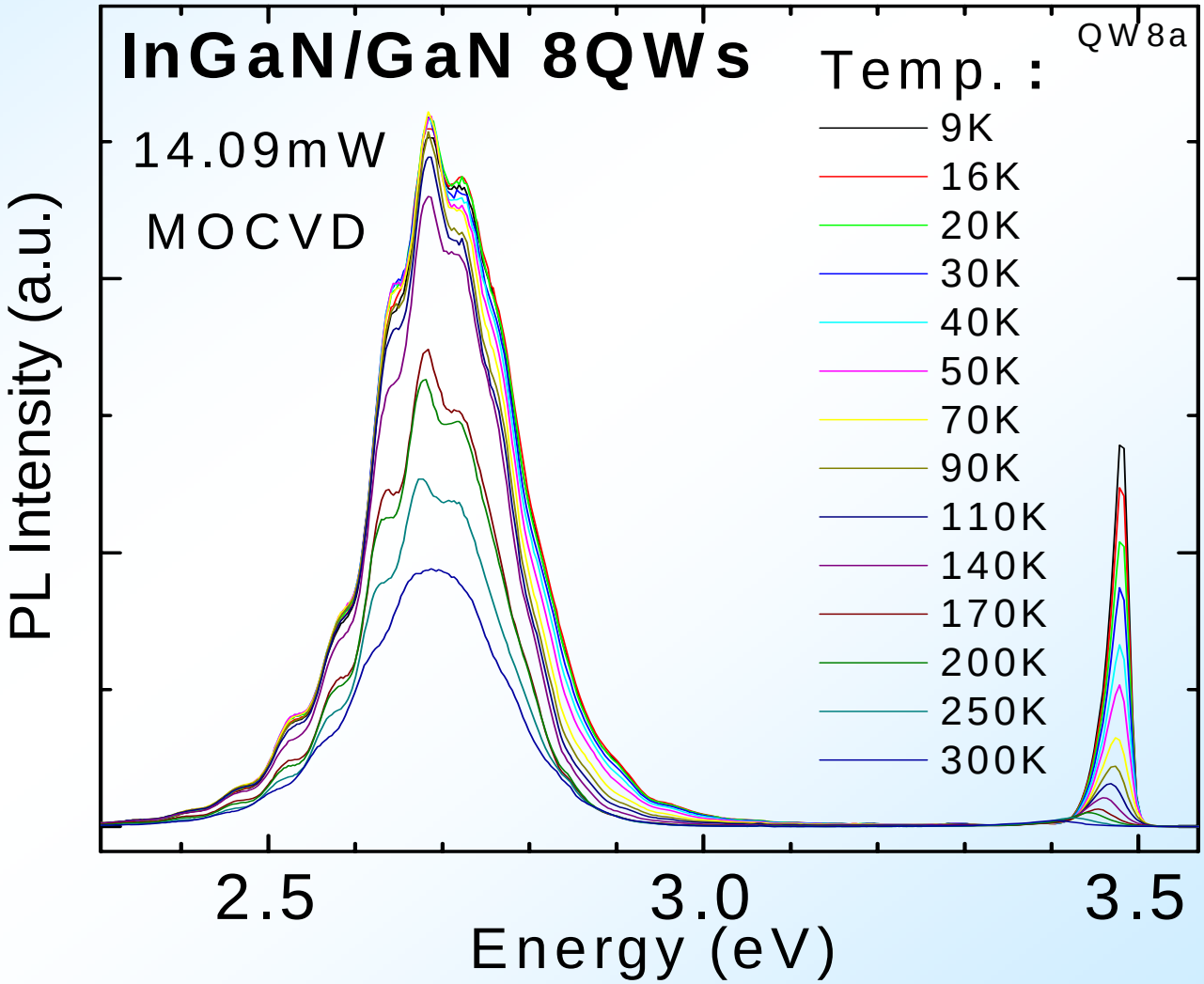

InGaN/GaN 8QWs: Peak position & Arrhenius plot

(W) 1.2nm / (B) 3nm x 8 x(In) : 17.8%

Varshni Eq. for E_g(GaN) – T:

$E(T)=E(0)-\alpha T_2/(\beta+T)$

$E(0)=2.7015$ eV

$\alpha = 0.368$ meV/K, $\beta = 618$ K

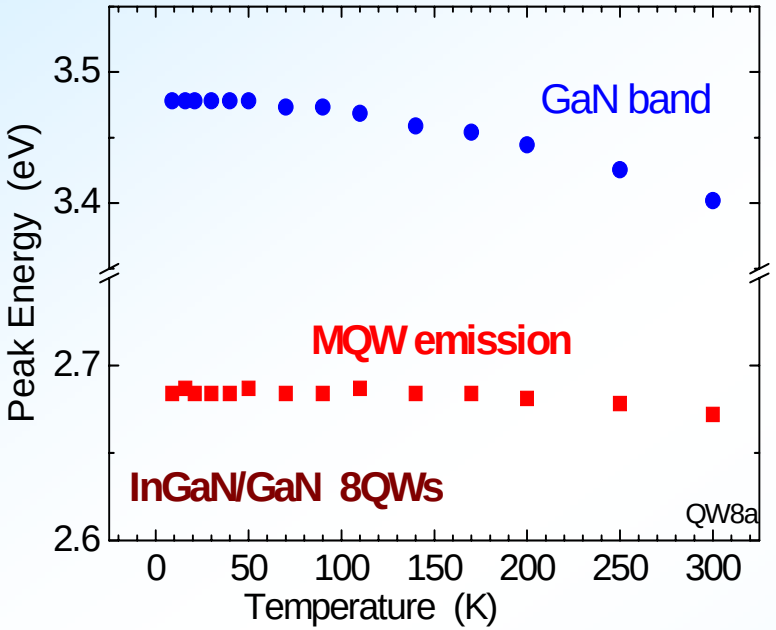

PL peak position versus T (9–300 K)

Anomalous T-behavior of MQW PL peak is attributed to band-tail states due to inhomogeneities in the InGaN-based material.

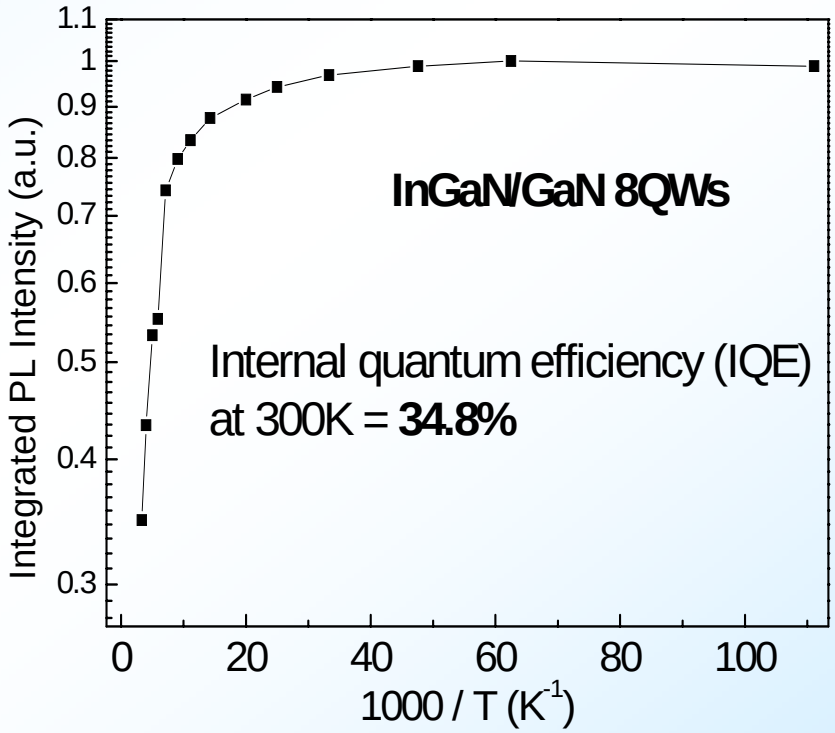

η (Internal Quantum Efficiency):

The time integrated photoluminescence intensity at room temperature normalized to a low temperature (9K) value

Temperature-dependent Behavior

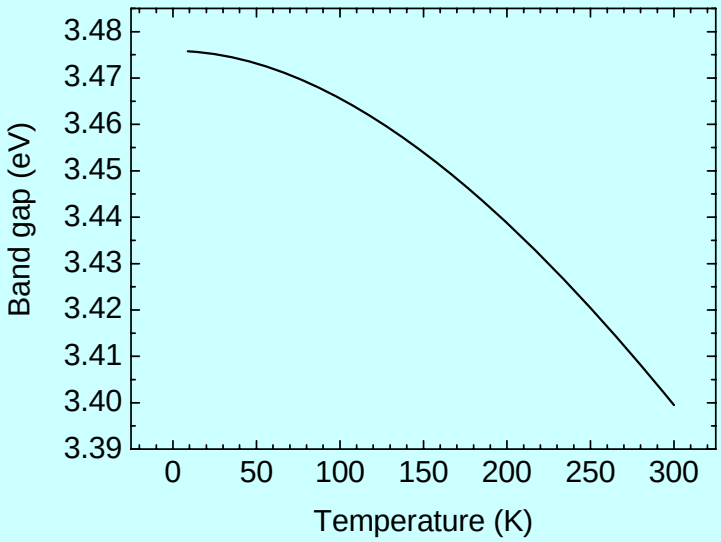

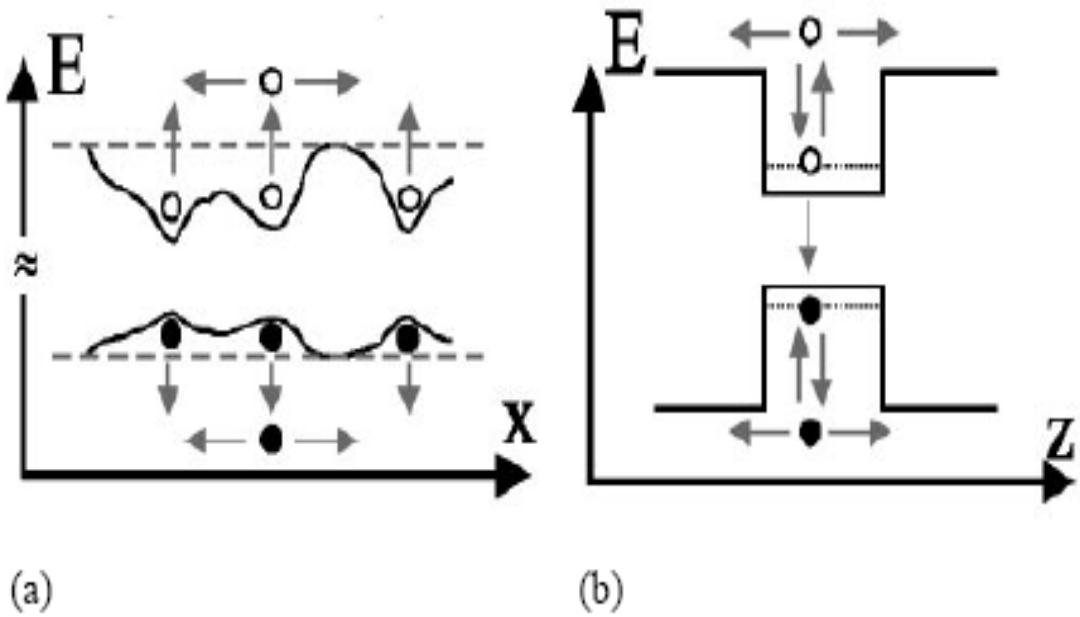

圖 4-2(a)(b) 載子逃脫量子井形成非輻射結合機制示意圖

Varshni's Law

$$E(T) = E(0) - \frac{\alpha T^2}{\beta + T}$$

$$E(T) = E(0) - \frac{\alpha T^2}{T + \beta} - \frac{\sigma^2}{k_B T}$$

Band-tail model

: degree of localization effect

Band gap shrinkage of GaN

Arrhenius Formula:

$$I_{PL}(T) = \frac{I_0}{1 + Ae^{(\frac{-E_a}{K_B T})}}$$

Photoluminescence excitation (PLE)

InGaN/GaN 8QWs: PL & PLE spectra

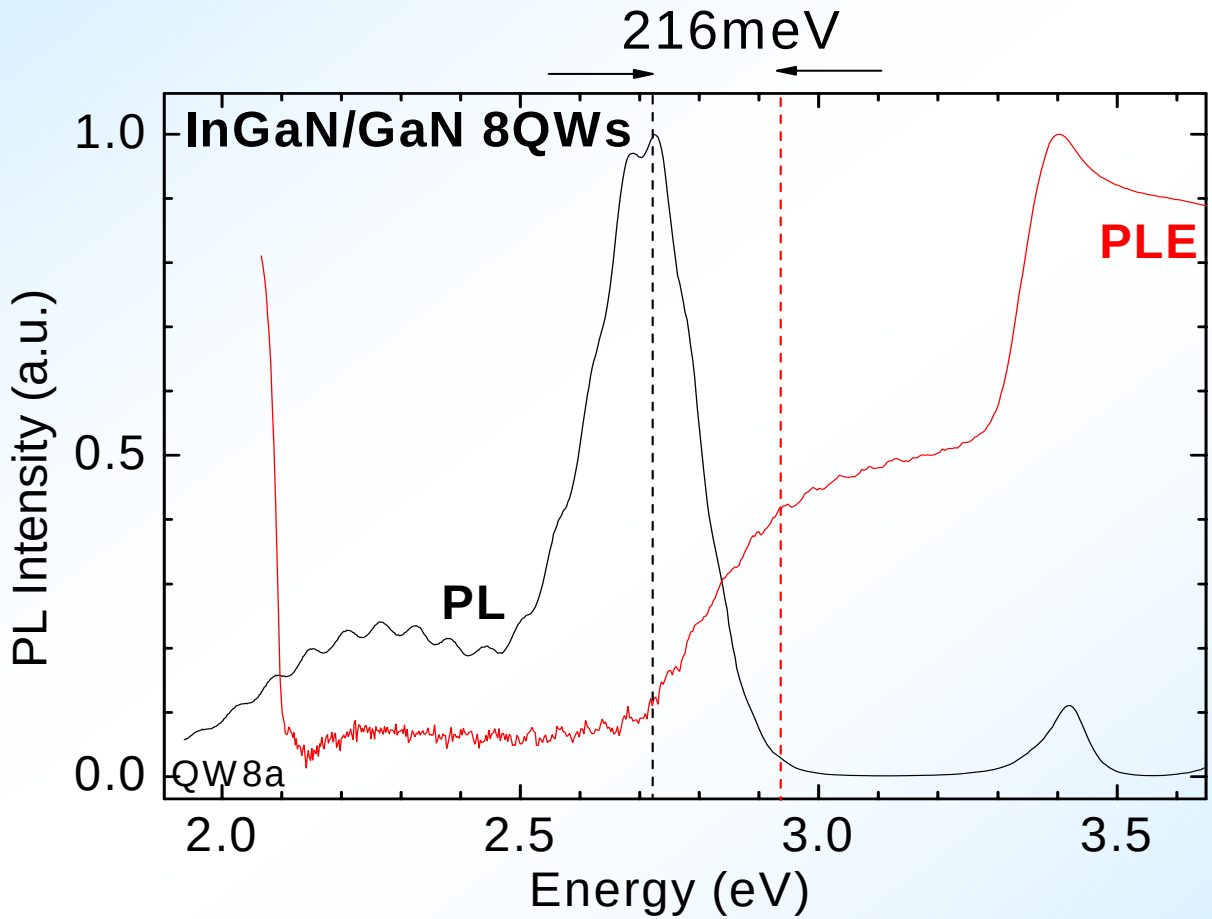

Comparison of RT PL and PLE spectra from a MOCVD-grown InGaN-GaN MQW (8-QWs) sample – Quantum confined Stark effect (QCSE).

TRPL of InGaN/GaN MQWs: dependence on E, T

(A pulsed laser 374 nm)

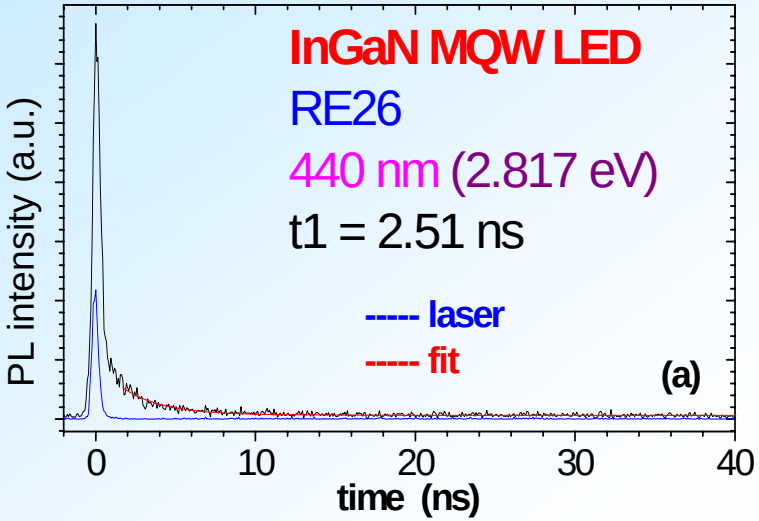

•A single-exponential fit - determine lifetime.

• *TRPL data and fittings at λ =440 nm. Fitting begins at about 1.5 ns in order to avoid the laser response.*

• *The RT TRPL was measured from 436nm to 492nm, with 15 points. The t_{PL} values increase with decreasing photon energy.*

• *This is characteristic of the localized system. The depth of localization can be evaluated by assuming the exponential distribution of the density of tail states and by fitting the photon energy dependence of the t_{PL} values using the equation:*

$$\tau_{PL}(E) = \frac{\tau_{rad}}{1 + \exp\dfrac{E - E_{me}}{E_0}},$$

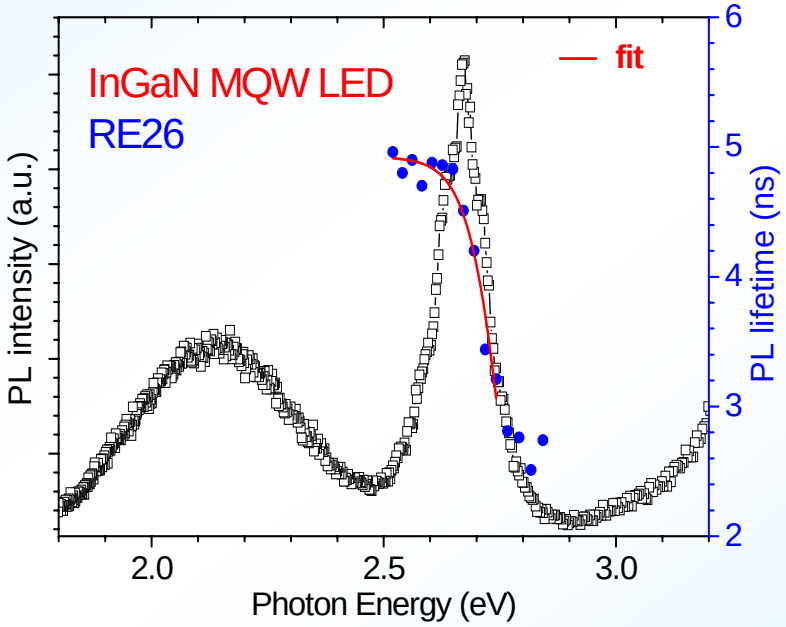

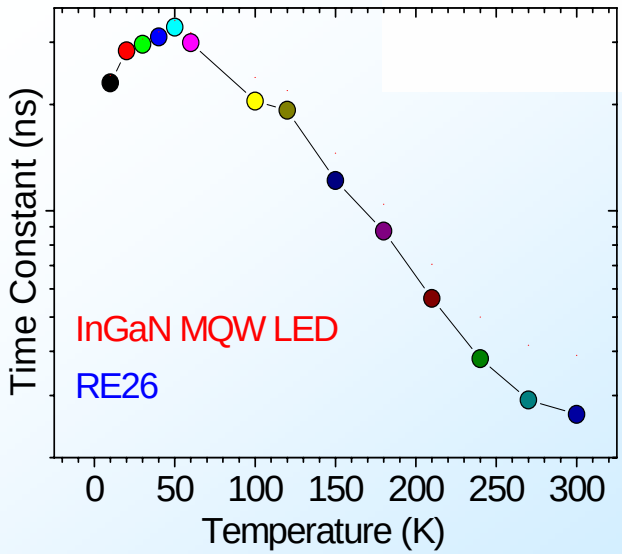

• **T-dependence of lifetime (10-300 K), measured at PL peak - 462 nm.**

Nano-structures and luminescence mechanisms of InGaN/GaN multiple quantum well light emitting diodes

(a)
QW1

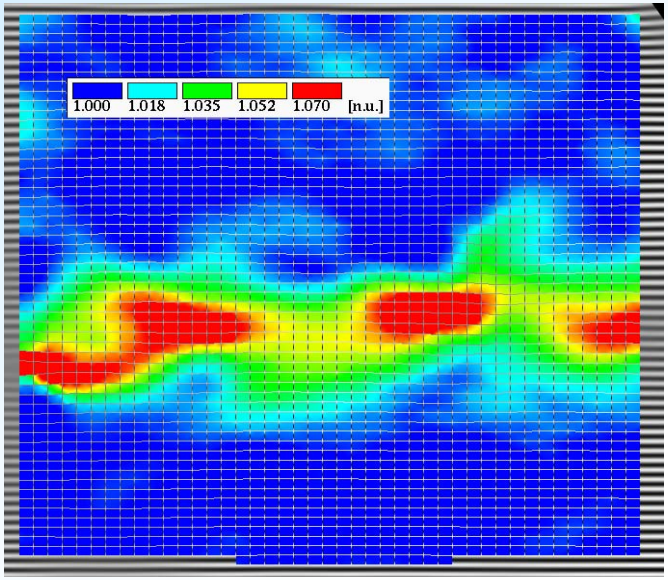

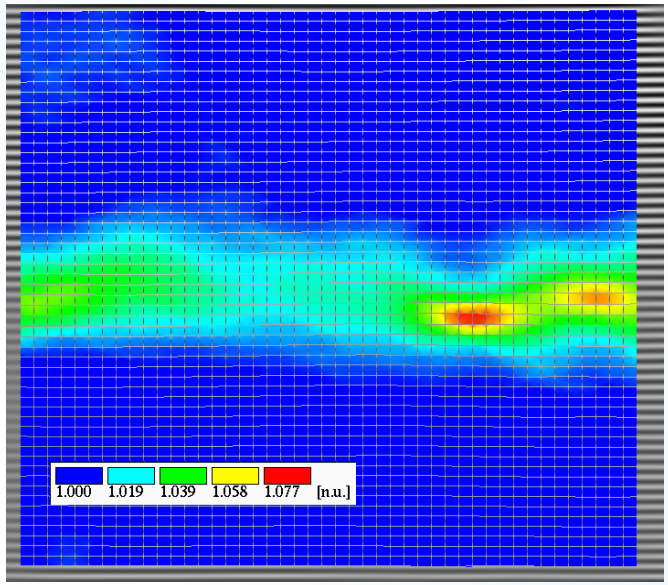

(e)
QW5

(G978)

The color-coded map of the local In concentration in an InGaN/GaN QW structure, which contains 5 InGaN layers. (a) is QW1 just next to the capping layer and (e) is QW5 at the bottom of the active layer.

Another opinions:
Monolayer fluctuations in InGaN QWs

Digital Analysis of Lattice image technique - *showing QD-like structures*

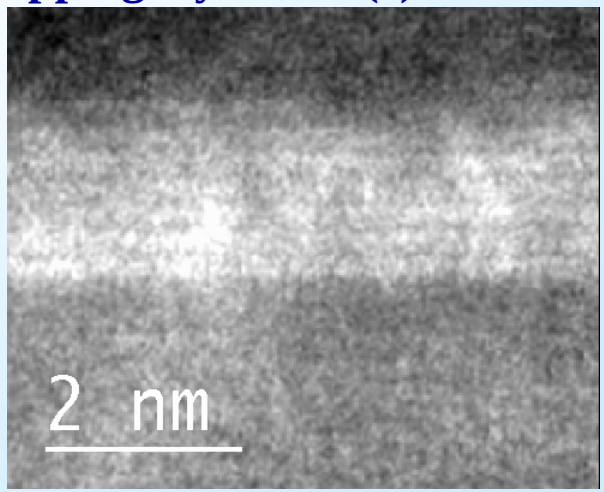

InGaN QWs are not automically flat

From Humphries et al.

V-defects & HAADF STEM images of the InGaN/GaN MQW

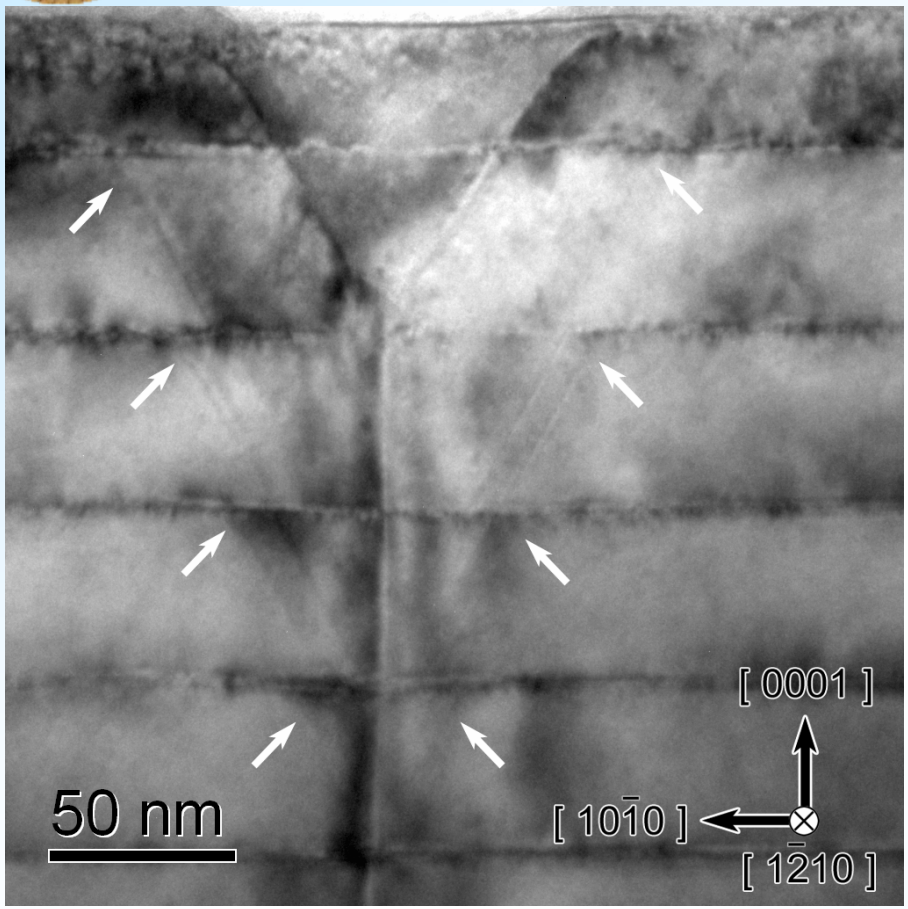

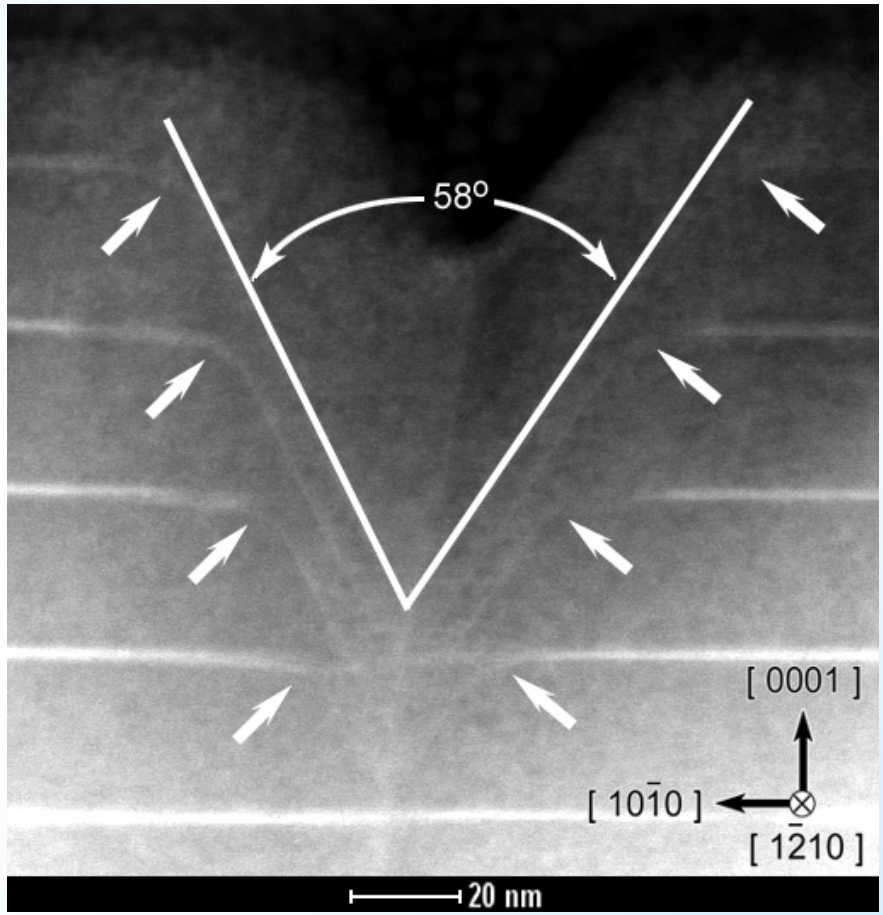

Threading dislocation originating from GaN/sapphire interface to disrupt the InGaN/GaN MQW, and to initiate the V-defect, which have inverted the hexagonal pyramid-shaped {10-10} side walls.

(G978)

New designs & developments of InGaN/GaN MQW LEDs

Specially designed InGaN/GaN MQW structure with AlGaN/GaN SL strain-released buffer for LEDs/LDs *{JAP, in press}*

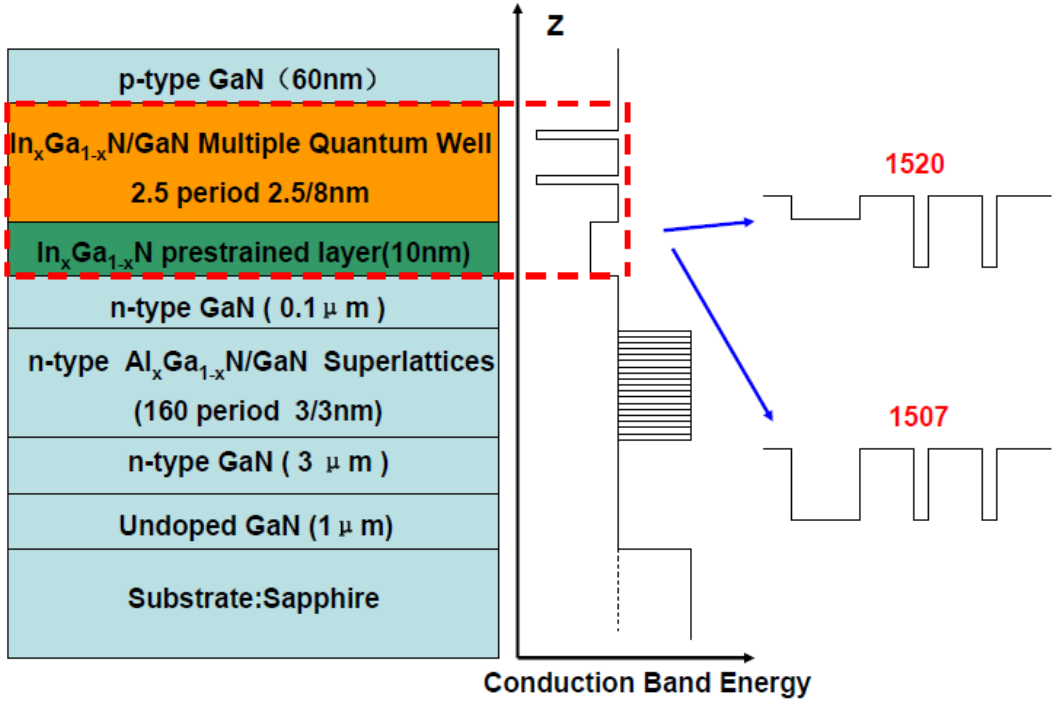

FIG. Schematic diagrams of sample structure and energy bands

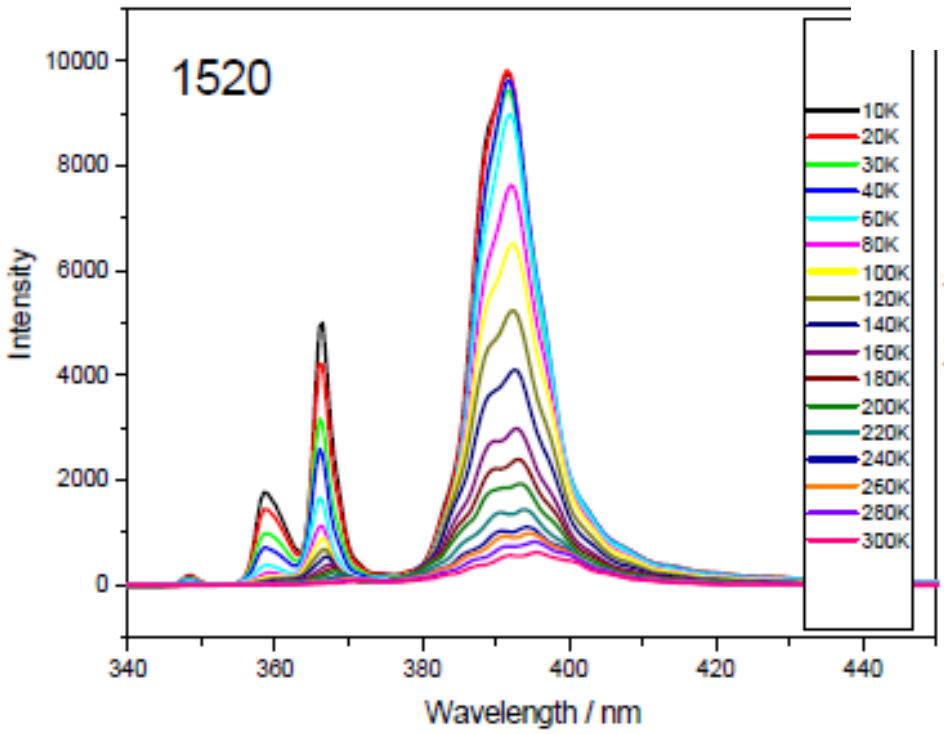

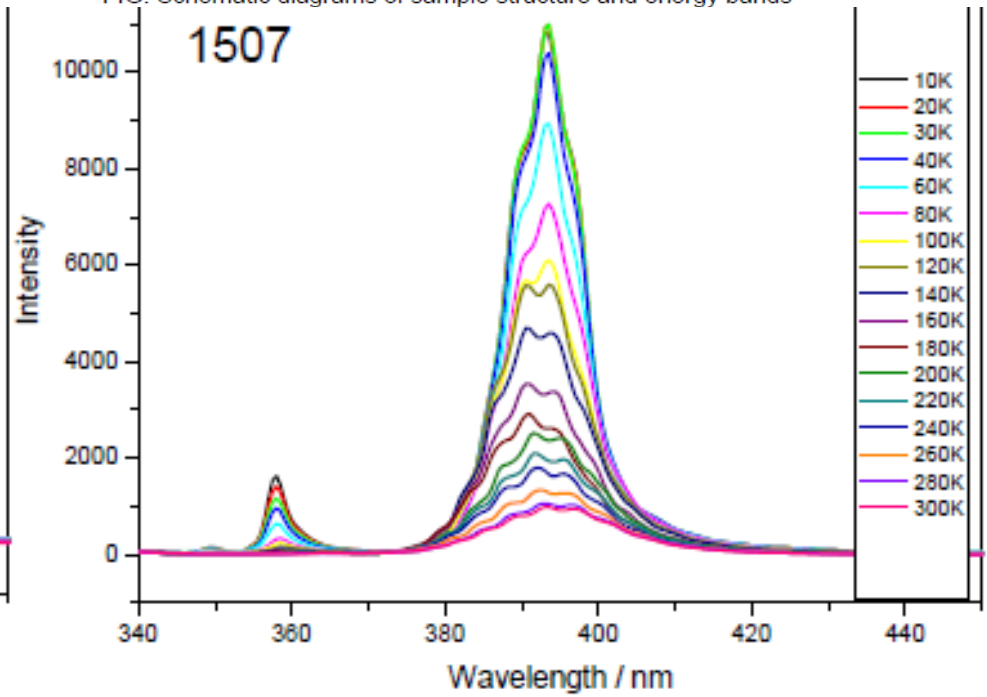

Time-Resolved and Temperature-Varied Photoluminescence of InGaN/GaN Multiple Quantum Well Structures

Lei Liu, Wenjie Wang, J.-L. Huang, Xiaodong Hu, Peng Chen, J.-J. Huang, Zhe Chuan Feng, SPIE **8484**-38, oral, San Diego, 16 August 2012. ***{SCI}***

Structure	Sample number
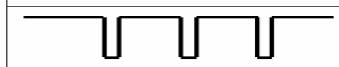	1505 (PL peak: ~420 nm)
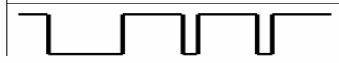	1506 (PL peak: ~420 nm)

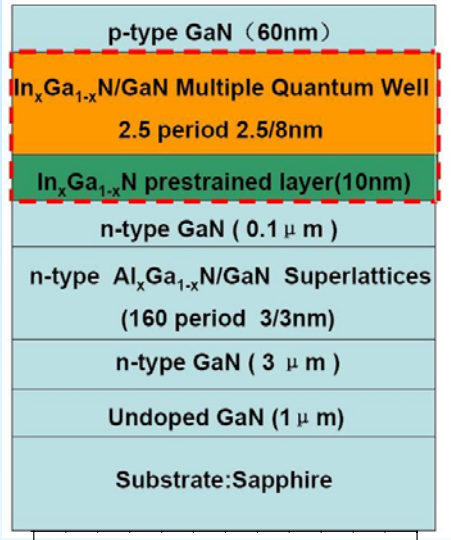

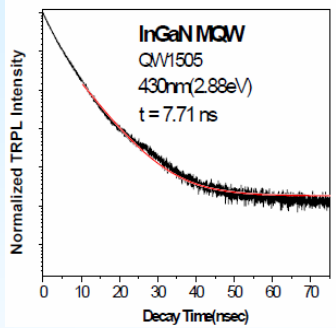

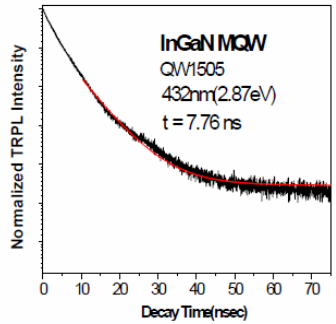

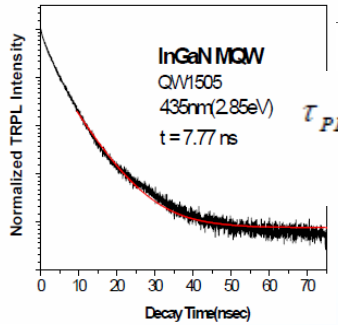

$$\tau_{PL}(E) = \frac{\tau_{rad}}{1 + \exp\dfrac{E - E_{me}}{E_0}}$$

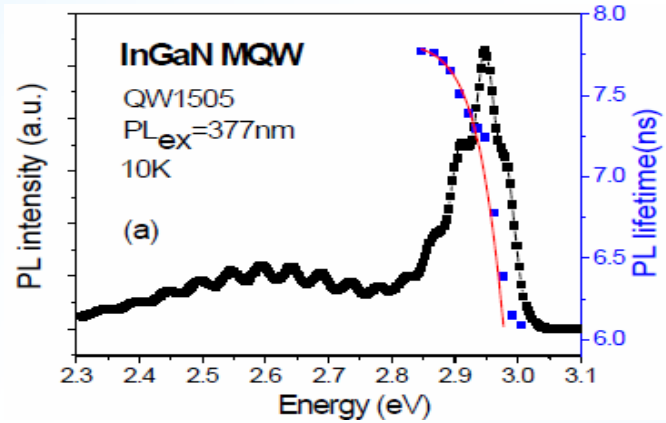

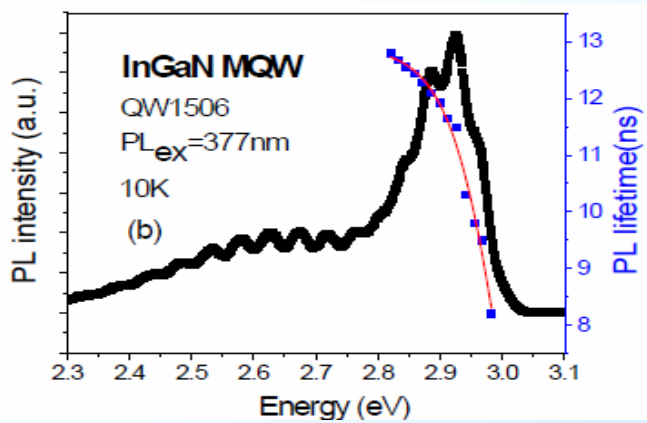

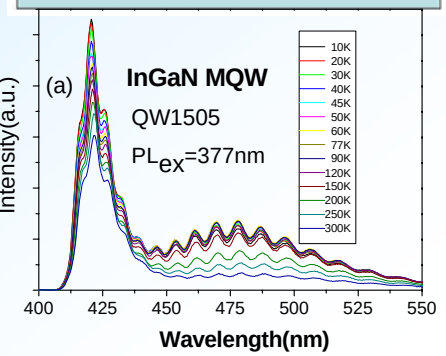

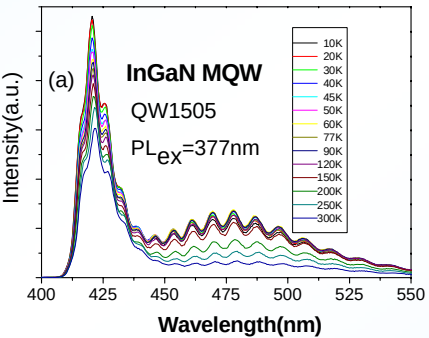

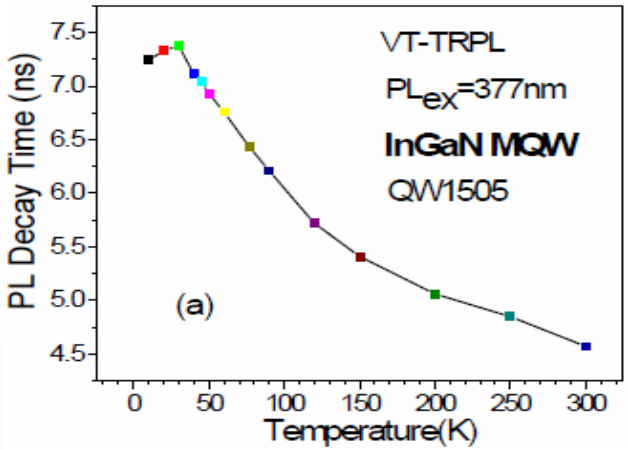

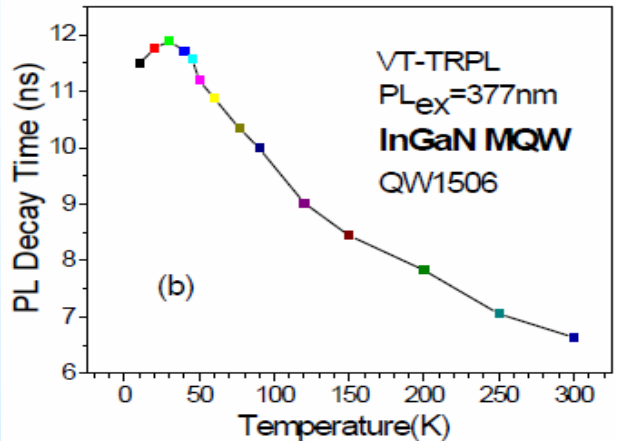

Charge Asymmetric Resonance Tunneling (CART)

MQW structure for dual-wavelength LEDs

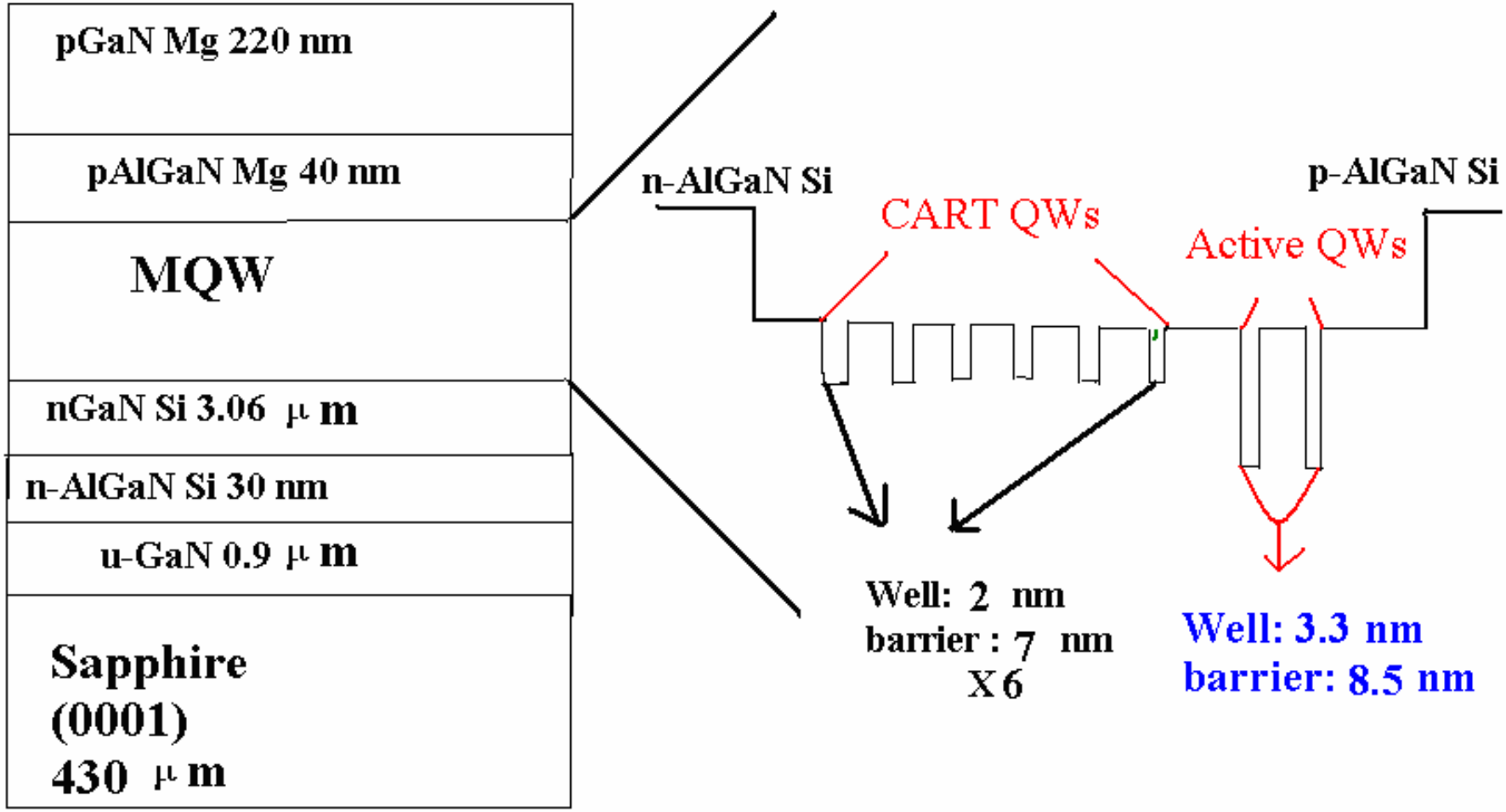

Well growth-temperature of 797^{0}C (GF03) and 782^{0}C (GF195) (TMIn flow: 940 SCCM).

Optical and structural studies of dual wavelength InGaN/GaN tunnel-injection light emitting diodes grown by metalorganic chemical vapor deposition

Z.C. Feng, T.W. Kuo, L.H. Zhu, C.Y. Wu, H.L. Tsai, B.L. Liu, and J.R. Yang, ***Thin Solid Films***, doi: 10.1016/j.tsf.2012.05.038 (2012). ***{SCI}***

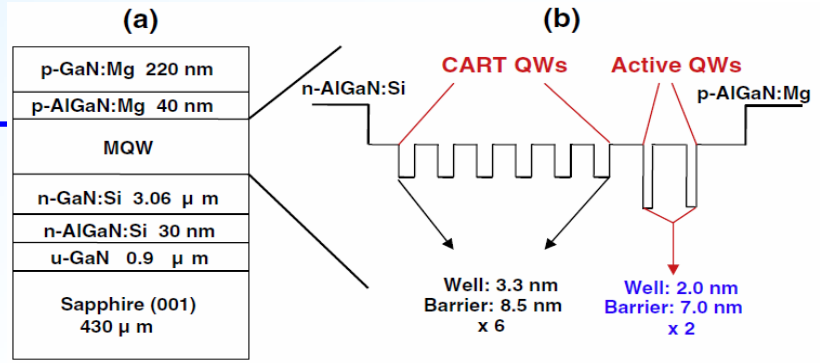

Fig. 1. (a) Schematic diagram and (b) conduction band diagram of the InGaN/GaN CART LEDs used in this study.

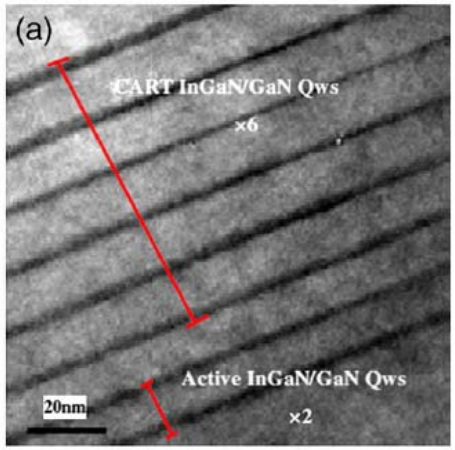

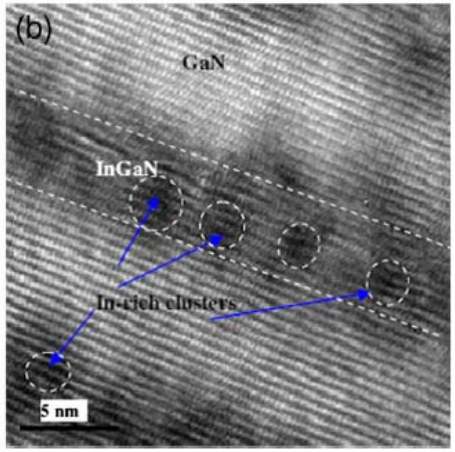

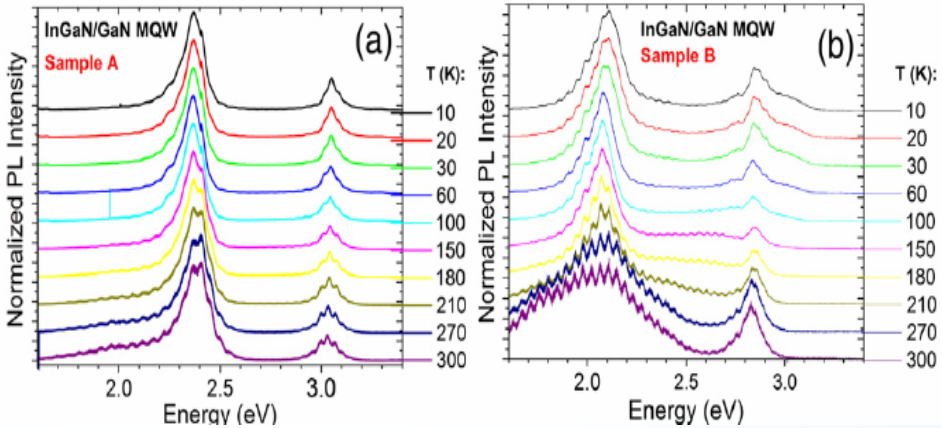

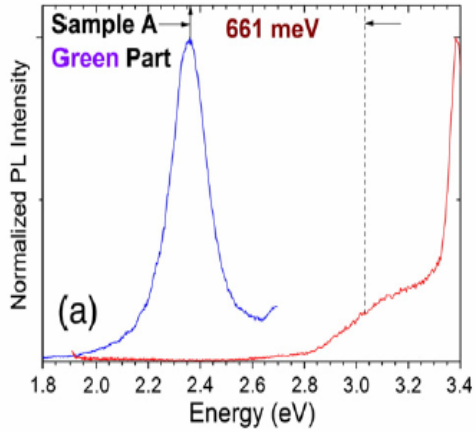

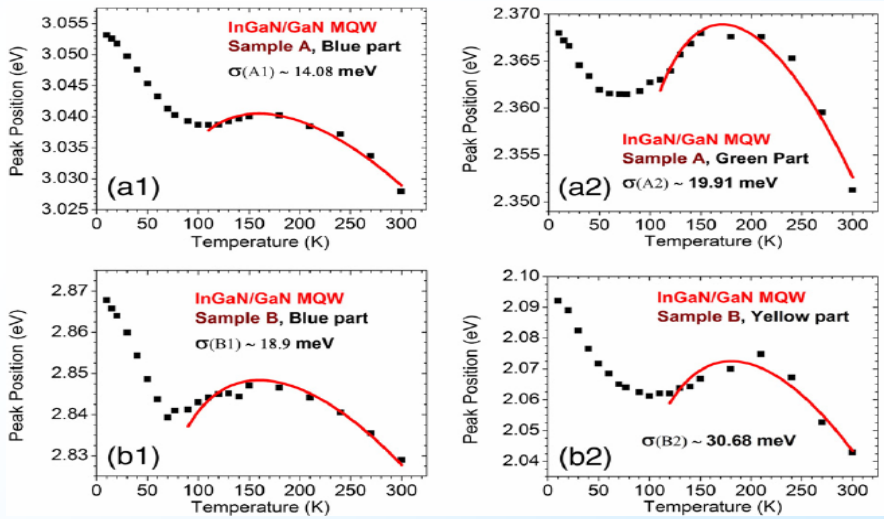

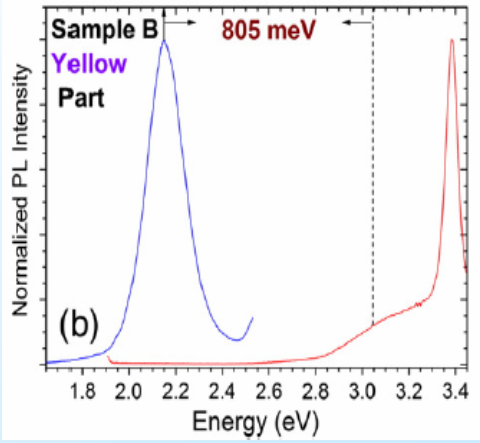

Photoluminescence Excitation (PLE)

Quantum Confined Stark Effects (QCSE)

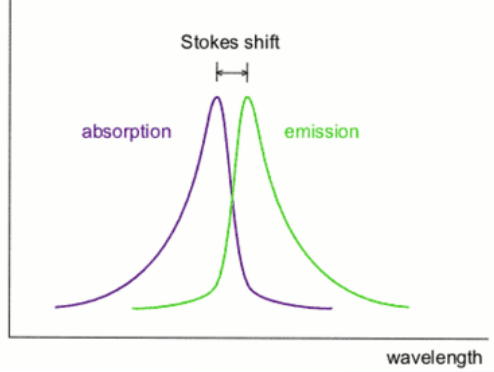

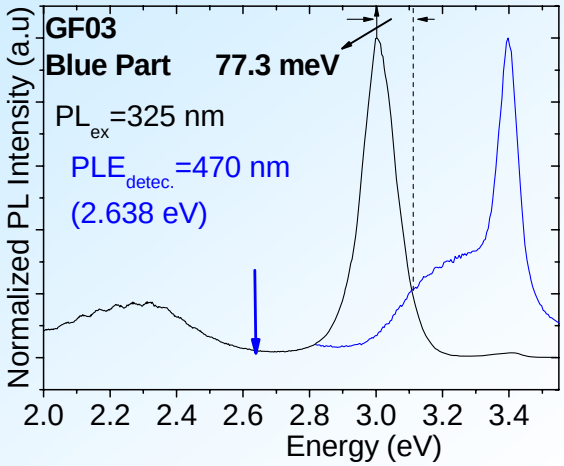

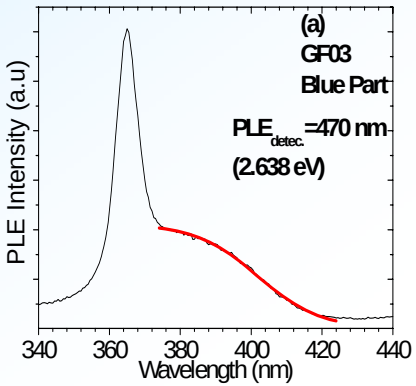

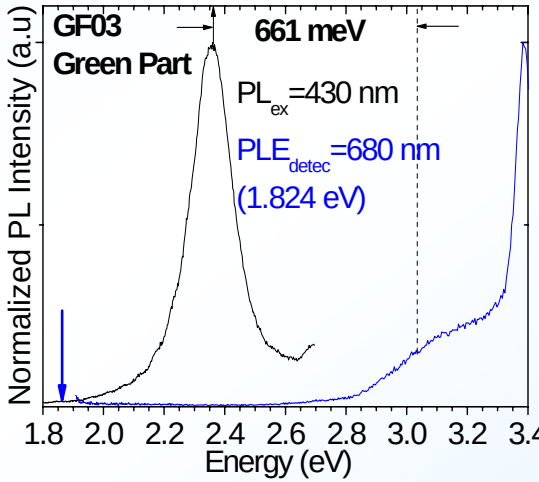

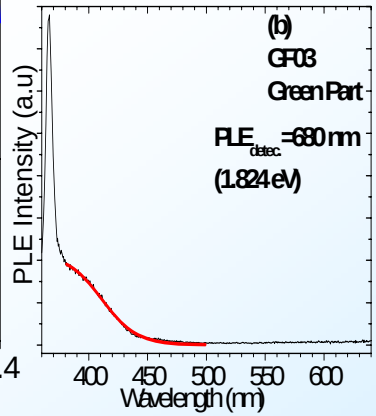

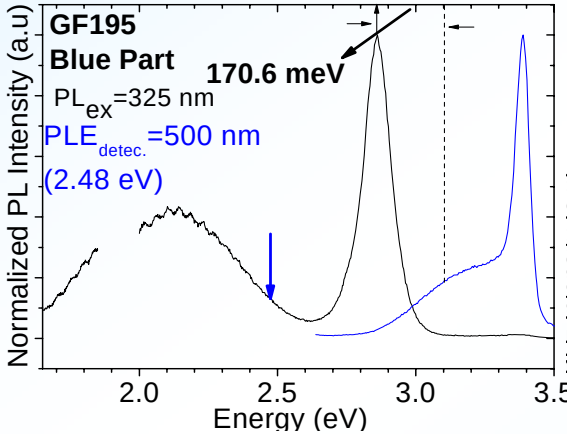

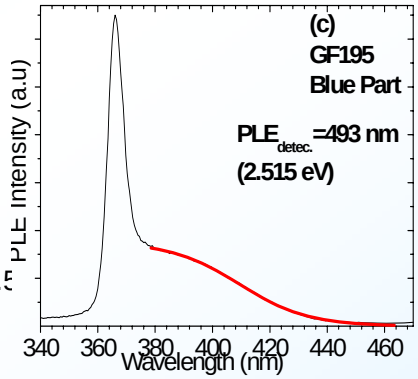

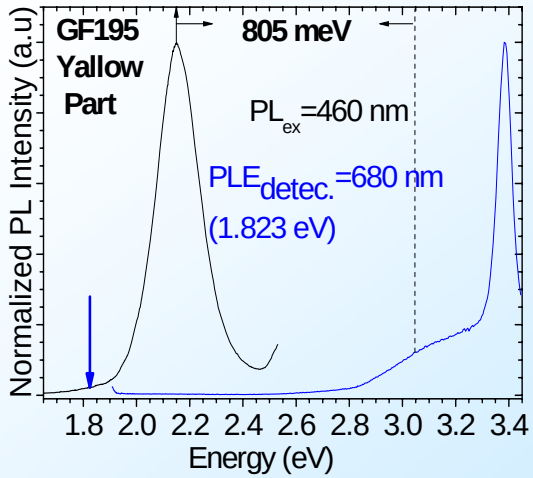

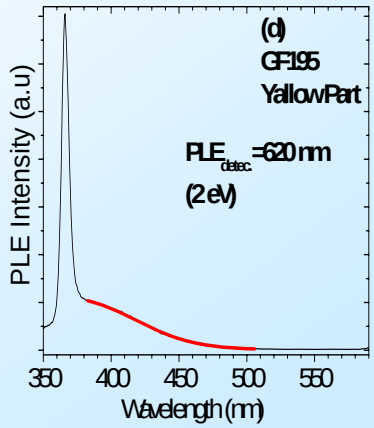

Figure . PL and PLE spectra at RT of InGaN/GaN MQW structure for GF03 & GF195.

Detection energy dependent Time-resolved PL (TR-PL)

Radiative lifetime, the energy similar to the mobility edge, and the depth of localization obtained from equation :

$$\tau_{PL}(E) = \frac{\tau_{rad}}{1 + \exp\dfrac{E - E_{me}}{E_0}}$$

- The radiative lifetime at low-energy side of the InGaN peak is longer, with a deeper localization depth & a larger Stokes shift for thicker well.

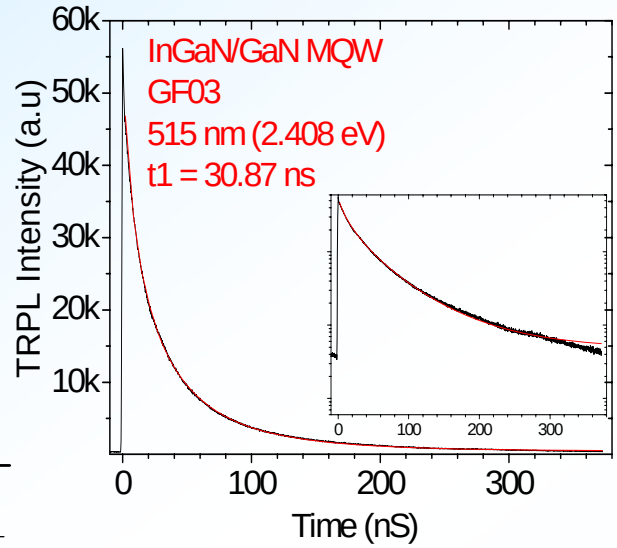

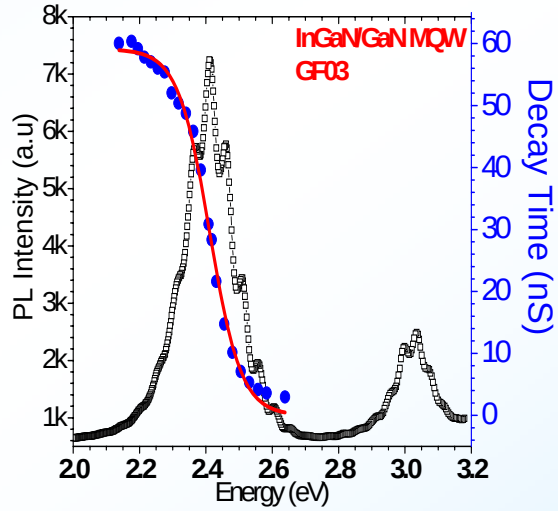

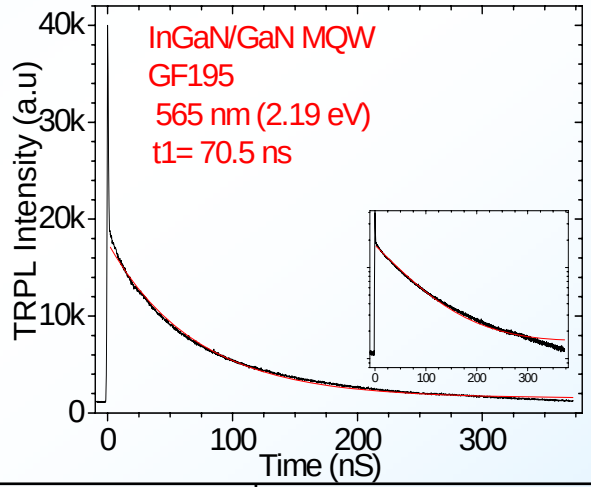

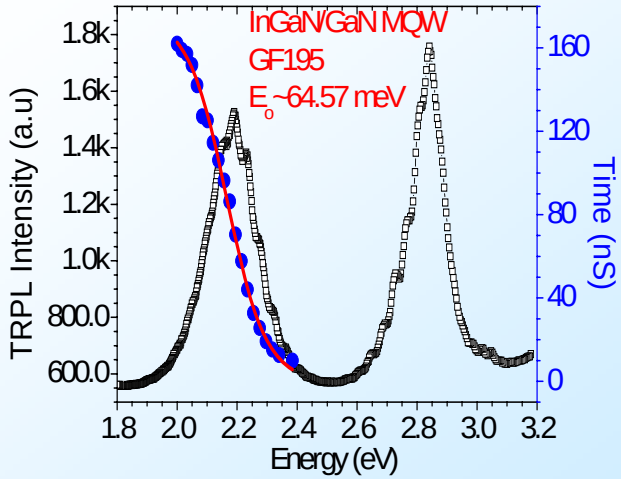

Sample	τ_{rad} (nS)	E_{me} (eV)	E_0 (meV)
GF03 Green Part	59.1	2.41	47.5 meV
GF195 Yellow Part	175.15	2.16	64.57 meV

Investigation of the light emission properties and carrier dynamics in dual-wavelength InGaN/GaN multiple-quantum well light emitting diodes

L. Liu, L. Wang, D. Li, N. Liu, X. Hu , Z.C. Feng, C.Y. Wu, H.L. Tsai, Y.C. Lee and J.R. Yang, ***J. Appl. Phys.*** in press (2012)

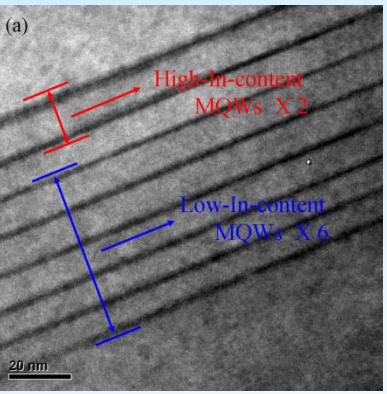

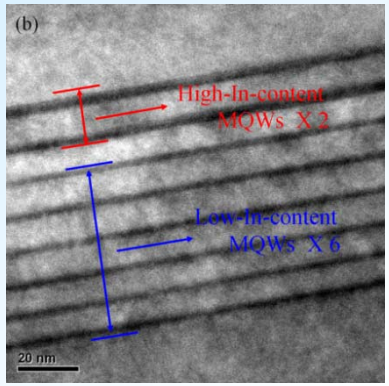

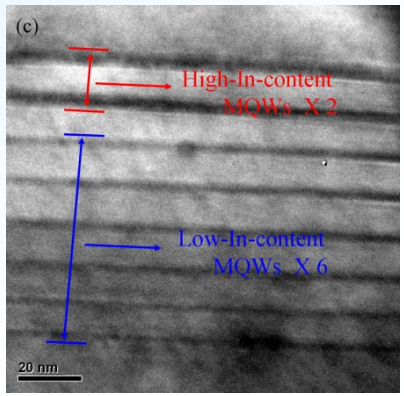

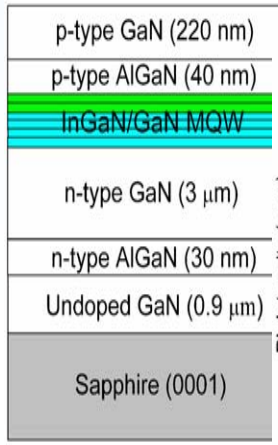

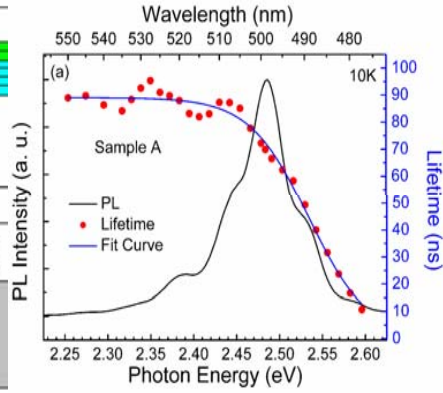

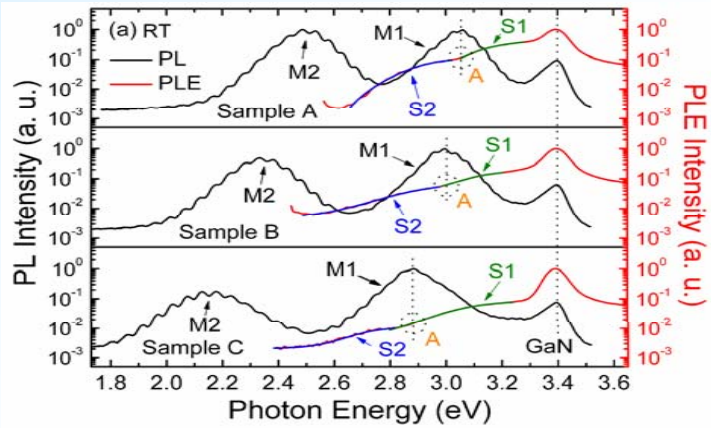

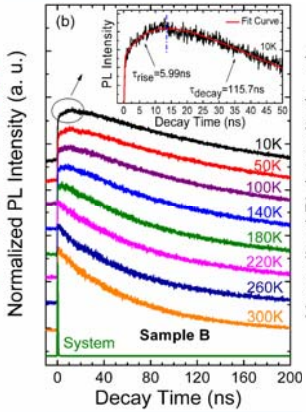

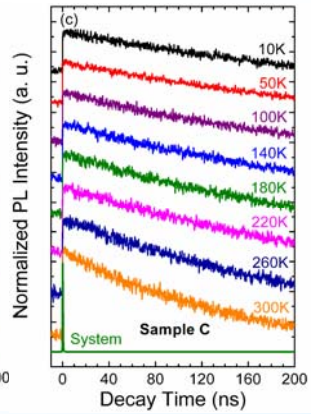

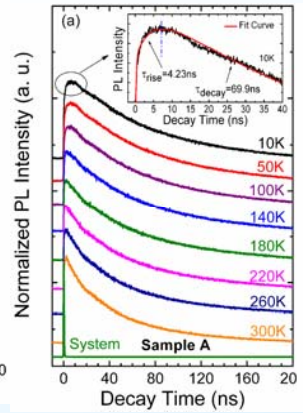

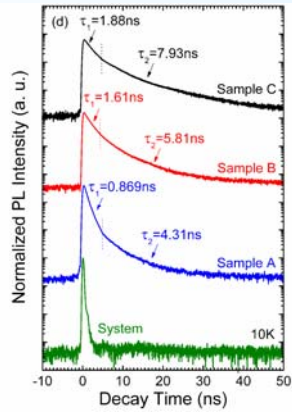

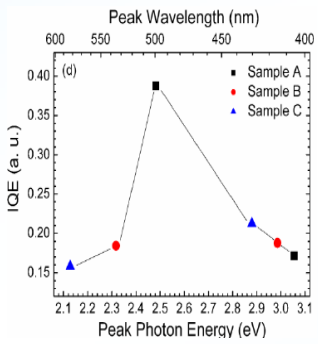

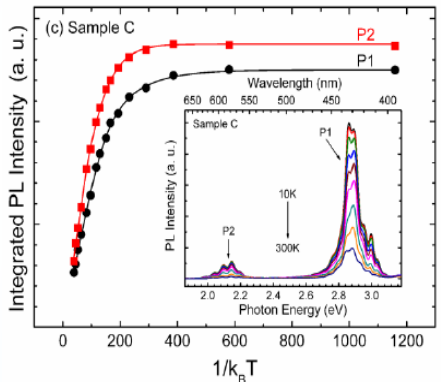

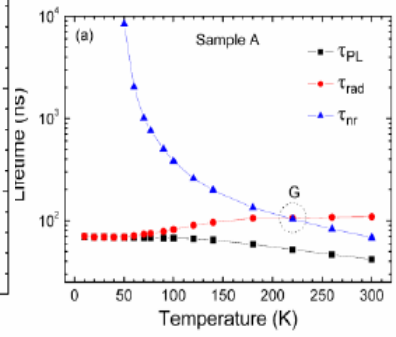

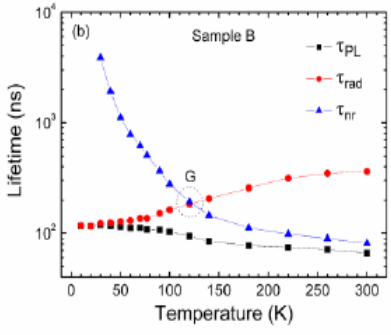

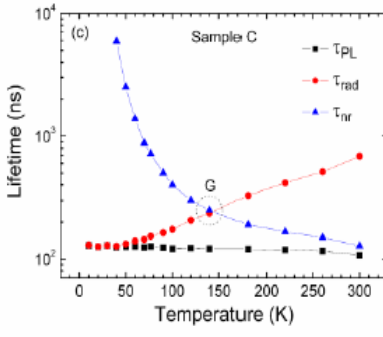

Shallow–Deep InGaN Multiple-Quantum-Well System for Dual-Wavelength Emission Grown on Semipolar (11-22) Facet GaN

L. Wang, Z. Lu, S. Liu, Z. C. Feng, *J. Elect. Materials* **40**, 1572-77 (2011)

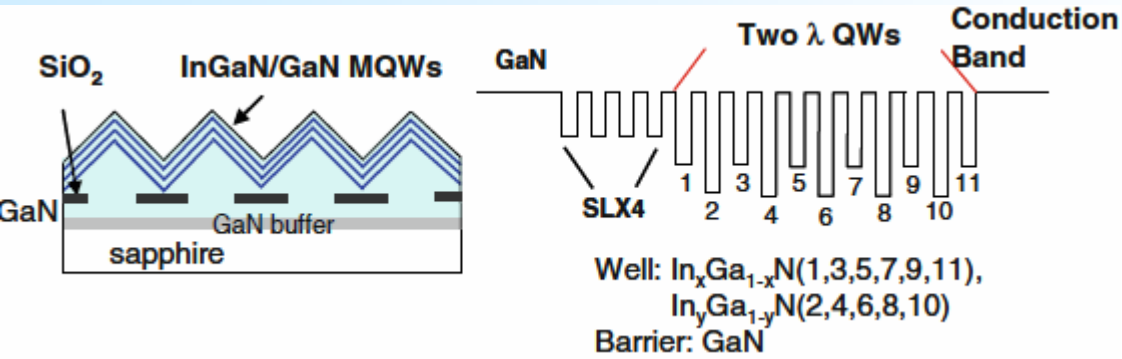

Fig. 1. Schematic of the shallow–deep InGaN multiple-quantum-well system grown on (11-22) facet GaN (a), and schematic energy band diagram of the shallow–deep InGaN quantum well system (b).

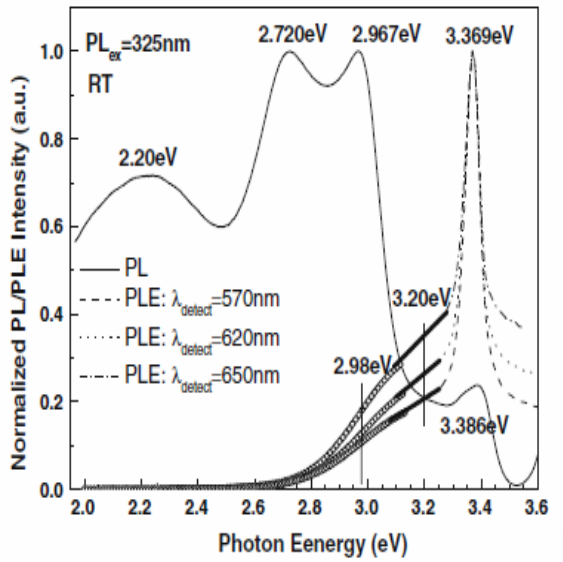

Fig. 3. Room-temperature PL and PLE spectra of the (11$\bar{2}$2) InGaN MQW system. The black solid line corresponds to the PL spectrum, and broken lines correspond to the PLE spectra.

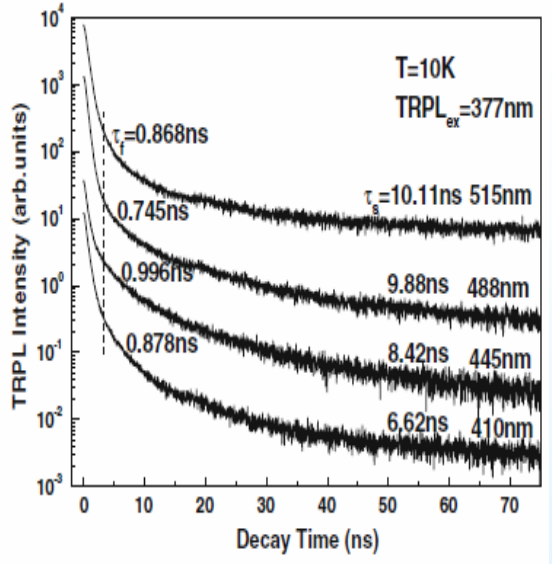

Fig. 4. Low-temperature time-resolved photoluminescence decay curves of the (11$\bar{2}$2) InGaN/GaN MQW system measured with detection wavelengths at 410 nm, 445 nm, 488 nm, and 515 nm.

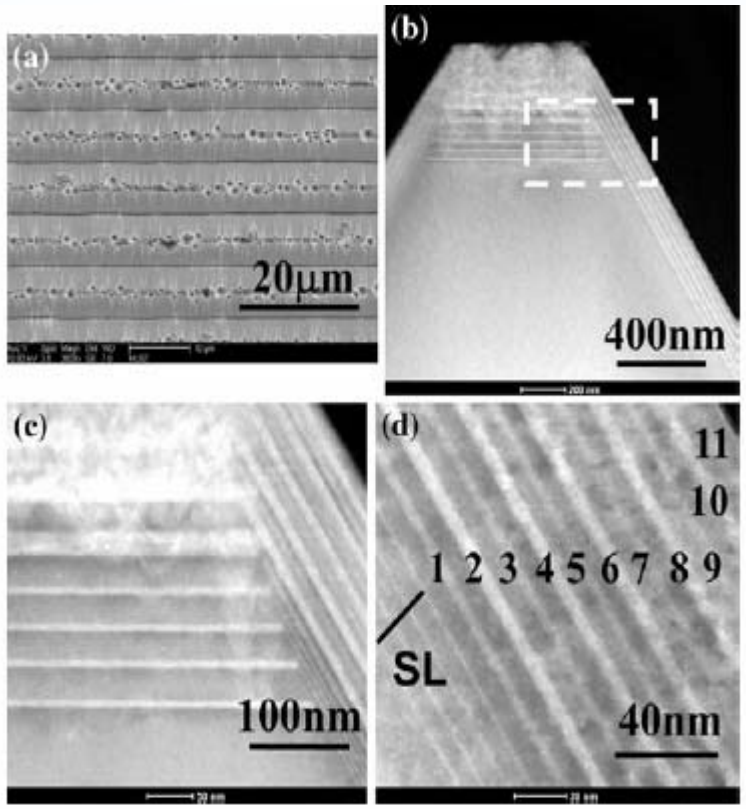

Fig. 2. (a) Plan-view SEM image of the shallow–deep InGaN multi-ple-quantum-well system grown on (11$\bar{2}$2) facet GaN, and (b–d) cross-sectional scanning transmission electron microscopy (XSTEM) images of the InGaN/GaN MQW system on the (11$\bar{2}$2) facet GaN taken in [1$\bar{1}$00] direction: (b) complete structure of the InGaN/GaN MQW system; (c) enlarged image of the box in (b), showing the MQW system on both the (11$\bar{2}$2) facet and the (0001) flat top facet; and (d) enlarged image of the box in (b), but only clearly showing the (11$\bar{2}$2) InGaN/GaN MQW system.

Important points

- **InGaN/GaN multiple quantum well light emitting diode (LED) structures are attractive and promising for the next generation high efficiency solid state lighting.**
- **Basic scientific research needed to fully understand the luminescence origins in this materials.**
- **Materials growth must be closely coupled to advanced characterization techniques to elucidate physical mechanism**
- **Experienced research team has been assembled which will guarantee the success of the proposed study**

Attractive Researches on III-Nitrides & Semiconductors in recent years

Wide Gap Semiconductor Laboratory
Professor Zhe-Chuan Feng
Graduate Institute of Photonics and Optoelectronics, National Taiwan University

UV-Visible PL Microscopy of Si:GaN/Sapphire

RT UV Photoluminescence

measured by an UV micro-PL system, excitation 325 nm

RT PL spectra of six MOCVD-grown GaN/sapphire with different SiH4 flows, i.e. different n-type or Si-doping levels.

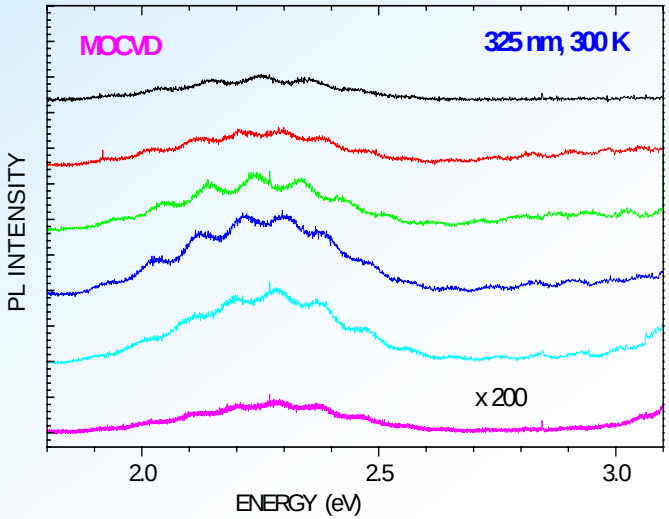

(defects emission , 1.8-3.1 eV)

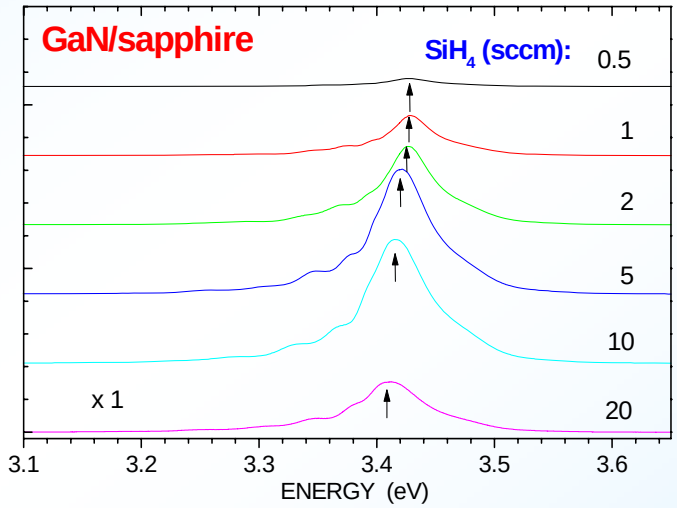

(near edge emission, 3.1-3.65 eV)

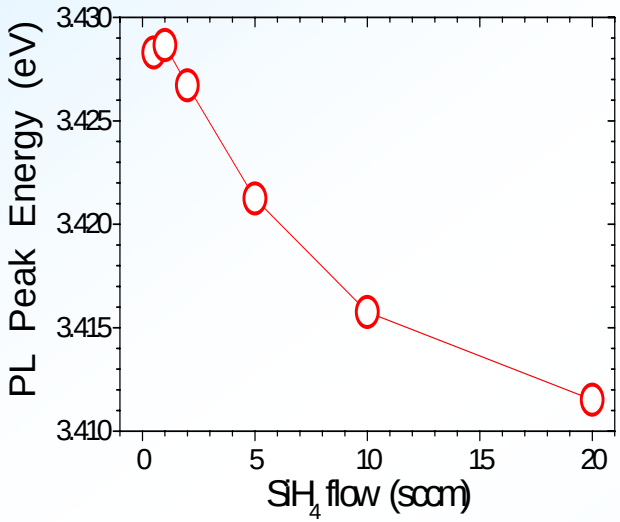

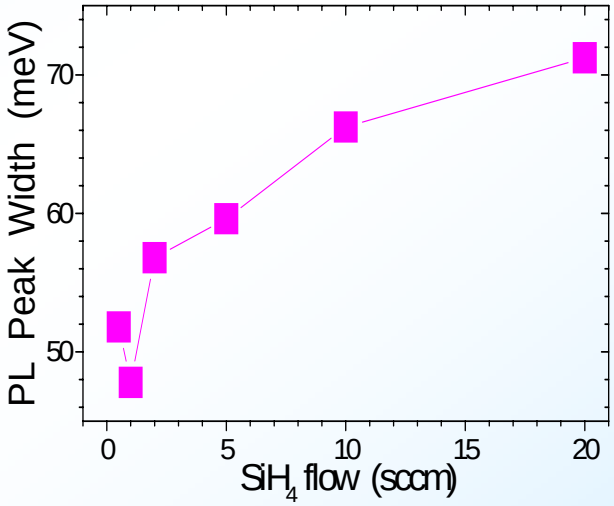

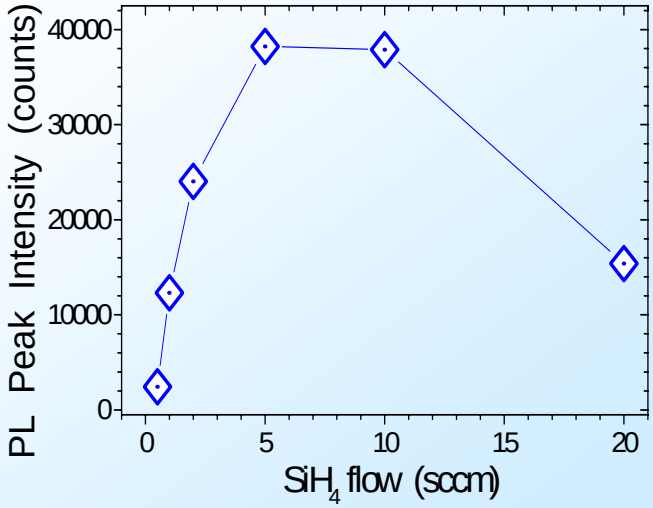

Numerical data displays of the dependences of RT PL peak energy, width and intensity on the SiH_4 flow rate from a series of MOCVD-grown n-GaN/Sapphire.

Raman measurements on Cross-section of GaN thin films

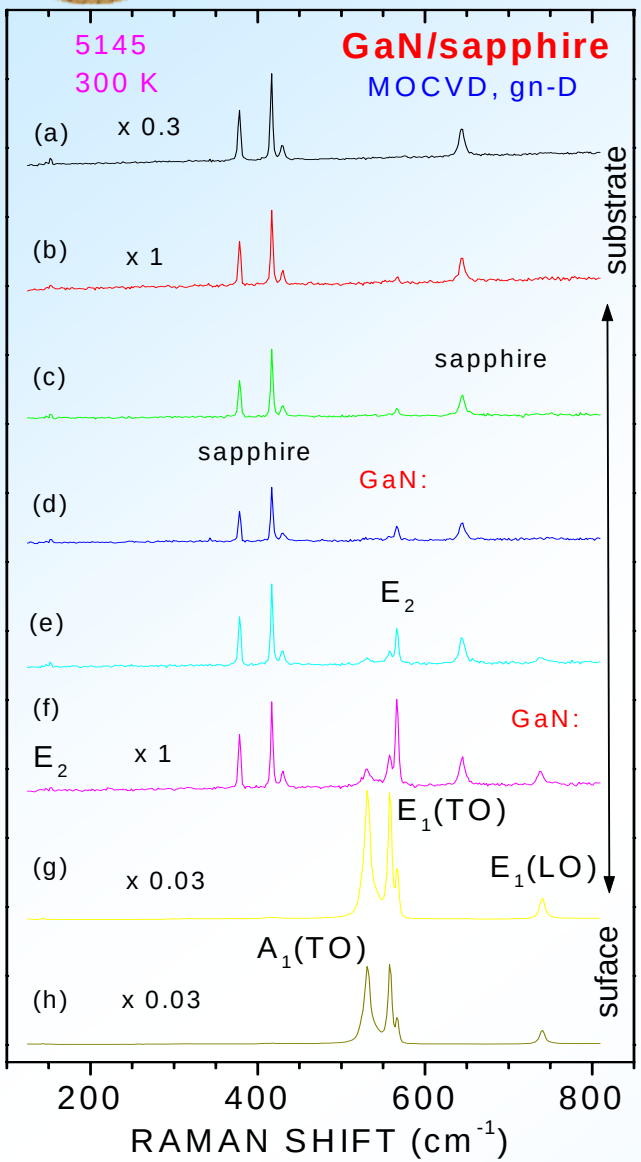

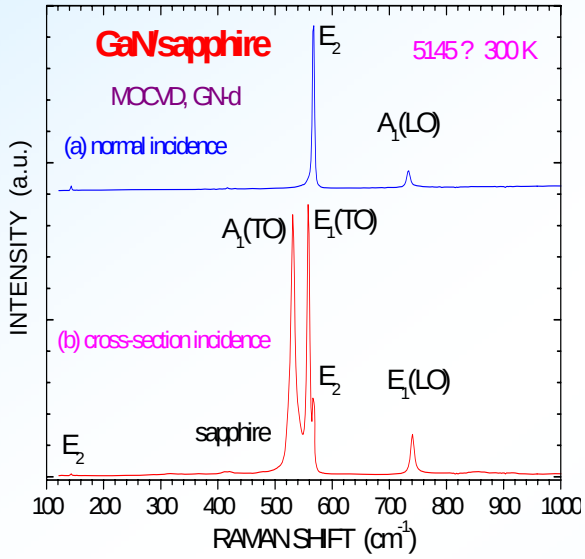

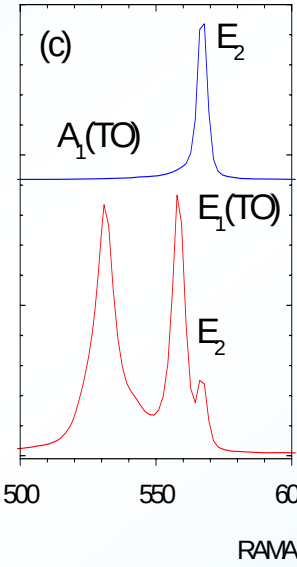

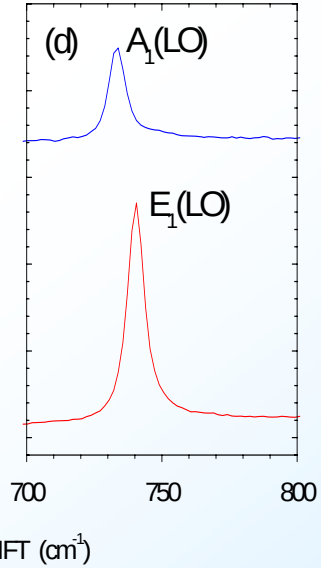

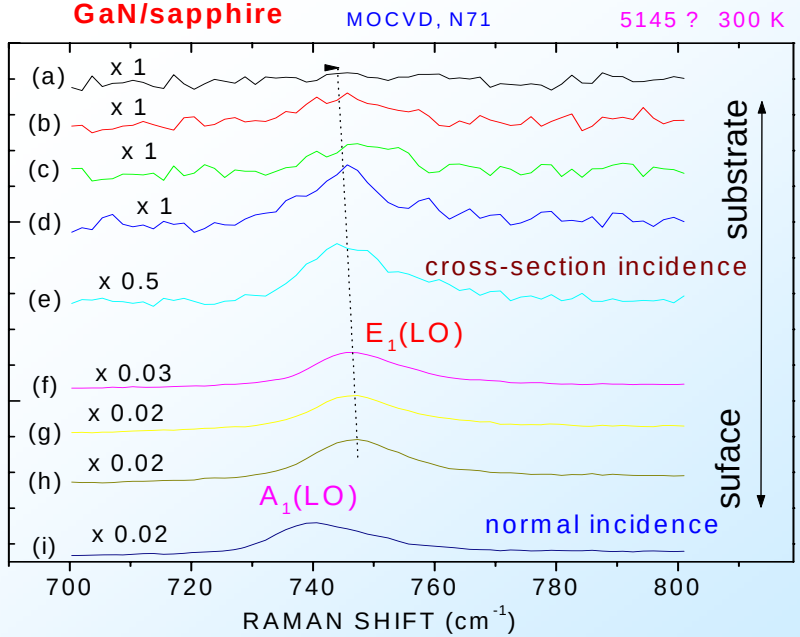

Anisotropic Properties of GaN Studied by Raman Scattering

Key notes

Study the phonon anisotropy using angular dependent Raman spectroscopy on MOCVD-GaN crystal, via polarized Raman scattering spectra from the cross-section of c-axis oriented GaN films as a function of the angle between the polarization direction of the incident laser with three different polarization configurations, in combination of theory and experiments.

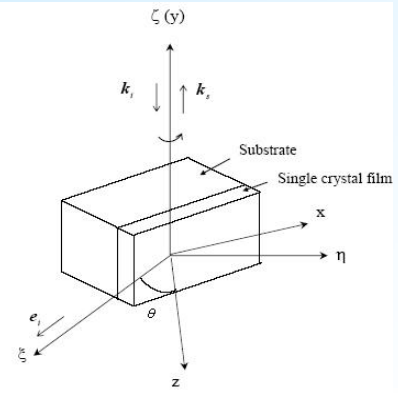

Fig.1 the two experimental coordinate systems. The ζ η ζ is the laboratory coordinate system while the xyz coincide with the crystal axes of the sample.

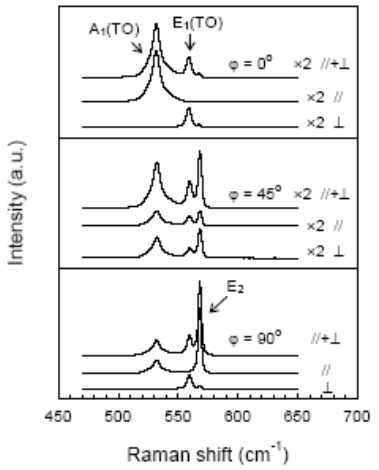

Fig.2 plots some typical spectra at several rotation angles. It is clearly seen that the Raman intensities of the three modes strongly depend on the rotation angle.

J. Appl. Phys. V.105, 036102 (2009).

Theory and Discussion

Raman intensity: $I_s \propto | e_i \cdot R \cdot e_s |^2$

Raman tensor:

$$A_1(\Gamma_1)=\begin{bmatrix} a & & \\ & a & \\ & & b \end{bmatrix} \quad E1(\text{planar})\ (\Gamma_5)=\begin{bmatrix} & & -d \\ & & d \\ -e & e & \end{bmatrix} \quad E_2(\Gamma_6)=\begin{bmatrix} f & f & \\ f & -f & \\ & & \end{bmatrix}$$

i. Perpendicular

$$I_{A1}^{\perp} \propto \left(\frac{a^2+b^2}{4}-\frac{|a||b|}{2}\cos(\phi_{a-b})\right)\sin^2 2\theta,$$

$$I_{E1}^{\perp} \propto e^2\cos^4\theta+d^2\sin^4\theta-\frac{|e||d|}{2}\sin^2 2\theta\cos\phi_{e-d}, \quad I_{E2}^{\perp} \propto \frac{1}{4}f^2\sin^2 2\theta$$

ii. Parallel

$$I_{A1}^{//} \propto a^2\sin^4\theta+b^2\cos^4\theta+\frac{|a||b|}{2}\sin^2 2\theta\cos(\phi_{a-b}),$$

$$I_{E1}^{//} \propto \left(\frac{e^2+d^2}{4}+\frac{|e||d|}{2}\cos(\phi_{e-d})\right)\sin^2 2\theta, \quad I_{E2}^{//} \propto f^2\sin^4\theta$$

iii. Unpolarized

$$I_{A1} \propto a^2\sin^2\theta+b^2\cos^2\theta, \quad I_{E1} \propto d^2\sin^2\theta+e^2\cos^2\theta,$$

$$I_{E2} \propto f^2\sin^2\theta$$

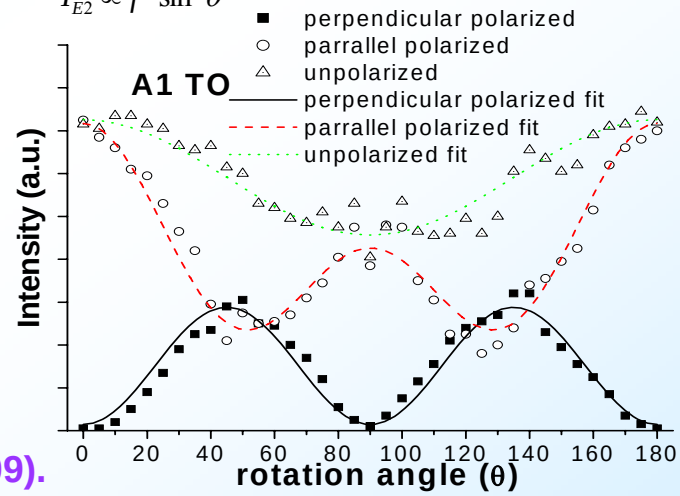

Fig.3 Raman Intensities of A1 (TO) : a sinusoidal tendency

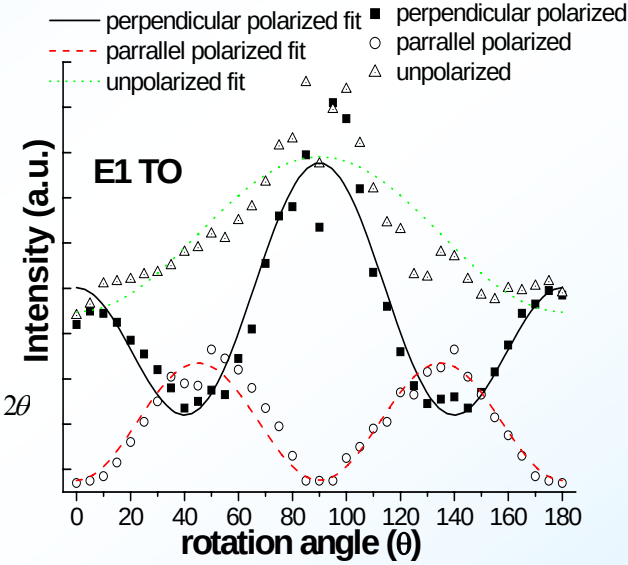

Fig.4 Raman Intensities of E1 (TO) mode with rotation angle, same as A1(TO).

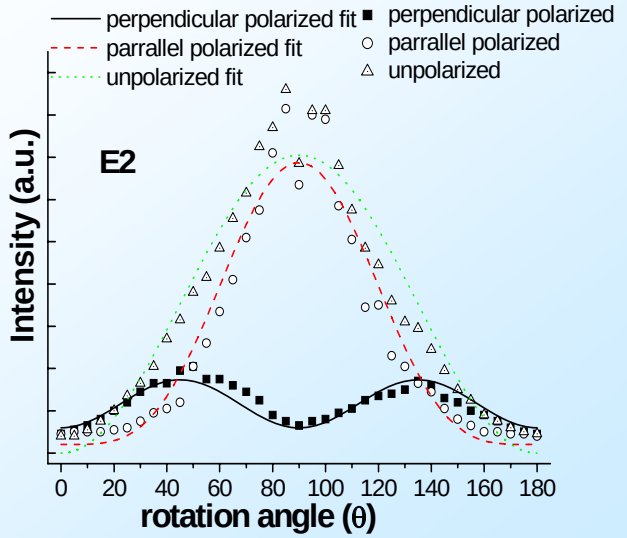

Fig.5 E2 Intensity with rotation angle, quite different to A1 and E1, because E2 mode has the same vibrating elements but the A1 and E1 have two types of the elements.

Polarized and diameter-dependent Raman scattering from individual AlN nanowires: the antenna and cavity effects

H.C. Hsu, G.M. Hsu, Y.S. Lai, Z.C. Feng, A. Lundskog, U. Forsberg, E. Janzén, K.H. Chen, L.C. Chen, ***J. Appl. Phys.***, in review.

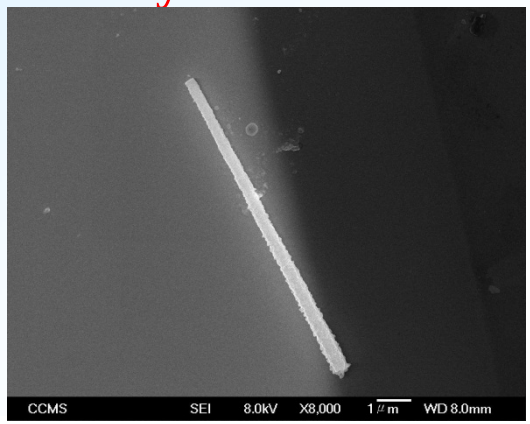

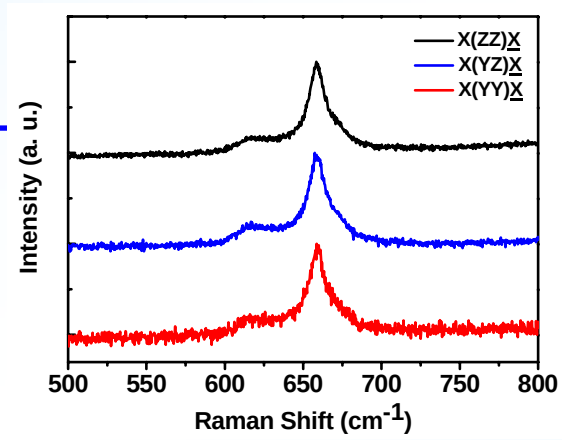

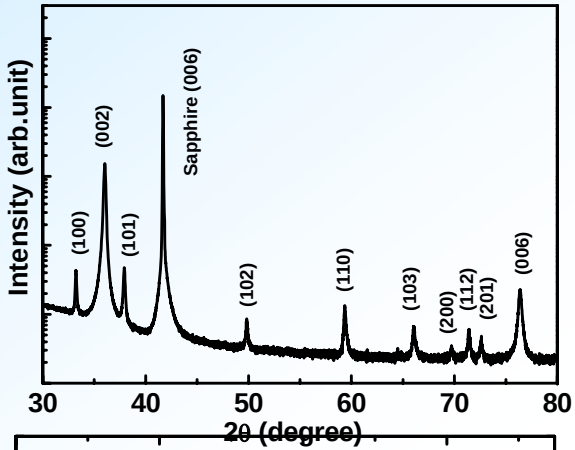

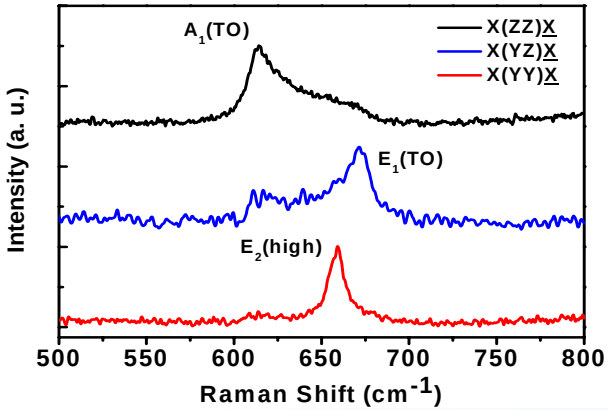

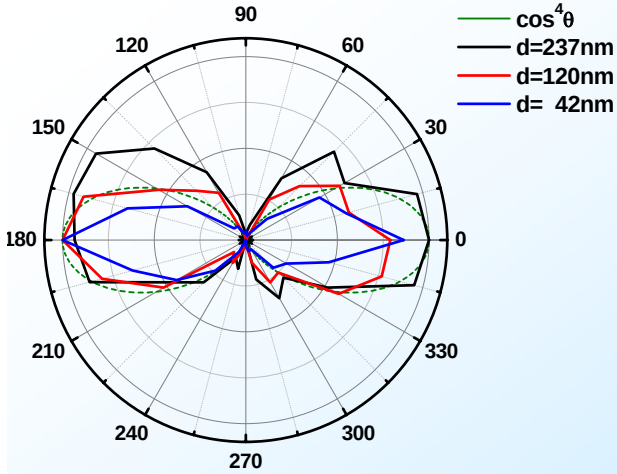

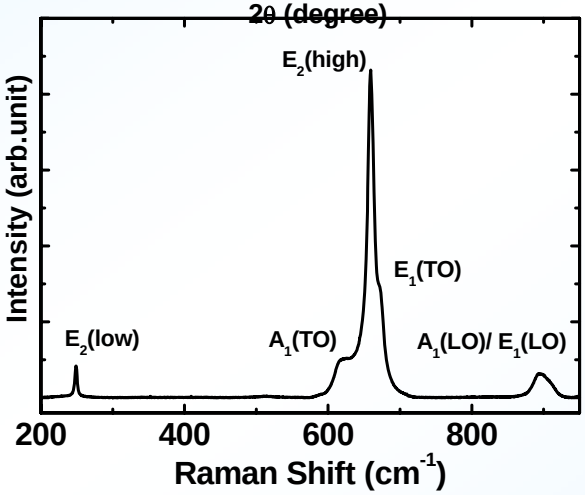

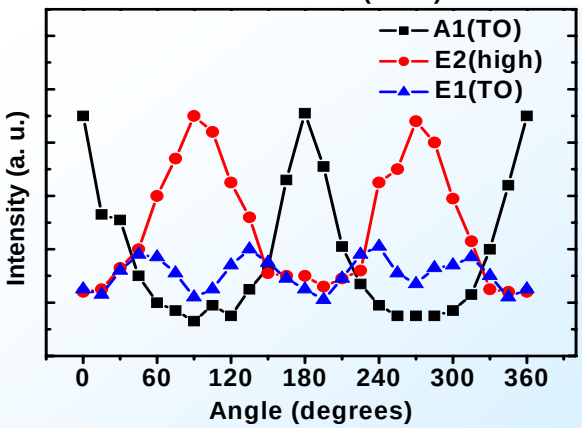

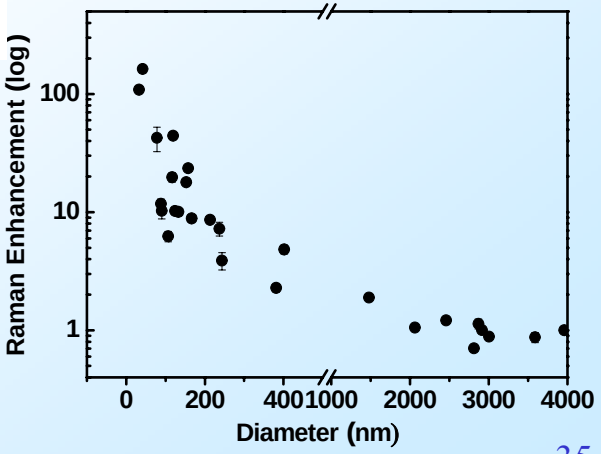

Polarized Raman scattering of a-axis single GaN nanowires

Key notes

CVD growth & Raman scattering on GaN nanowires: A1(TO), E1(TO), E2(high), and A1(LO). Phonon modes - strongest as electric vector is along the nanowire long axis but lowest ones as polarization of electric field is perpendicular to the nanowire, which is related to the quantum reflection interacting between light and nanostructures.

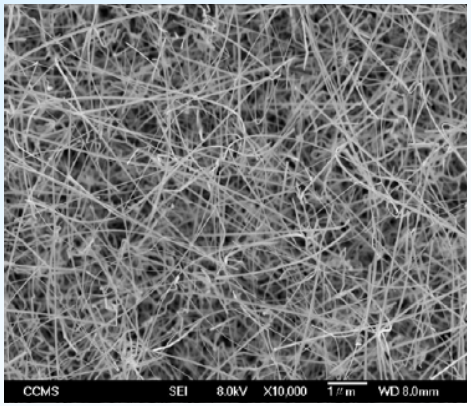

Fig. 1 The SEM image of ensemble GaN na

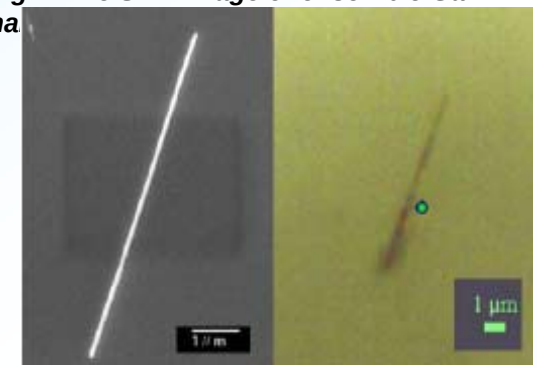

Fig. 2 SEM (left) and CCD camera (right) image of single GaN nanowire.

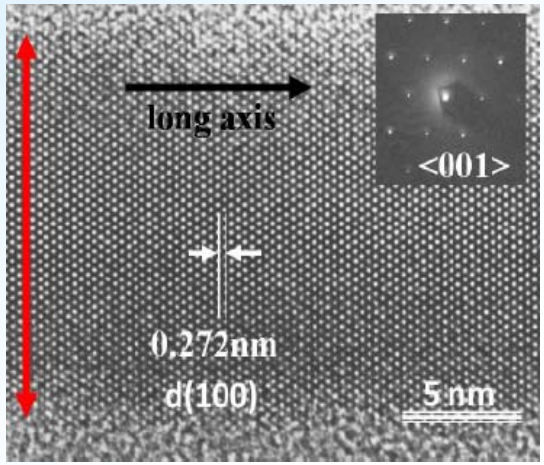

Fig.3 HR-TEM image of GaN nanowire (inset) The SAED pattern taken from [001] zone axis

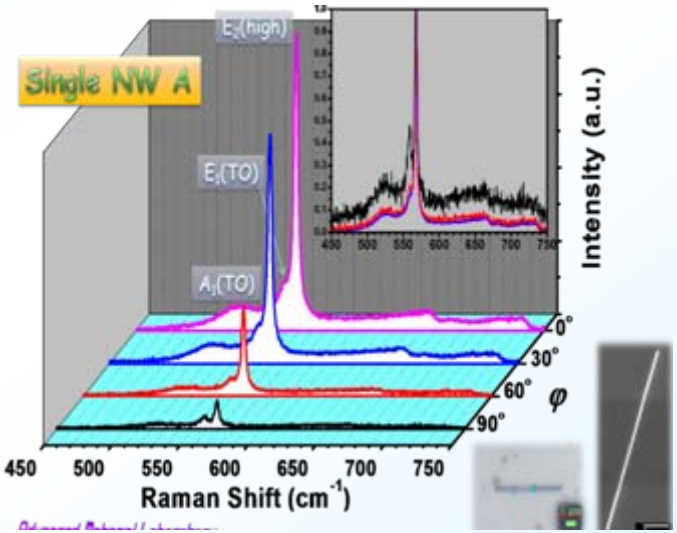

Fig. 4 Raman spectra of ensemble GaN nanowires

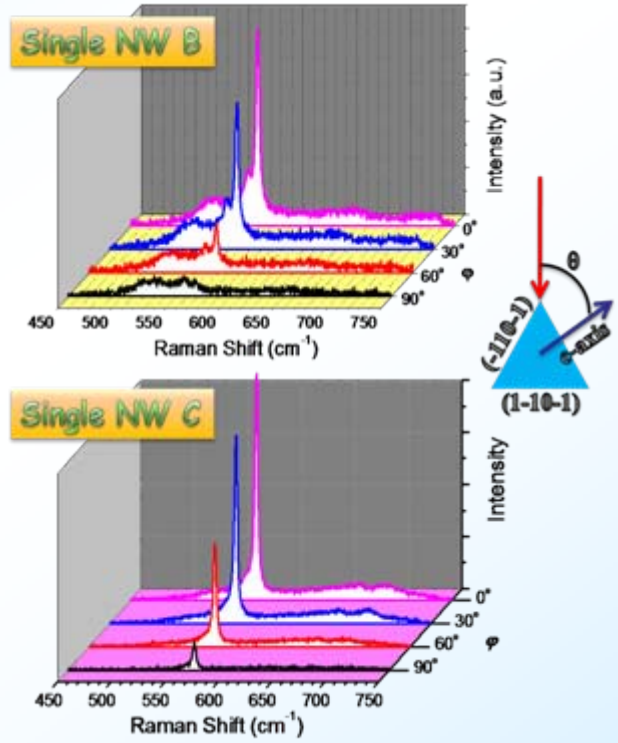

Fig.5 Raman spectra of other two nonowires.

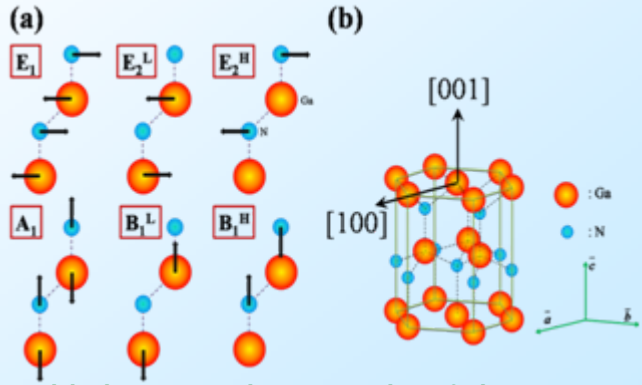

Fig. 6 (a) The geometric symmetries of phonon vibrations in hexagonal structure (b) The scheme of GaN unit cell.

{Reported at TW-MRS & IWN 2008}

Raman scattering and Rutherford backscattering studies on InN films grown by plasma-assisted molecular beam epitaxy

Yee Ling Chung, Xingyu Peng, Ying Chieh Liao, Shude Yao, Li Chyong Chen, Kuei Hsien Chen, Zhe Chuan Feng, *Thin Solid Films* **519**, 6778-82 (2011)

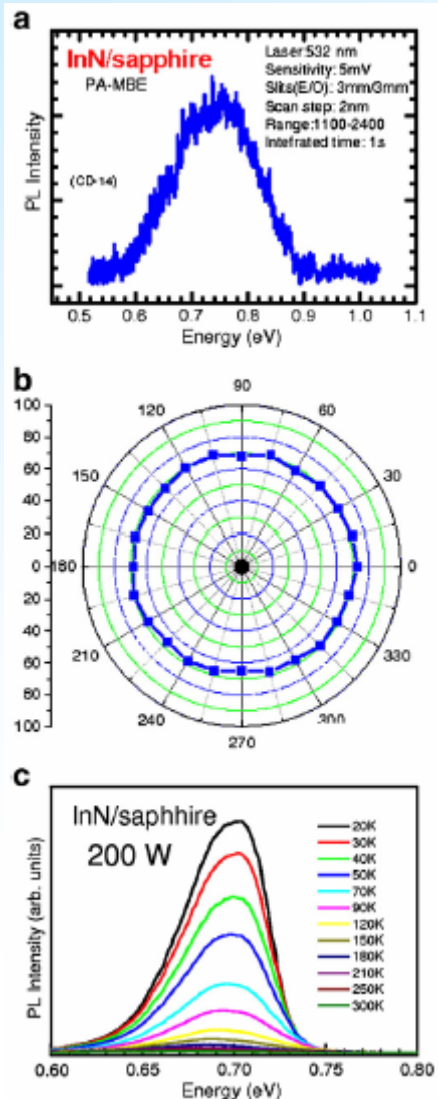

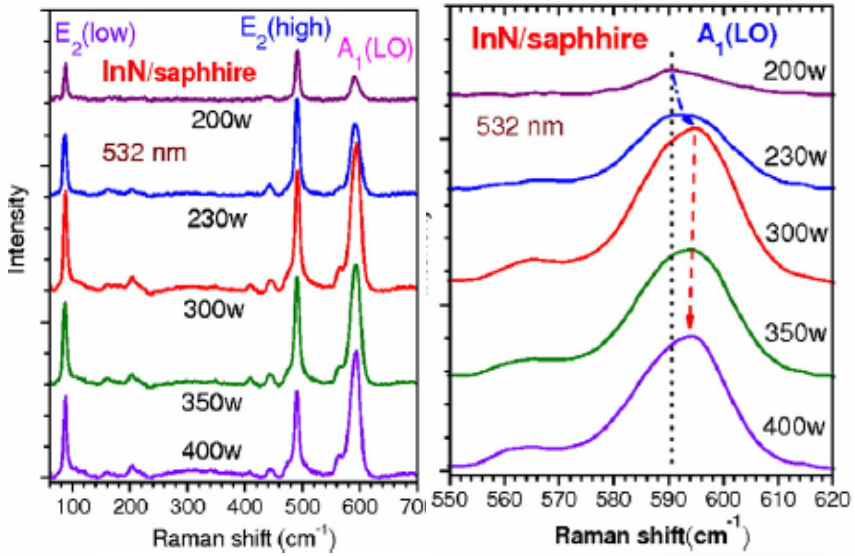

Fig. Raman spectra for A1 (LO) mode of InN films grown with plasma power at 200, 350 and 400 W.

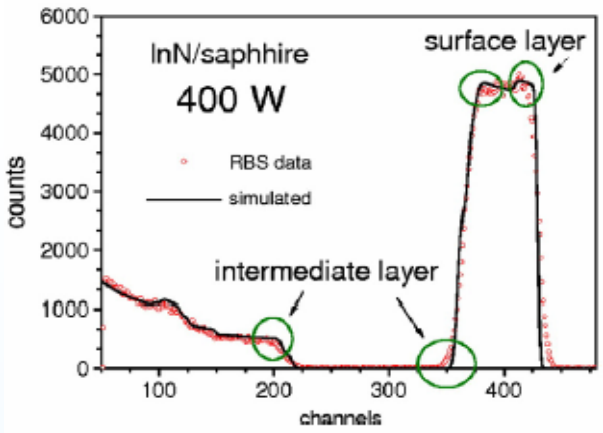

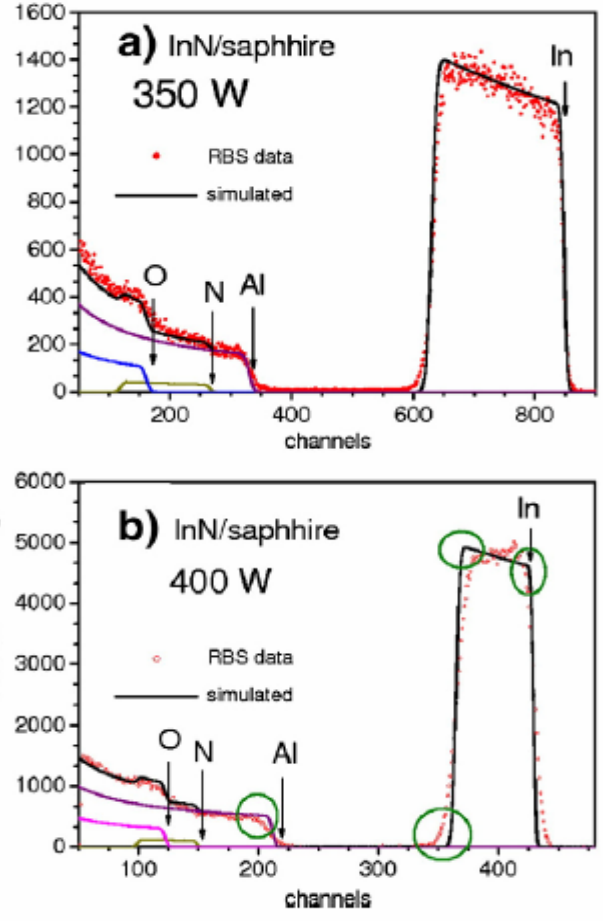

Fig. Random (circle) and simulated (solid line) RBS spectra of InN film with plasma power at (a) 350W and (b) 400 W.

m-plane (10-10) InN heteroepitaxied on (100)-γ-$LiAlO_2$ substrate: Growth orientation control and characterization of structural/optical anisotropy,

C.L. Hsiao, J.T. Chen, H.C. Hsu, Y.C. Liao, P.H. Tseng, Y.T. Chen, *Z.C. Feng*, L.W. T
M.M.C. Chou, L.C. Chen & Kuei-Hsien Chen, J. Appl. Phys. **107**, 073502 (2010).

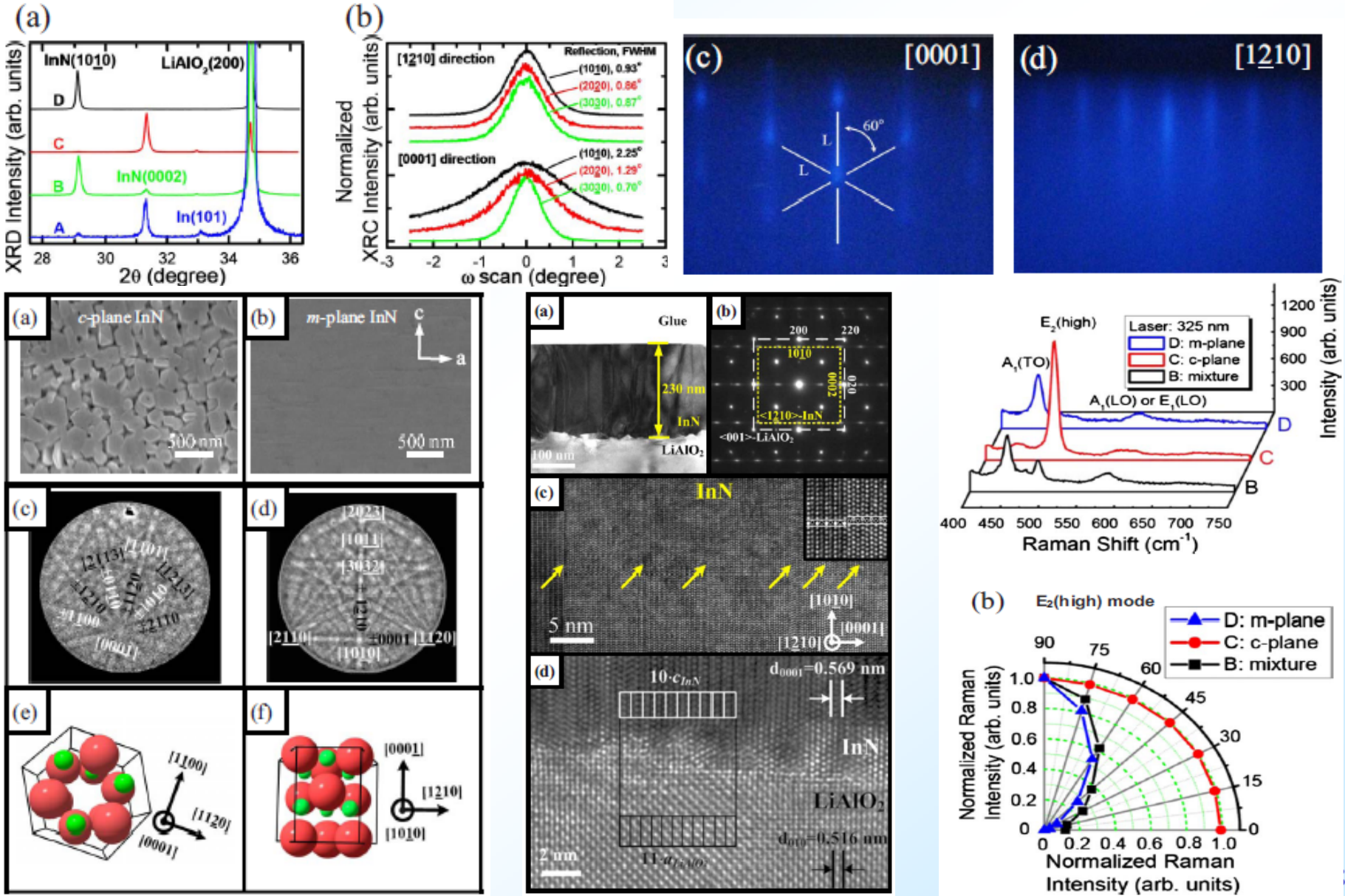

Temperature dependence of Raman scattering in m-plane GaN with different Ⅲ/Ⅴ ratios

Cheng Chen, Xiang Ping Shu, Hua Yang Sun, Zhi Ren Qiu, Ting-Wei Liang, Li-Wei Tu, and Zhe Chuan Feng,
Advanced Materials Research, in press. ***{EI}***

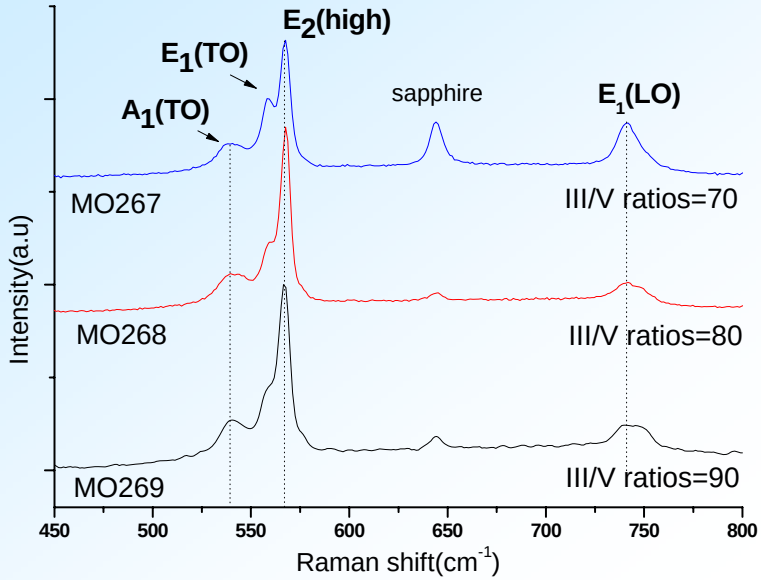

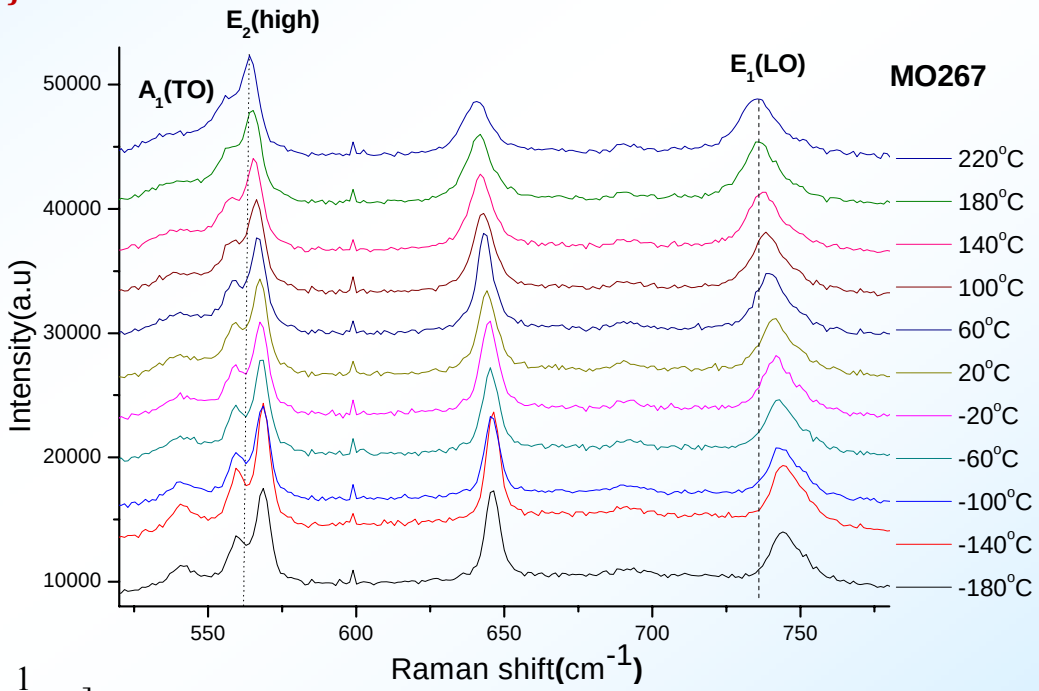

$$\omega(T) = \omega_0 + \omega^{(1)}(T) + \omega^{(2)}(T)$$

$$= \omega_0 \exp\left[-3\gamma \int_0^T \alpha(T')dt\right] + M_1[1 + \frac{1}{e^x - 1}] + M_2[1 + \frac{1}{e^y - 1} + \frac{1}{(e^y - 1)^2}]$$

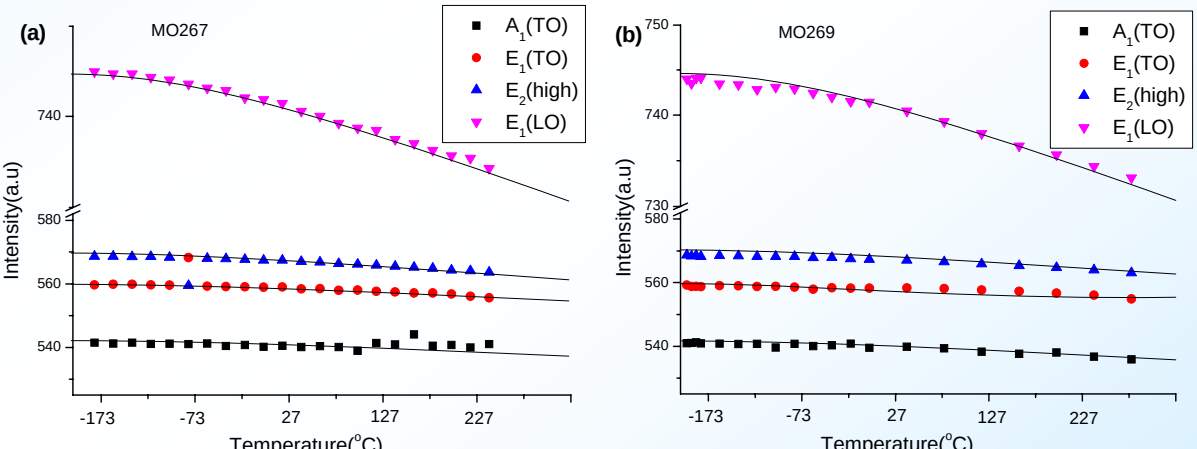

Th phenomenon should due to anharmonic coupling to phonons of other branches, or the heating of crystal, which cause volume expansion or lattice dilation. At last, the trend of Raman modes redshift was calculated by an equation combine three phonon process and four phonon process. The value of M1 and M2 reveals the three-phonon processes are dominant in the redshift of E1(LO) and E2(high).

Anomalous luminescence behavior in the InAlGaN thin film

Sheng-Yao Hu, Yueh-Chien Lee, Zhe-Chuan Feng, Shi-Hong Yang,

Journal of Alloys and Compounds **509**, 2300–2303 (2011)

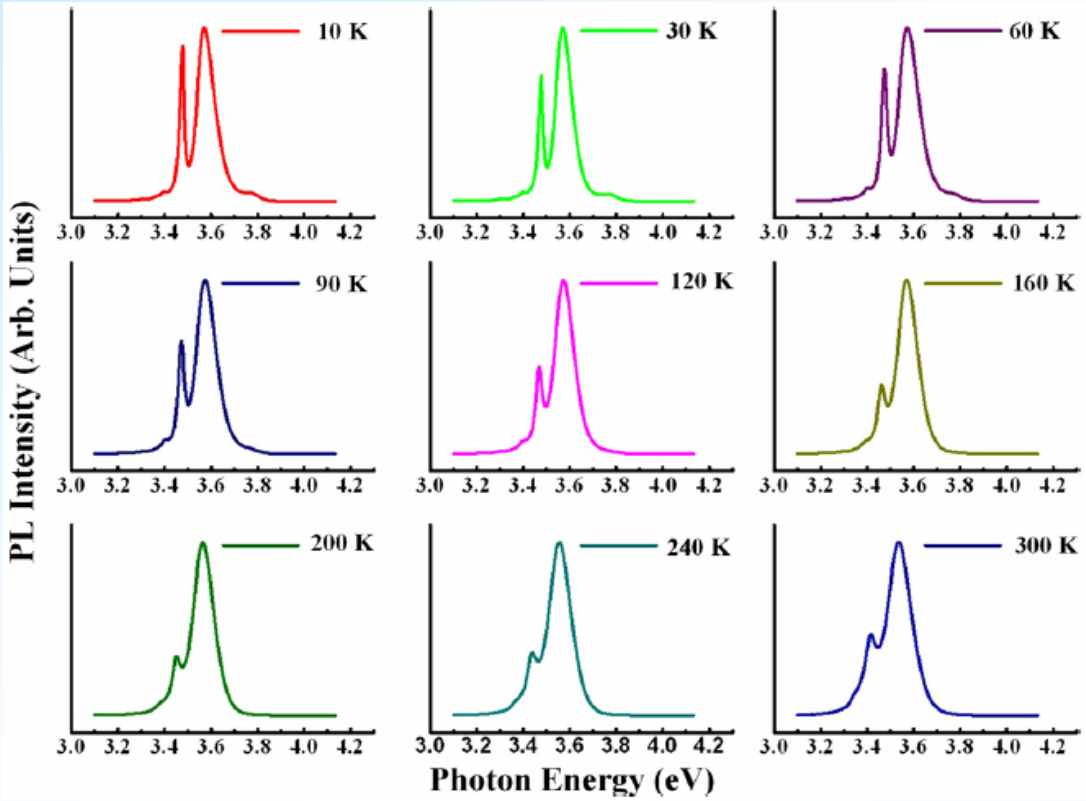

Fig. 1. PL spectra from the In0.014Al0.105Ga0.881N and the GaN substrate revealing the significant emissions at several different temperatures in the range of 10–300 K..

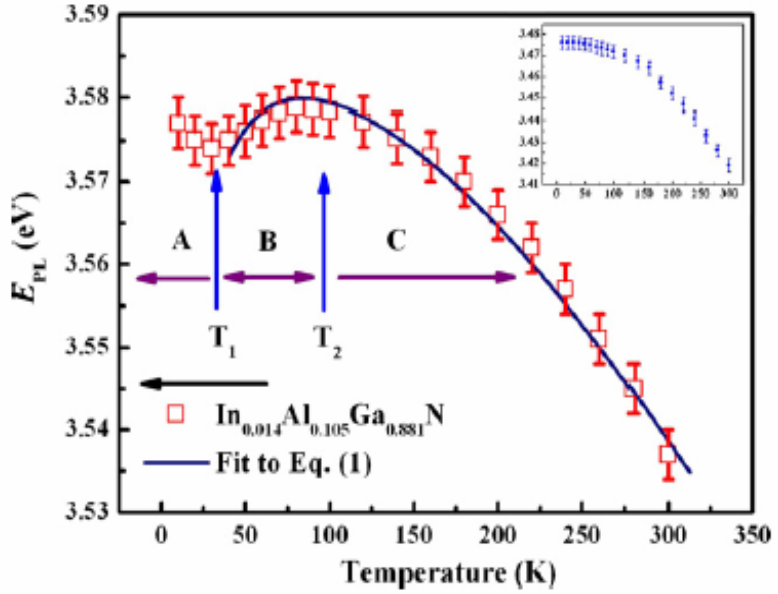

Fig. 2. The PL peak energy as a function of temperature for In0.014Al0.105Ga0.881N.

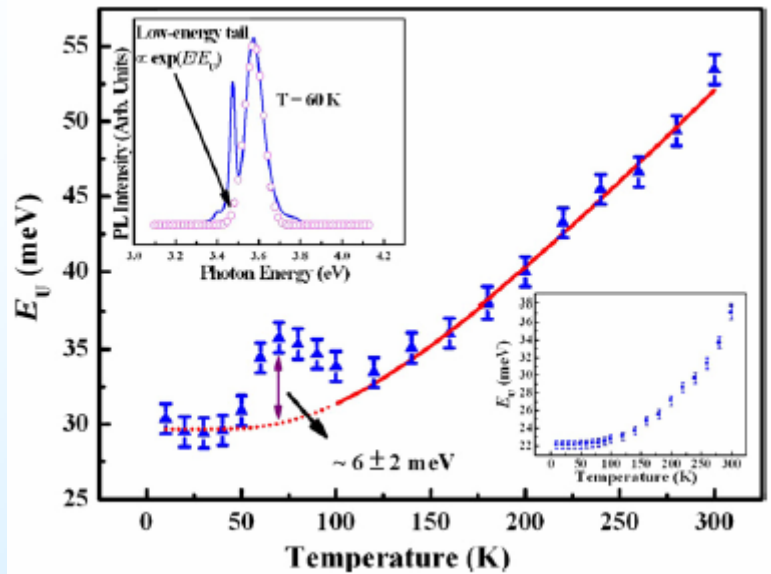

Fig. 3. Variation of Urbach energy (EU) against temperature for In0.014Al0.105Ga0.881N.

Journal of Luminescence 132 (2012) 1037–1040

Contents lists available at SciVerse ScienceDirect

Journal of Luminescence

journal homepage: www.elsevier.com/locate/jlumin

Investigation of defect-related optical properties in $Al_xIn_yGa_{1-x-y}N$ quaternary alloys with different Al/In ratios

S.Y. Hu [a,*], Y.C. Lee [b], Z.C. Feng [c], S.H. Yang [d]

Fig. 1 XRD spectra of three AlInGaN films.

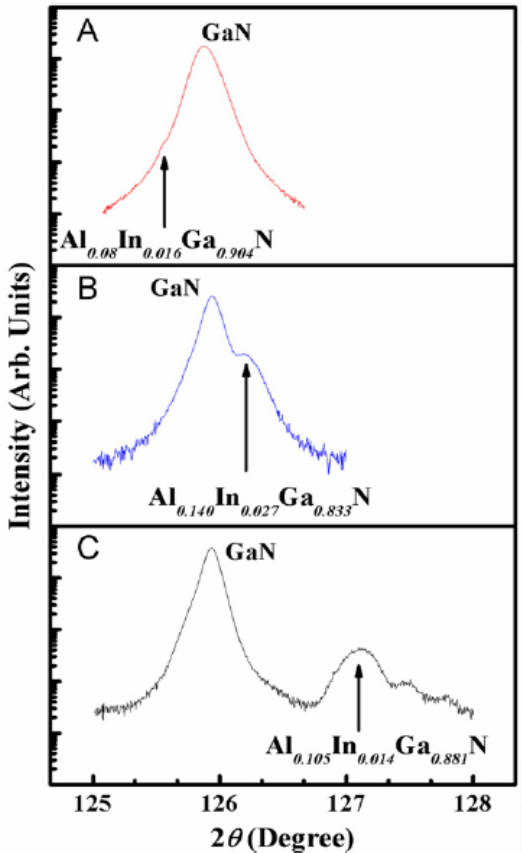

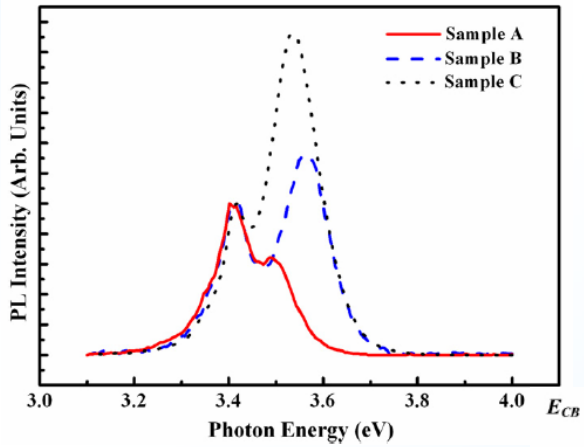

Fig. 2 PL spectra of three AlInGaN.

Fig. 3 PC spectra of three AlInGaN films.

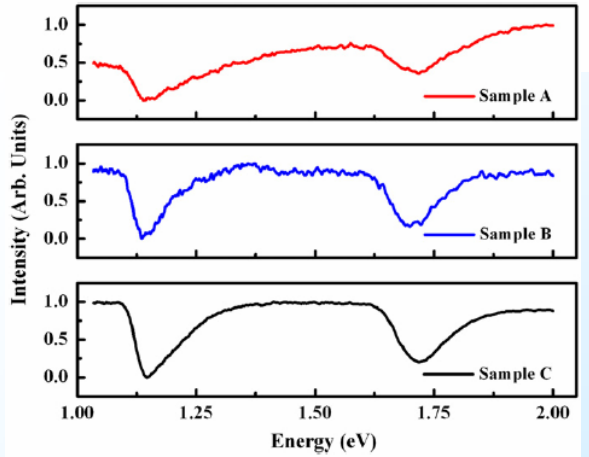

Fig. 4 defect levels of AlInGaN.

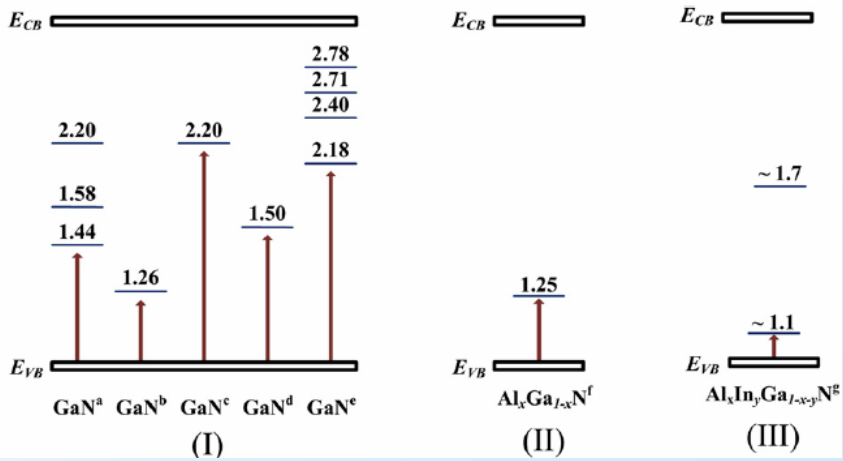

GaN:Gd - Sample Structure/RT PL

Priority Order	Sample #	Elemnt Doping	Concentration (theoretical)	Thickness (μ m)	Co-dopant
Gadolinium samples					
1	2816gdn	Gd	12%	0.5	Si:e17
2	2813gdn	Gd	12%	0.5	Si:e16
3	2819gdp	Gd	12%	0.5	Mg:e17
4	2798gd	Gd	12%	0.5	-
5	2796gd	Gd	2%	0.5	-

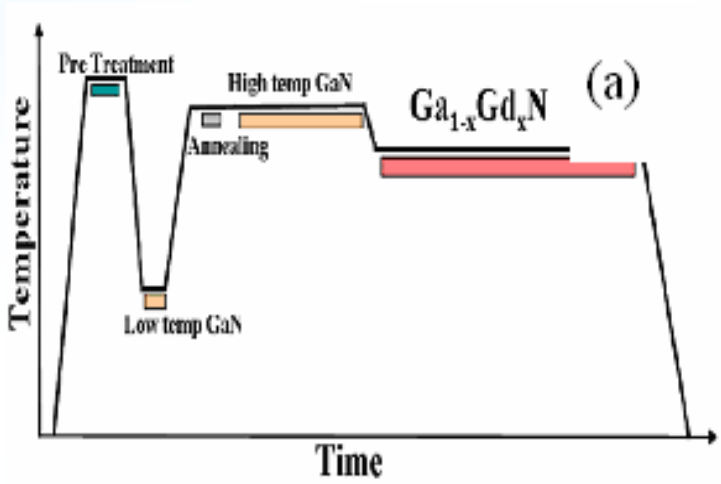

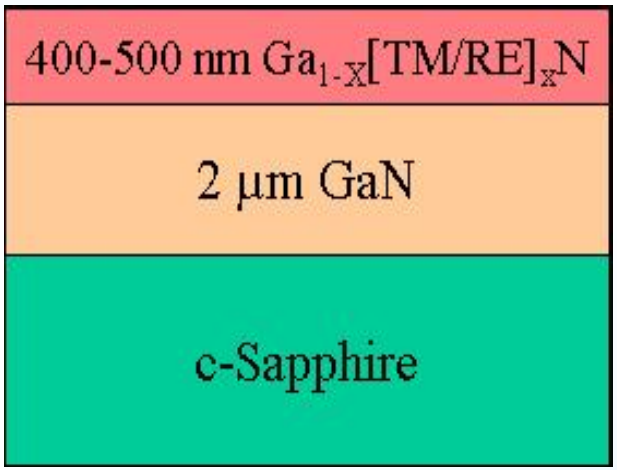

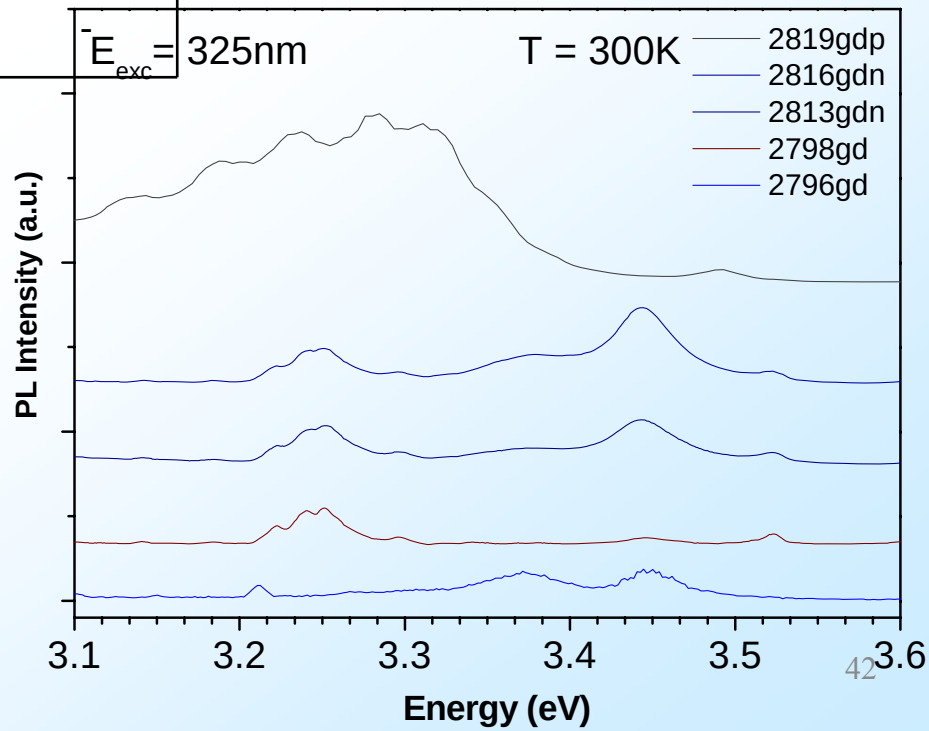

GaGdN: Temperature-dependent PL (i)

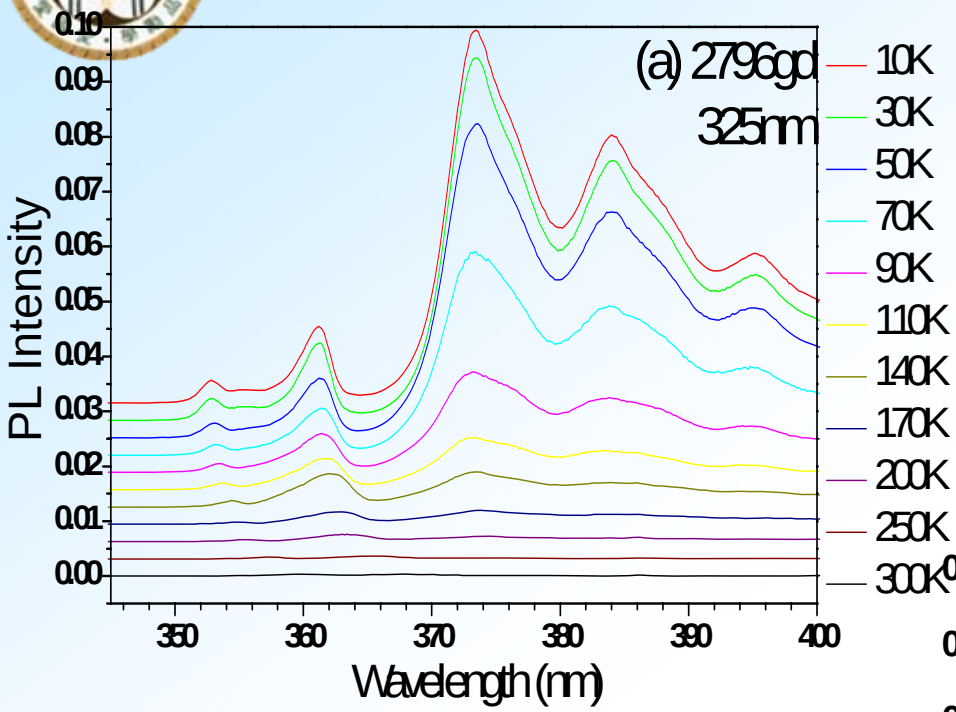

PL spectra of GaGdN thin films: sample 2796gd and 2798gd, in the temperature range from 10 to 300 K.

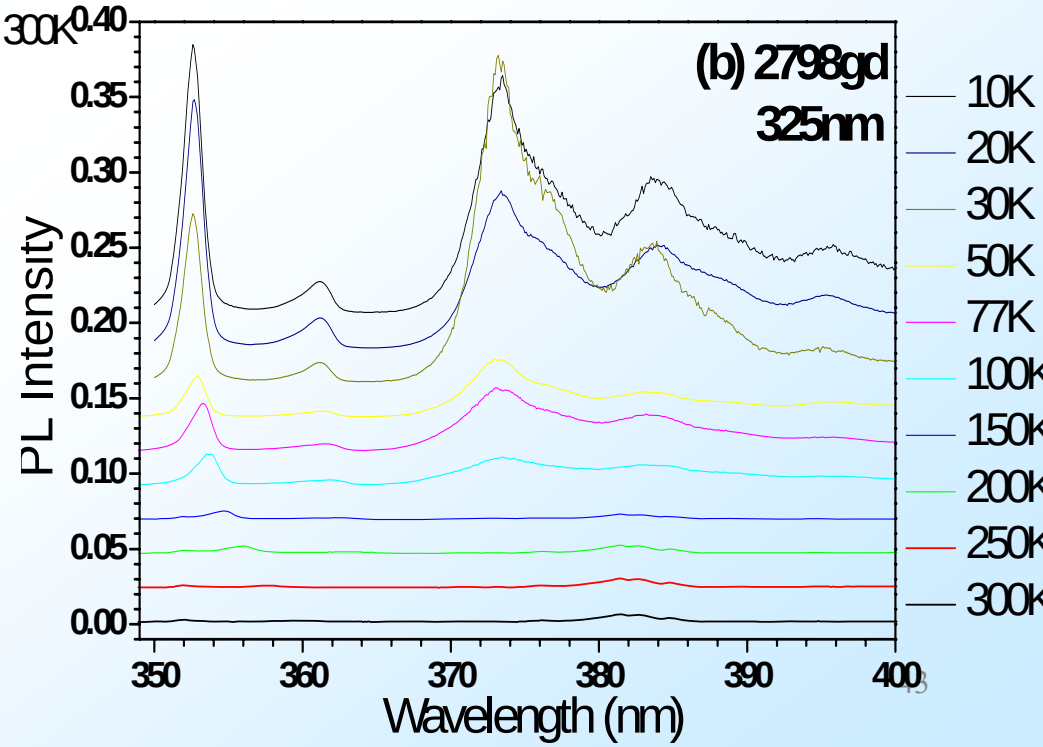

GaGdN: Temperature-dependent PL (ii)

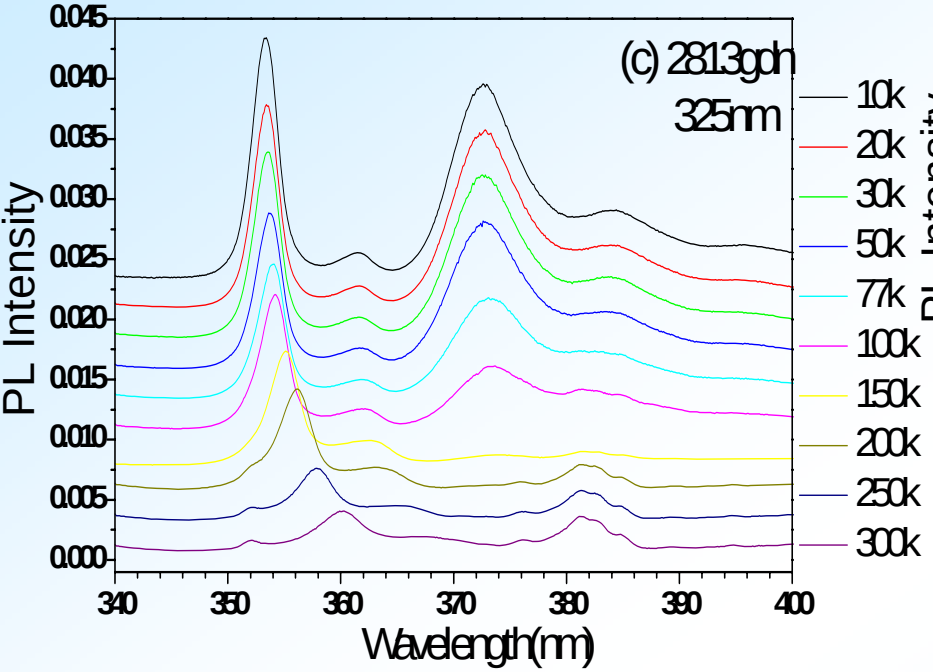

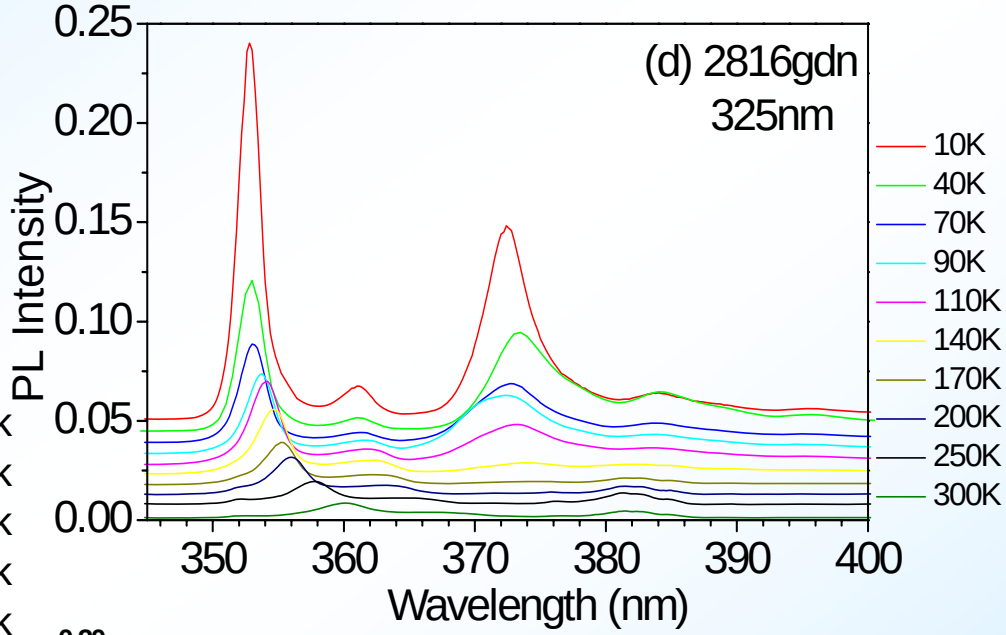

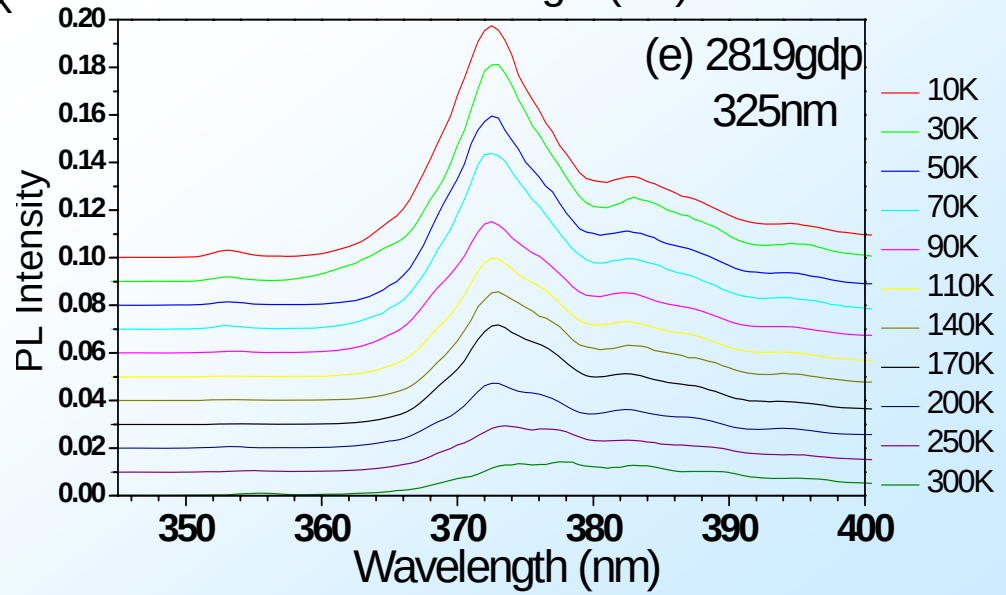

PL spectra of GaGdN thin films: sample 2813gd, 2816gdn and 2819gdp, 10 - 300 K.

GaGdN or GaCrN/sapphire: T-PL (iii)

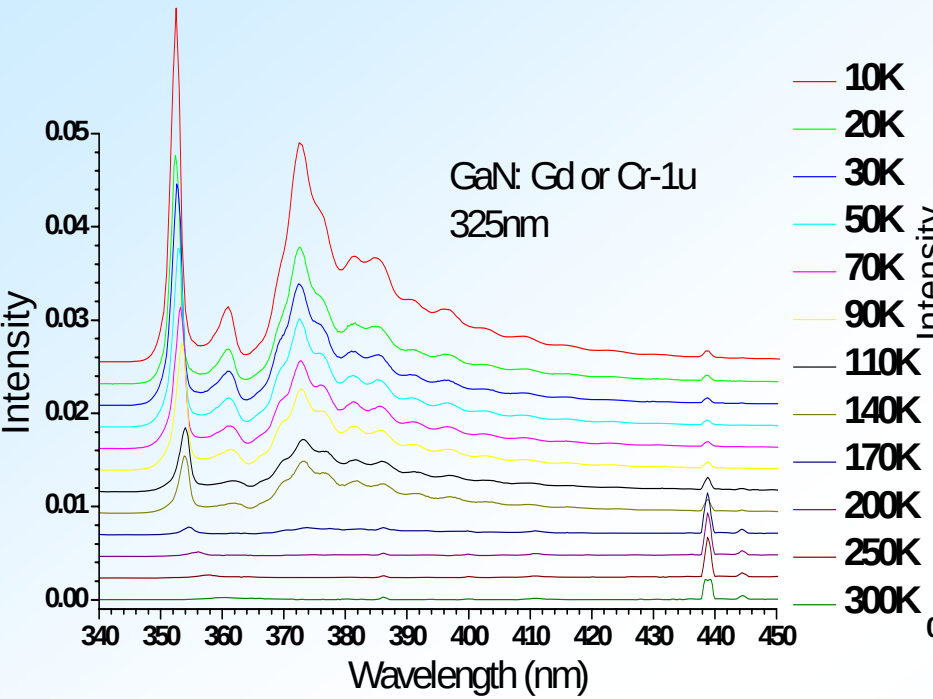

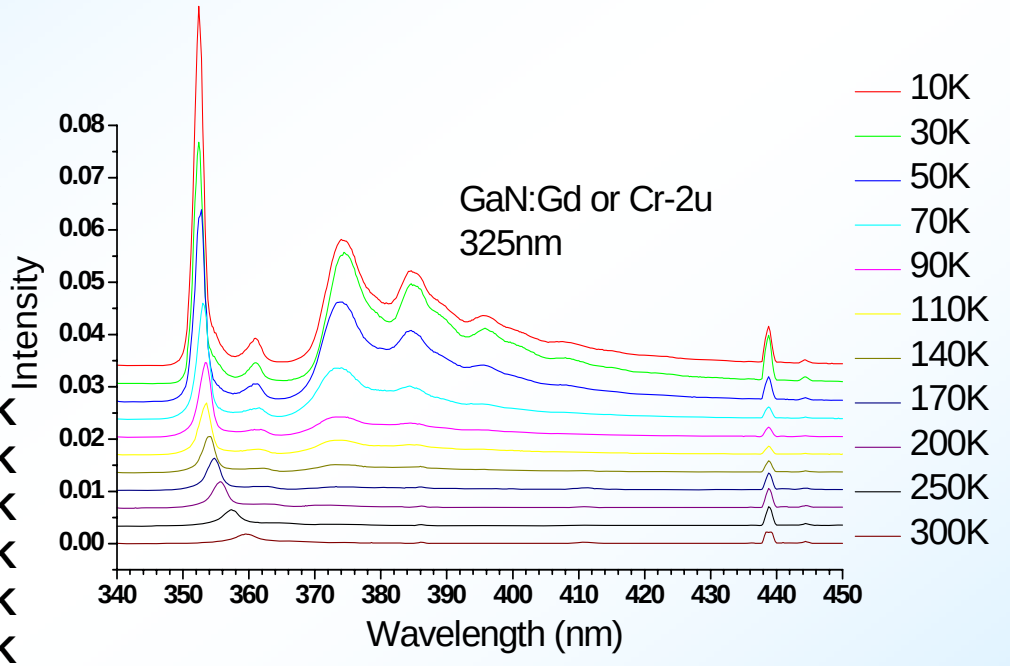

PL spectra of GaN:Gd or Cr-1u, -2u and -3u thin films, 10 - 300 K.

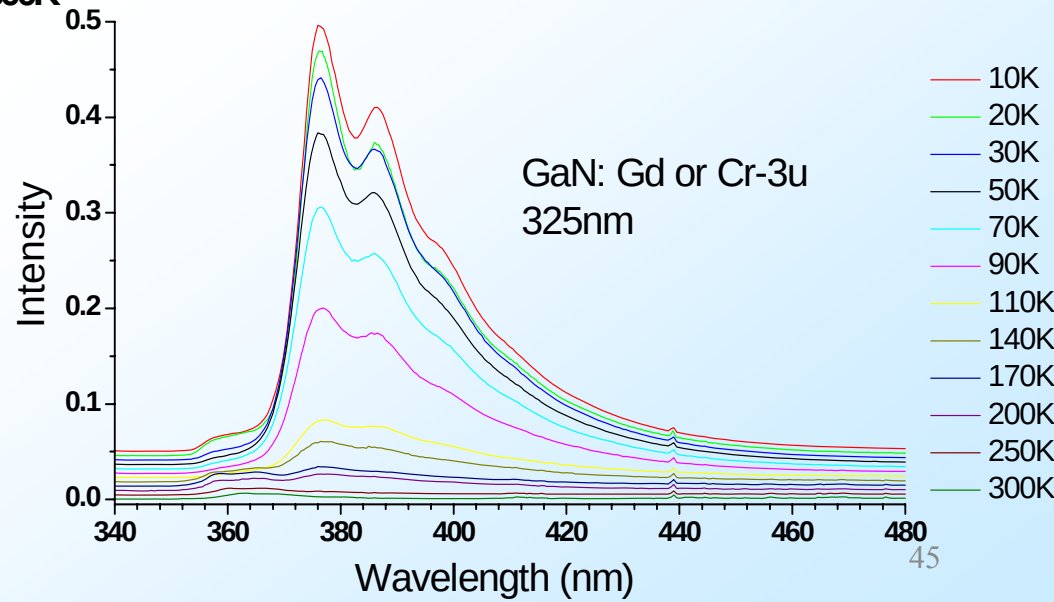

JOURNAL OF APPLIED PHYSICS 106, 1 (2009)

Temperature dependent and time-resolved photoluminescence studies of InAs self-assembled quantum dots with InGaAs strain reducing layer structure

Lingmin Kong,[1] Zhe Chuan Feng,[2,a)] Zhengyun Wu,[3] and Weijie Lu[4]
[1]*Department of Physics, Zhejiang Ocean University, Zhoushan 316000, China*
[2]*Department of Electrical Engineering, and Institute of Photonics and Optoelectronics, National Taiwan University, Taipei 106-17, Taiwan, Republic of China*
[3]*Department of Physics, Xiamen University, Xiamen 361005, China*
[4]*Department of Chemistry, Fisk University, Nashville, Tennessee 37208, USA*

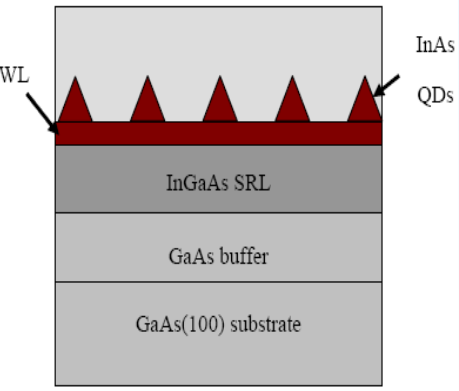

FIG. 1. Cross-section schematic of InAs QDs embedded in GaAs matrix with an InGaAs SRL.

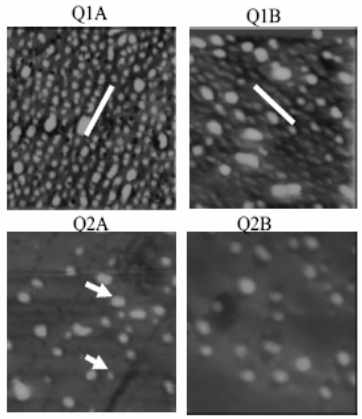

FIG. 2. AFM images of 4-InAs/GaAs QDs, all with measured area of 1x1 μm².

FIG. 8. Time-resolved spectra of InAs/GaAs QDs sample Q1A at 16 K. →

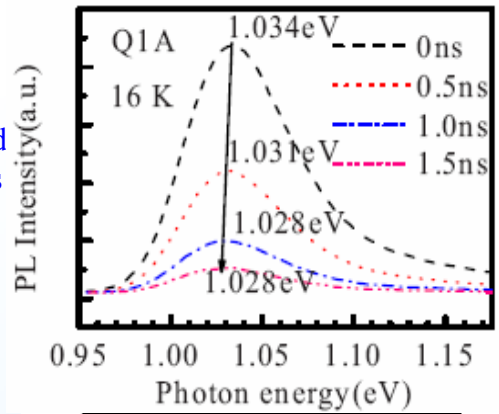

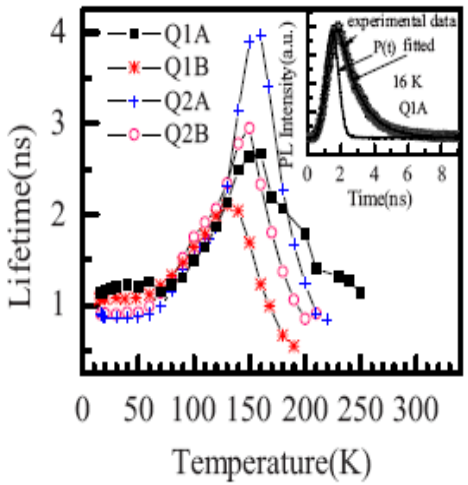

FIG. 6. PL peak lifetimes of 4-QDs at different-T; insert is a typical decay spectrum of Q1A & fitting.

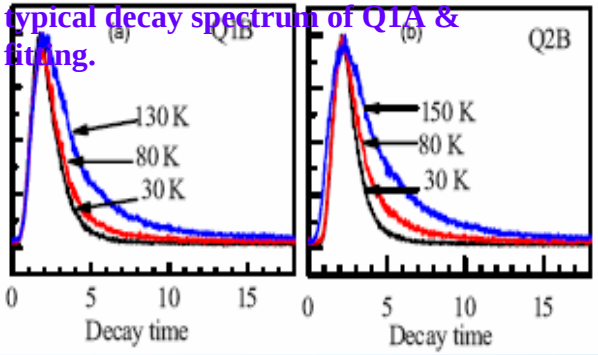

FIG. 9. Wavelength dependent PL lifetimes of Q1A at 16 K and Q2B at 120 K. The solid lines are PL spectra and the filled circular symbols are PL lifetimes at different detection wavelengths.

FIG. 7. PL decay spectra of Q1B and Q2B at different temperatures.

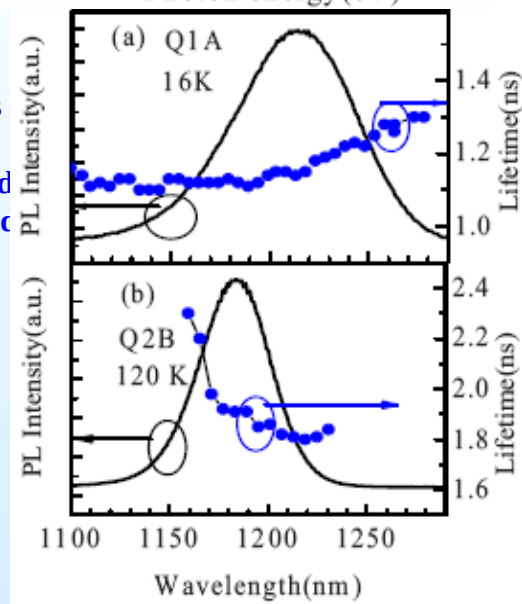

InAs self-assembled Quantum dots within InGaAs/GaAs Quantum well

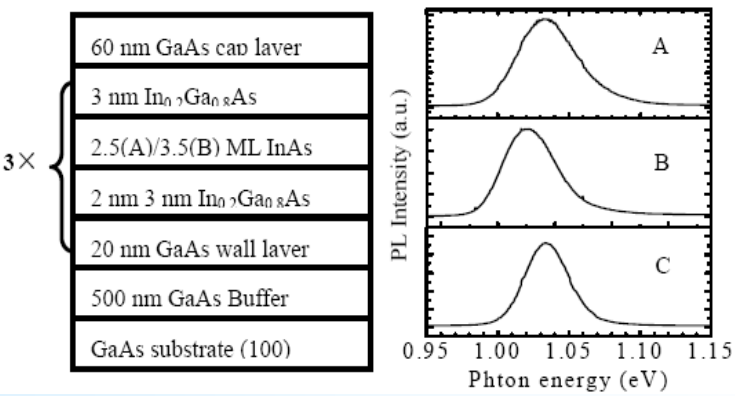

Fig. 1 (a) Schematic diagram for samples A and B. (b) PL spectra of three InAs QDs samples at 14 K, fitted with Gaussians.

- **Three different InAs QDs in InGaAs/GaAs QW were formed and studied by time-resolved and temperature dependent photoluminescence (PL).**
- **A strong RT PL at ~1.3 μm with a FWHM of only 28 meV.**
- **Dots-in-a-well (DWELL): strong stress release, large size QDs**
- **lead to PL narrowing/red-shift, enhancing carrier migration, increasing carrier density in QDs, achieving good PL lifetime stability on temperature, improving QD quality.**

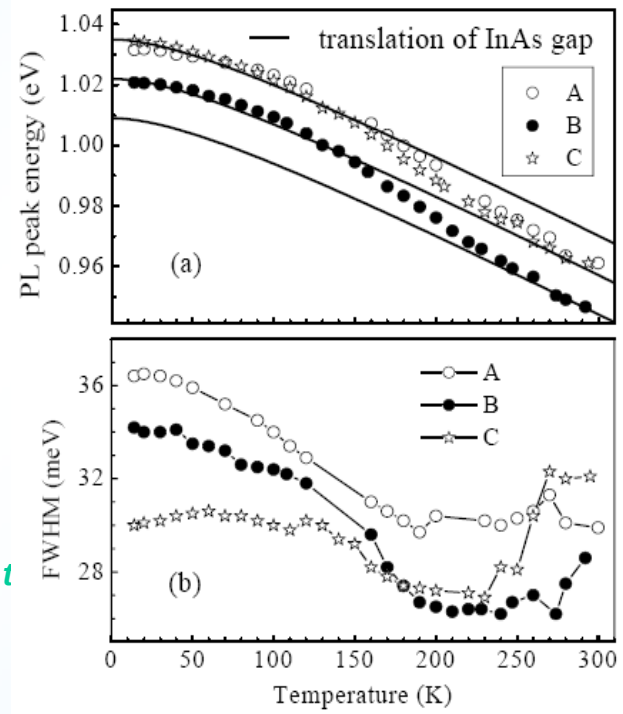

Fig. 3 PL energy and FWHM of t main peak versus temperature.

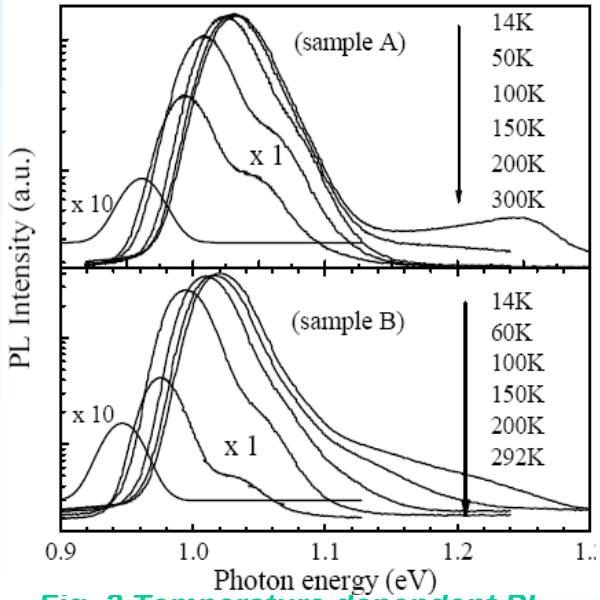

Fig. 2 Temperature dependent PL spectra for samples A and B.

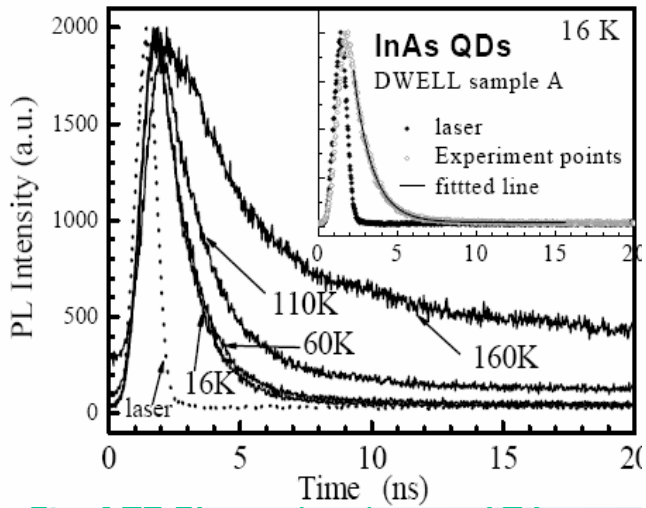

Fig. 4 TR PL spectra at several T for DWELL sample A, and decay curve fitting (insert) for a TRPL spectrum measured at 16 K.

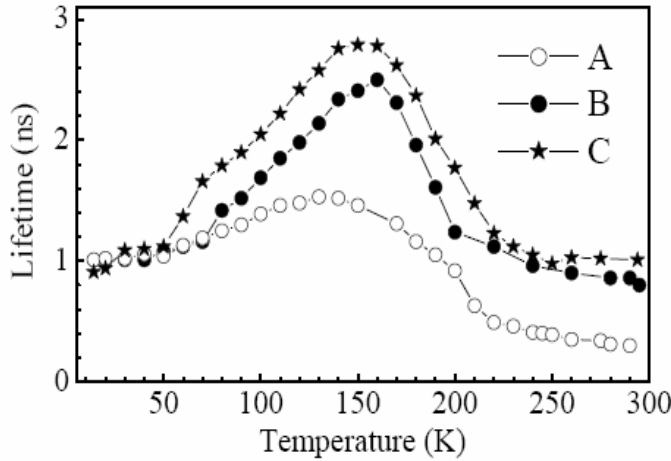

Fig. 5. Lifetime versus T for three DWELL samples A, B and C.

{SST23(08) 075044}

"Vibrational signatures of isotopic impurities and complexes in II-VI compound semiconductors"

Devki N. Talwar, Zhe Chuan Feng and Tzuen-Rong Yang, ***Phys. Rev. B 85****, 195203 (2012).*
{SCI}

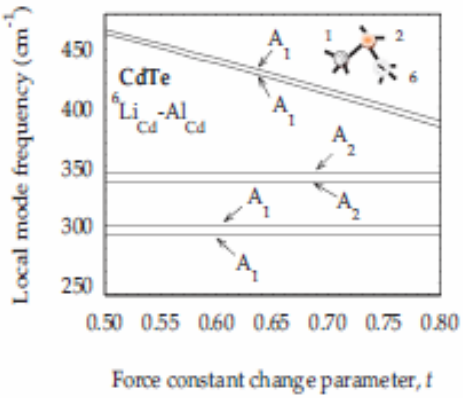

FIG. 5. (Color online) Green's function calculation for the variation of localized vibrational modes as a function of t (see text) for $^6Li_{Cd}$-Al_{Cd} second NN pair (with $v = -0.23$) in CdTe.

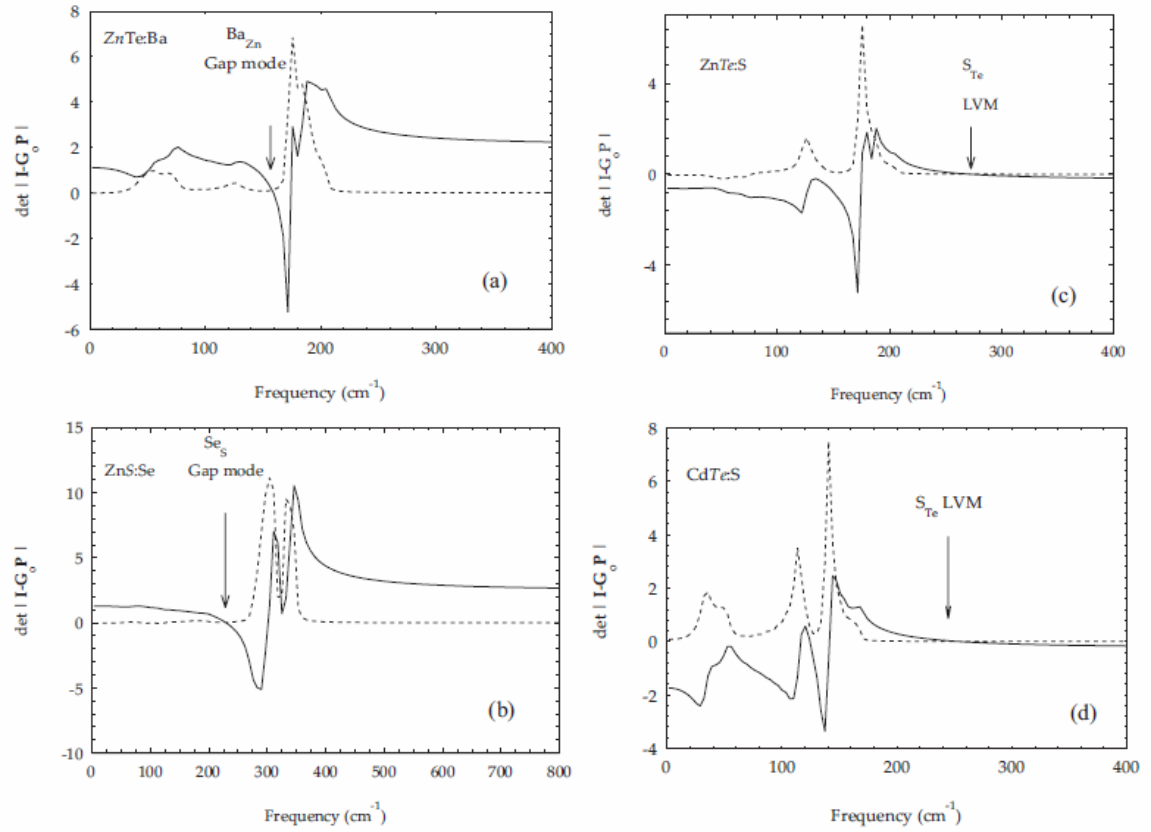

FIG. 3. Calculated real (solid line) and imaginary (dotted line) parts of the det $|\, I - G_0 P \,|$ (cf. Sec. II D) in the F_2 representation showing gap modes of (a) Ba_{Zn} in ZnTe, (b) Se_S in ZnS, and the local modes of (c) S_{Te} in ZnTe and (d) S_{Te} in CdTe.

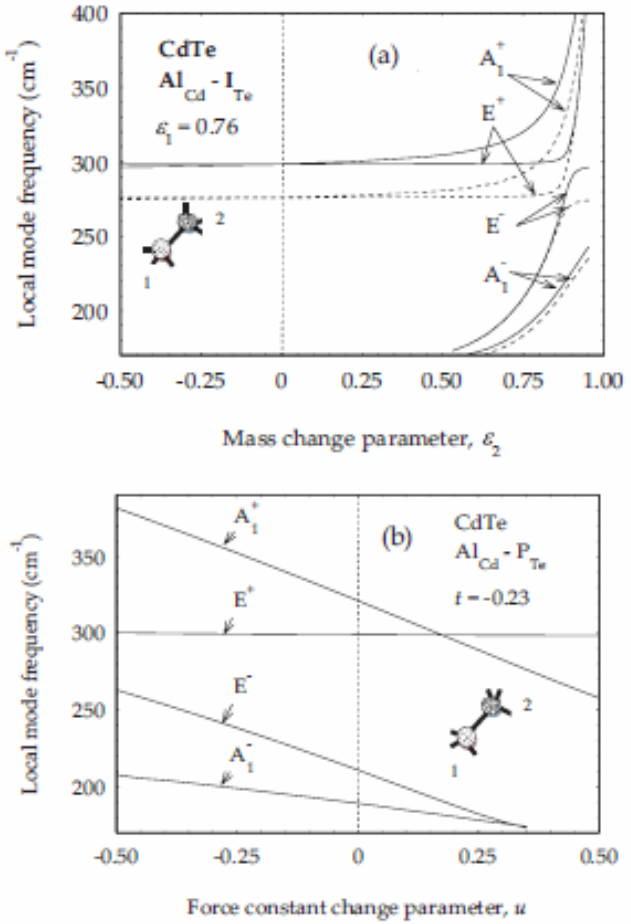

FIG. 4. (Color online) Green's function calculation of (a) the variation of localized vibrational modes as a function of ε_2 for Al_{Cd}, paired with other impurities on Te-site in CdTe; dotted lines, MDA; full lines with $t = -0.23$ (see text). (b) The variation of localized vibrational modes as a function of u for Al_{Cd}-P_{Te} pair keeping $t = -0.23$.

Room Temperature Deposition of Al-Doped ZnO Films on Quartz Substrates by Radio-Frequency Magnetron Sputtering and Effects of Thermal Annealing

W. Yang, Z. Wu, Z. Liu, A. Pang, Y.L. Tu & *Z.C. Feng*, **Thin Solid Films** **519**, 31-36 (2010)

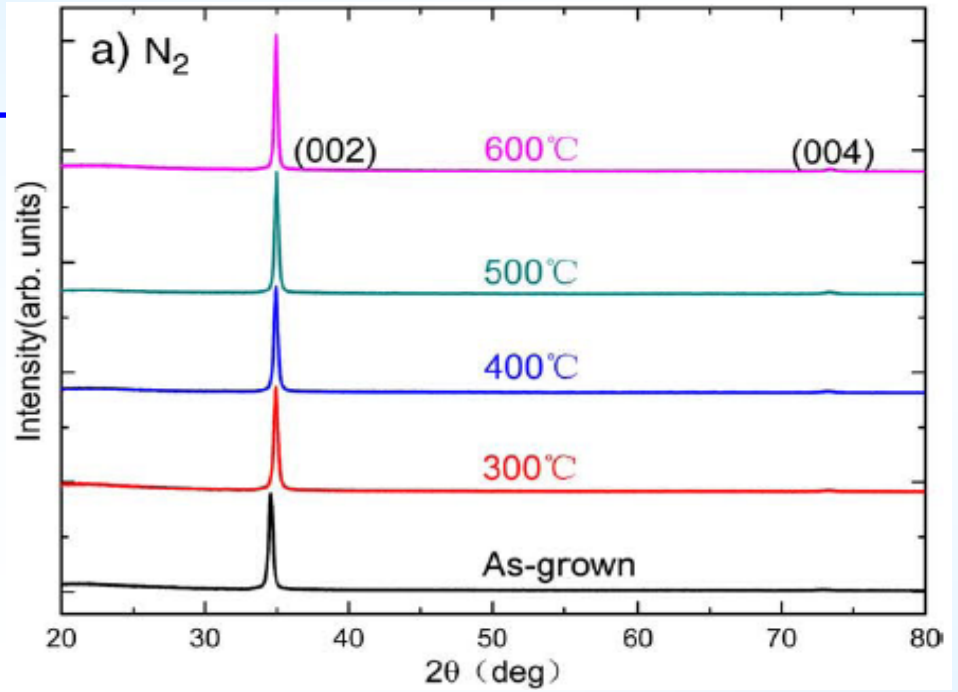

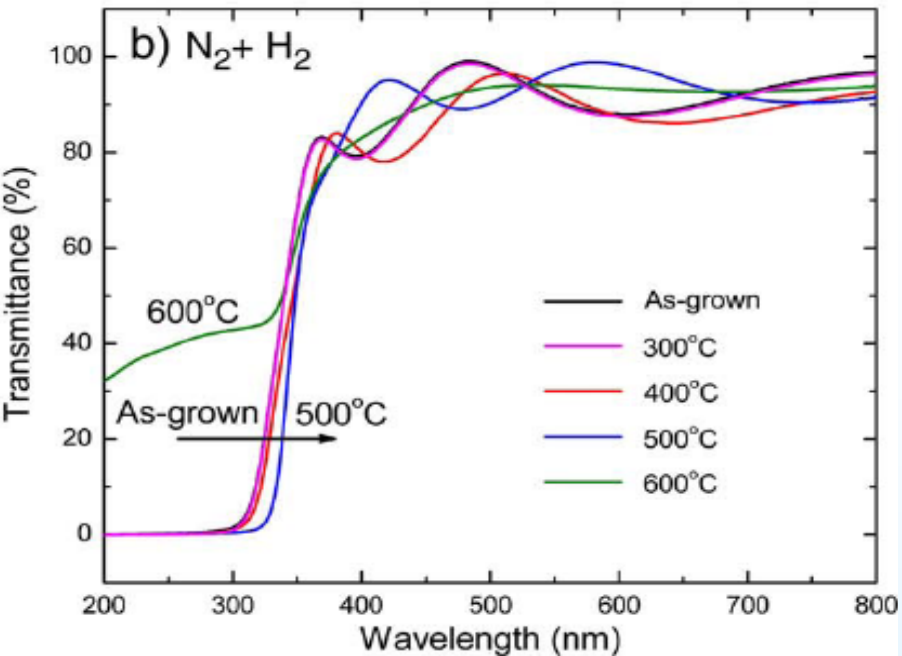

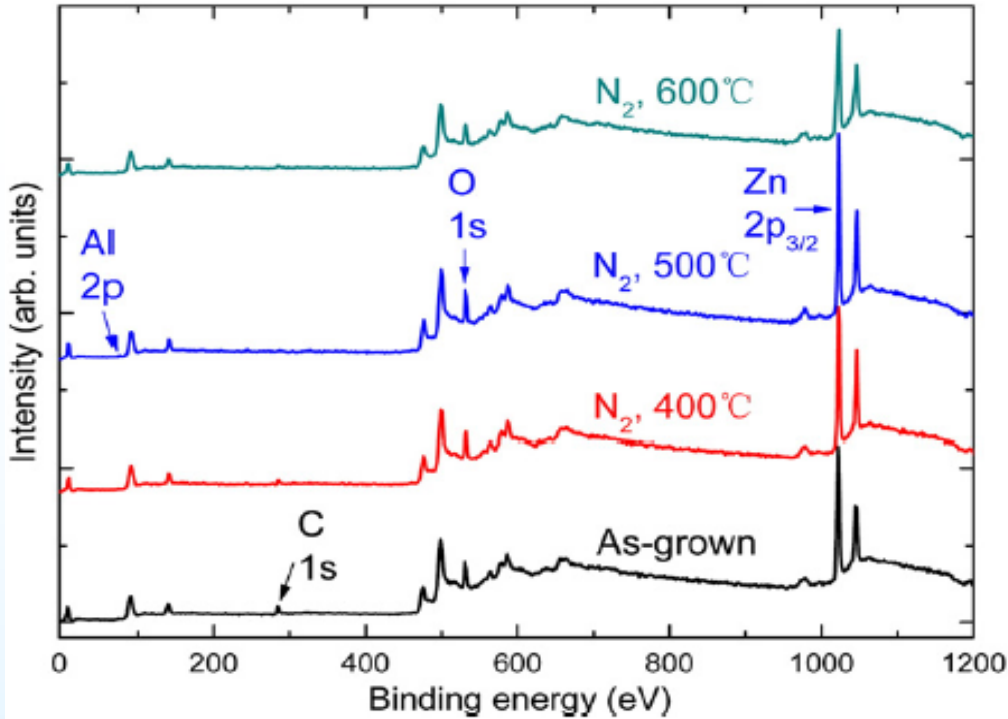

Synchrotron Radiation Technology, Nuclear and Surface Science Investigation

Wide Gap Semiconductor Laboratory

Professor Zhe-Chuan Feng
Graduate Institute of Photonics and Optoelectronics, National Taiwan University

National synchrotron radiation research center (NSRRC)

X-Ray Absorption Near Edge Structure of 6H-SiC with Different N-Dopants

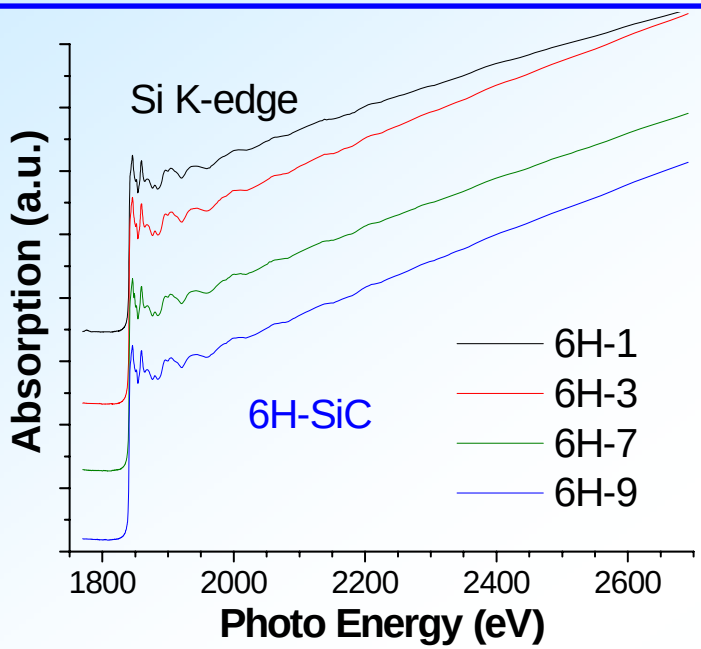

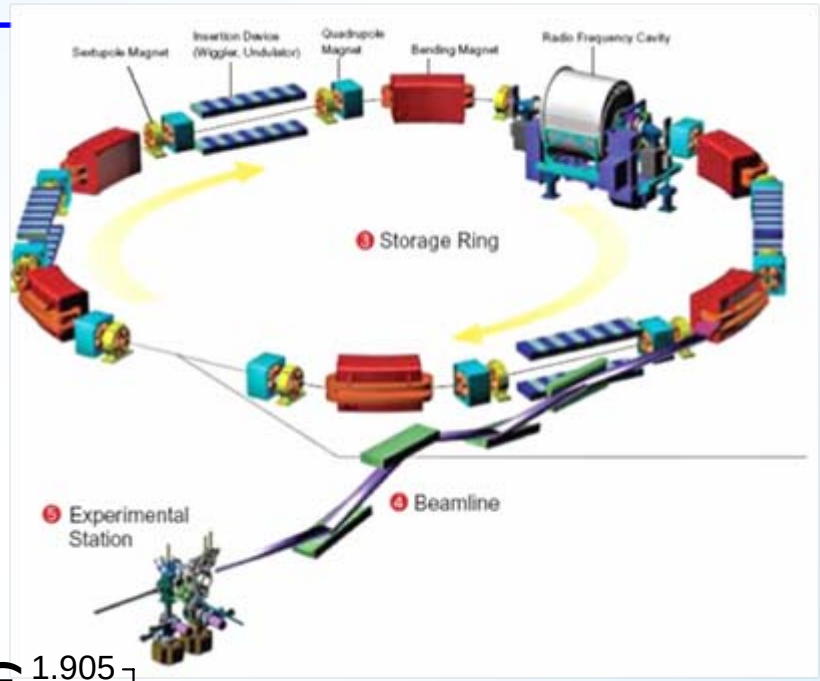

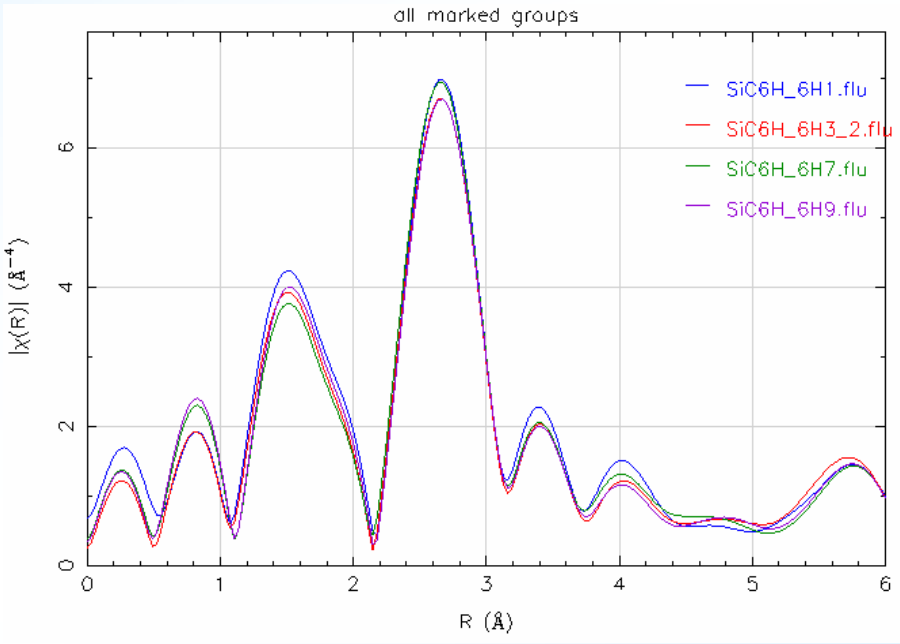

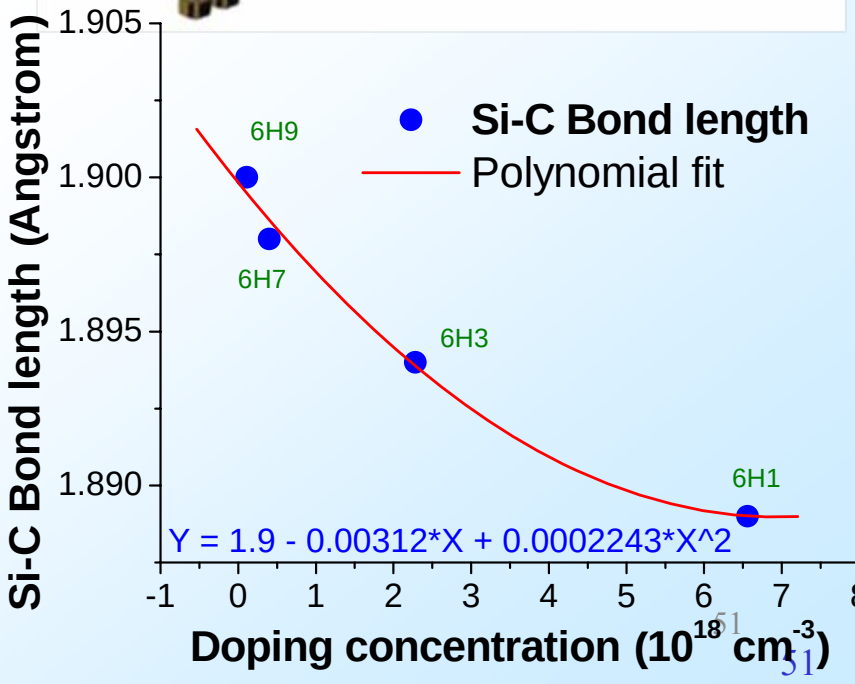

Synchrotron Radiation polarized X-ray absorption: GaN films

- Study local structure of MBE GaN/Si, MOCVD GaN/sapphire
- Determine interatomic distances in the second coordination shell around Ga: get in-plane and out-of-plane strains induced by heteroepitaxial growth

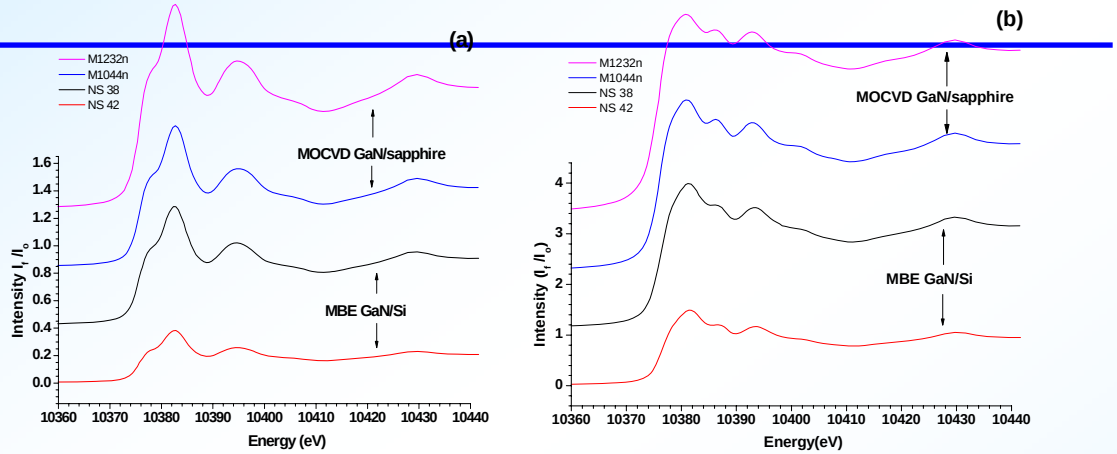

Fig. 1 X-ray absorption near edge spectra (XANES) around the Ga K-edge of the epitaxially grown GaN layers collected under (a) normal incidence and (b) grazing incidence, respectively .

Six Ga atoms lie in same (0001) basal plane as the central atom at a distance

$$R_{GaGa}(90^\circ) = a, \qquad (1$$

whereas the other six Ga atoms, positioned in parallel basal planes (three atoms above and three below), are at a distance

$$R_{GaGa}(15^\circ) = \sqrt{\frac{1}{3}a^2 + \frac{1}{4}c^2}, \qquad (2$$

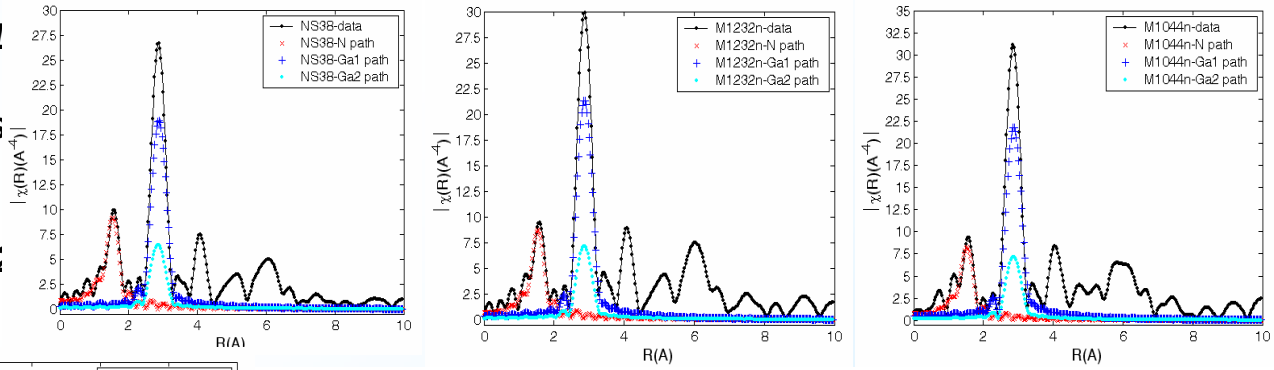

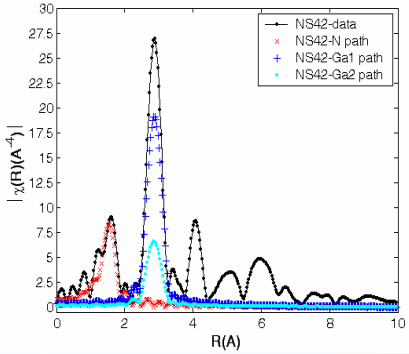

Fig. 2 Fourier transformed EXAFS spectra around Ga K edge of GaN on Si & sapphire. Light blue line - fits of normal incidence, Dark blue line - fits of grazing incidence of the X-ray, in each figure.

Table 2. Results of the quantitative XAFS analysis.

Sample	R_{GaN} ±0.002	σ^2_{GaN} ±0.002	$R_{GaGa}(15^\circ)$ ±0.003	$R_{GaGa}(90^\circ)$ ±0.003	Difference	σ^2_{GaN} ±0.0007
Bulk [3]	1.95000		3.17940	3.18780	-0.00840	
M1232n	1.93225	0.0013	3.17669	3.17630	0.00039	0.0045
M1044n	1.93036	0.0024	3.17515	3.17469	0.00046	0.0038
NS38	1.93347	0.0024	3.17318	3.18995	-0.01677	0.0049
NS42	1.93657	0.0024	3.17309	3.18109	-0.00800	0.0054

{submitted to JAP}

Synchrotron Radiation Technology for sub-50nm Si-IC, Si/Ge/Si, 3C-SiC/Si, AlN/sapphire, ZnO/sapphire, …, structures

- Many new scientific and technological issues appear, for example, stresses in 3-dimmensional distribution and their effects to the material properties will have become very important and they will affect the device functions and performance severely.
- Study by high energy and high intensity synchrotron radiation X-ray diffraction (SR-XRD) and X-ray photoelectron spectroscopy (SR-XPS) with rich data.

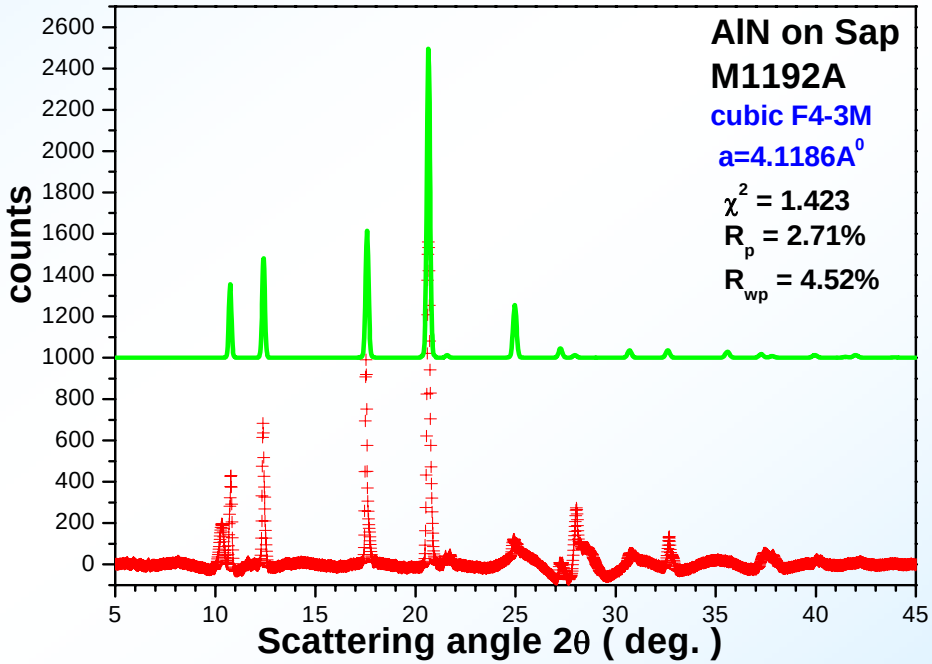

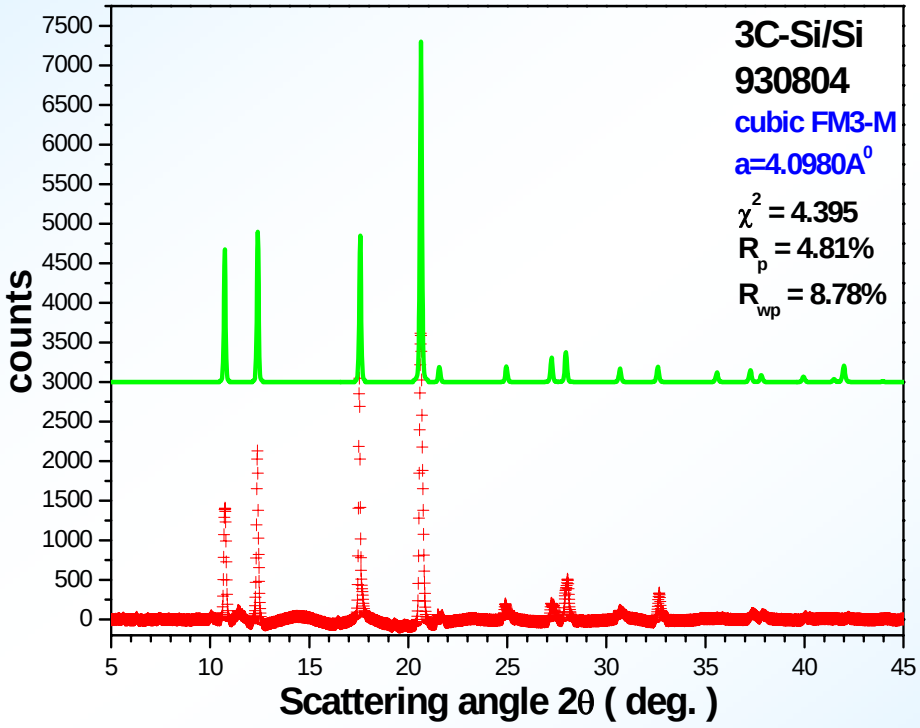

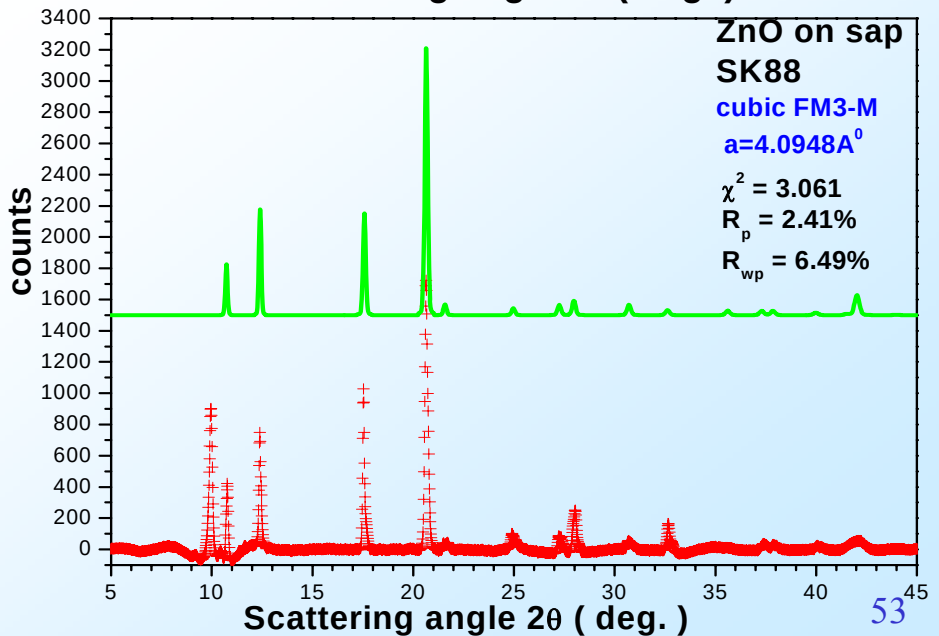

X-ray absorption and Raman study of GaN films grown on different substrates by different techniques

Y.L. Wu, *Z.C. Feng*, J.F. Lee, W. Tong, B.K. Wagner & I. Ferguson,
Thin Solid Films 518, 7775-9 (2010).

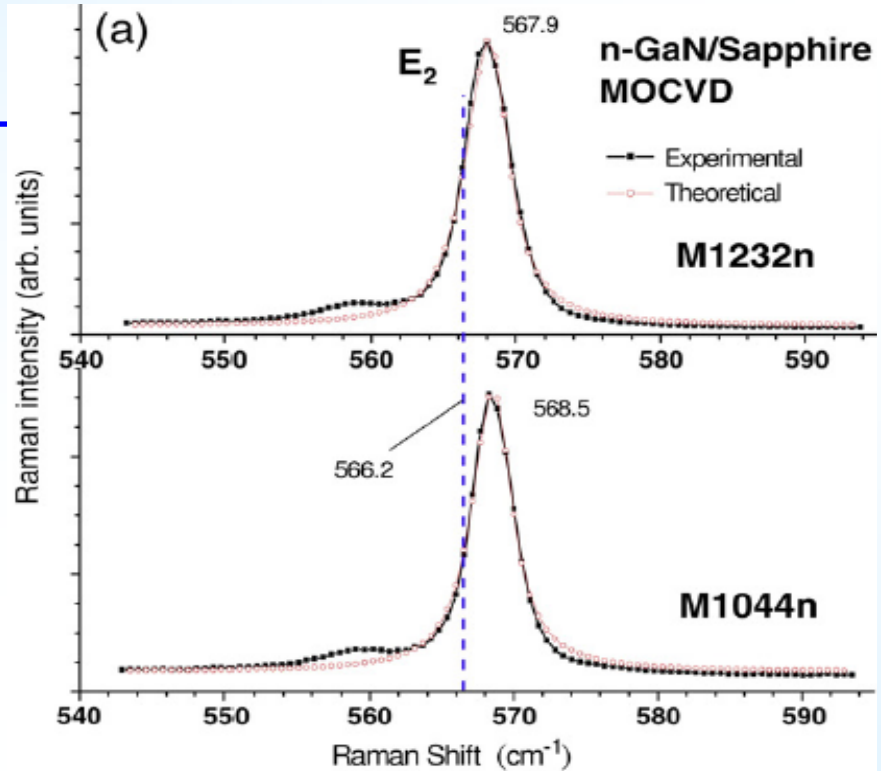

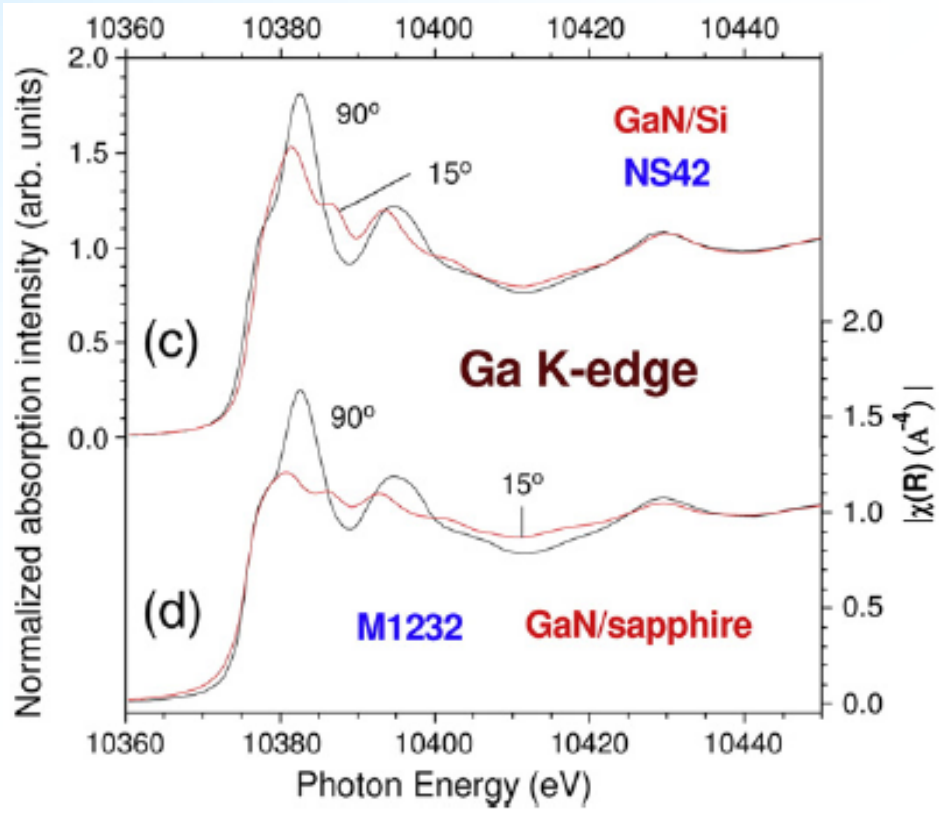

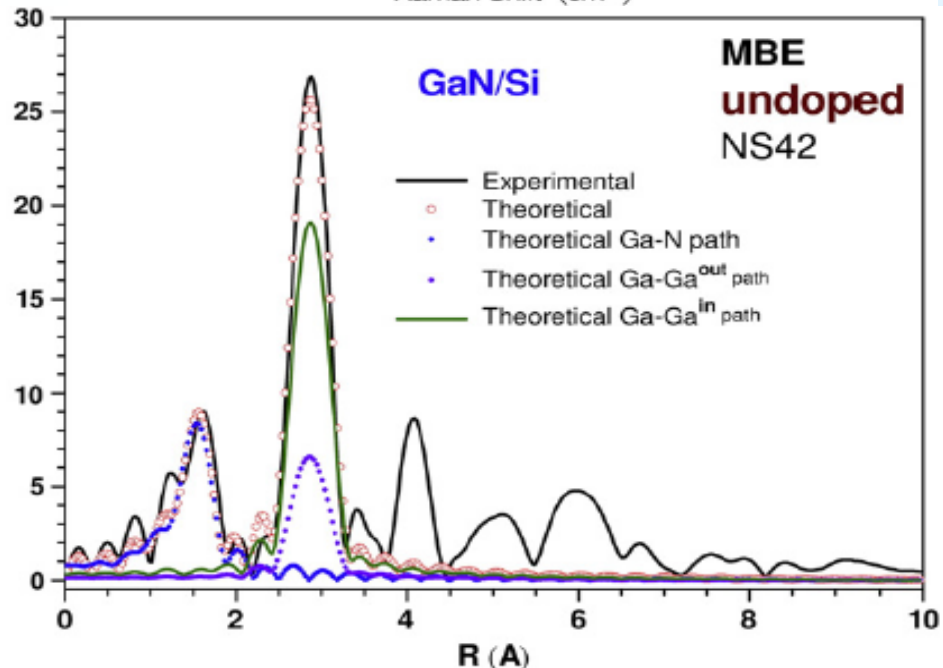

Rutherford backscattering of various semiconductors/oxides

Key notes

Rutherford backscattering (RBS) have been used to study more semiconductors and oxides heterostructures, obtain precise thickness and compositions

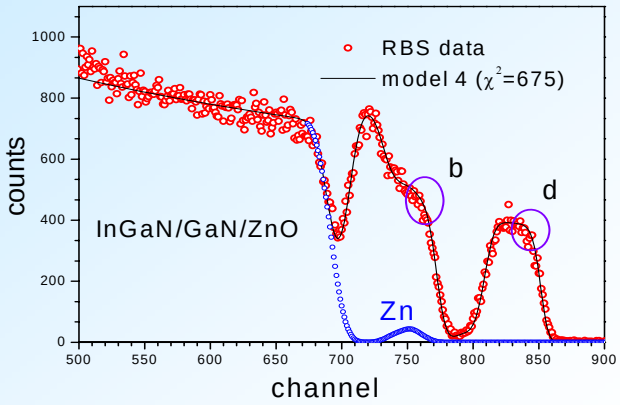

Fig. 1 *Random (open circles) and simulated (solid line) RBS spectra of* ***InGaN/GaN/ZnO*** *structure including the effects of Zn-diffusion, roughness, and interface fuzzy*

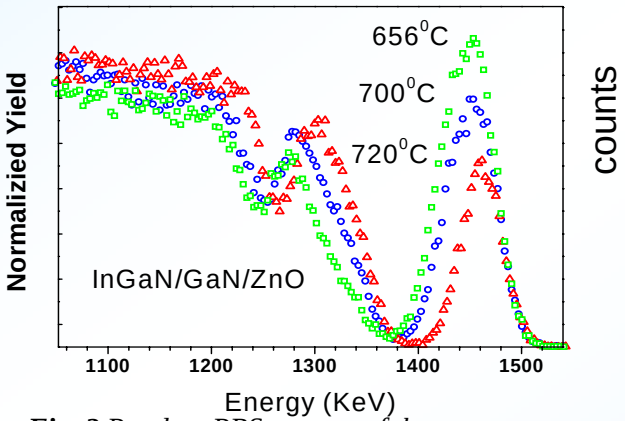

Fig. 2 *Random RBS spectra of three InGaN/GaN/ZnO samples with InGaN layer grown at 656, 700 and 720 ℃, respectively.*

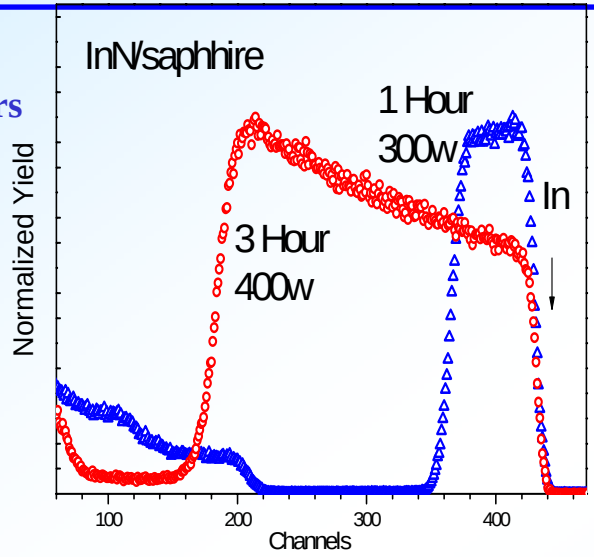

Fig.3 *Random RBS spectra of* ***InN films*** *with different growth times*

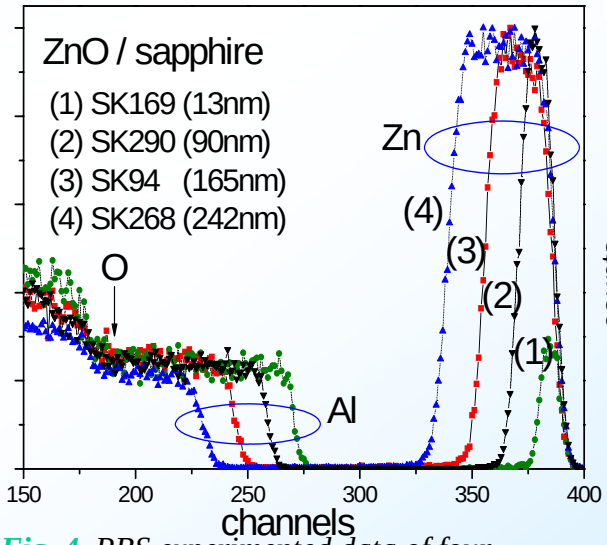

Fig. 4 *RBS experimented data of four different thickness* ***ZnO thin films on sapphire***

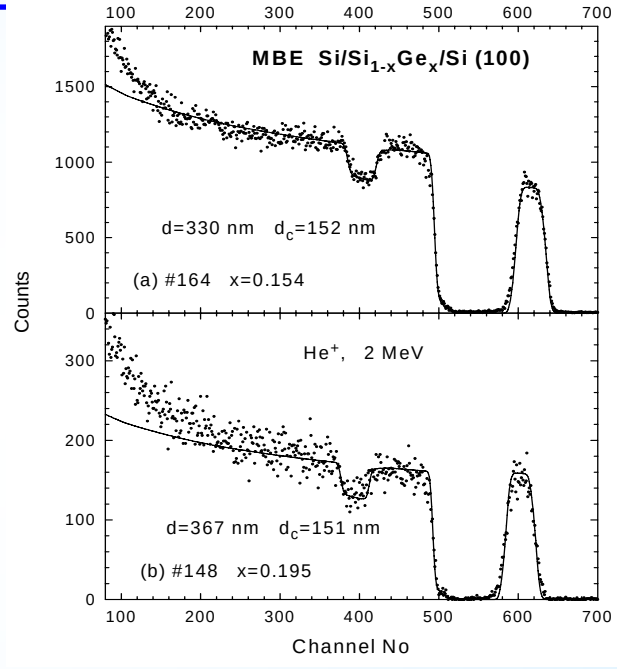

Fig.5 *Random and simulated RBS spectra of sanwitzed* ***Si/SiGe/Si.***

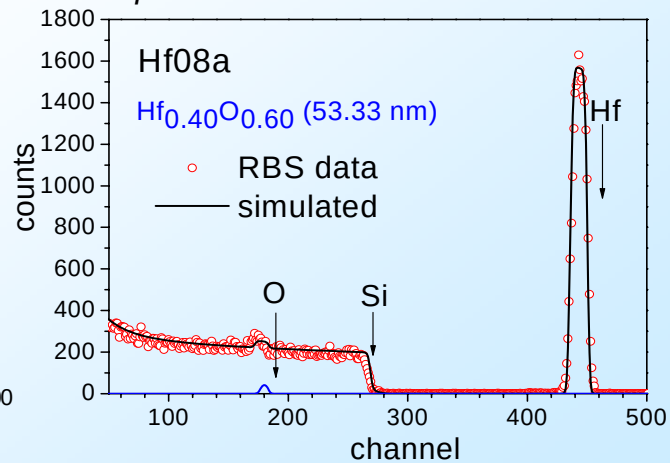

Fig. 6 *RBS & simulation for* ***HfO_2 film on Si.***

{best MS-thesis, 2010}

Raman scattering and X-ray absorption from CVD grown 3C-SiC on Si

Zhe Chuan Feng, Cheng Chen, Qiang Xu, Suwan P. Mendis, Ling-Yun Jang, Chin-Che Tin, Kung-Yen Lee, Chee Wee Liu, Zhengyun Wu, and Zhi Ren Qiu,

Materials Science & Forum **717-720**, 505-508 (**2012**). ***{EI}***

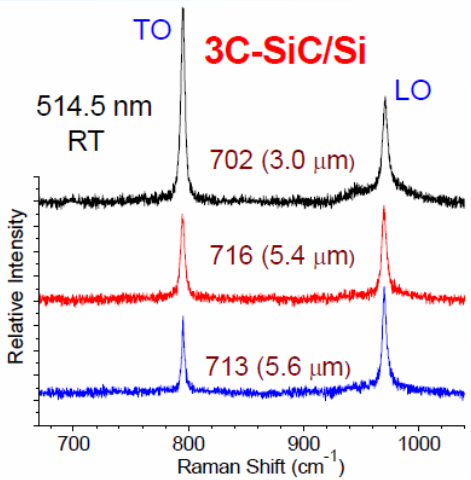

Fig. 1 Raman spectra of three CVD 3C-SiC/Si (100).

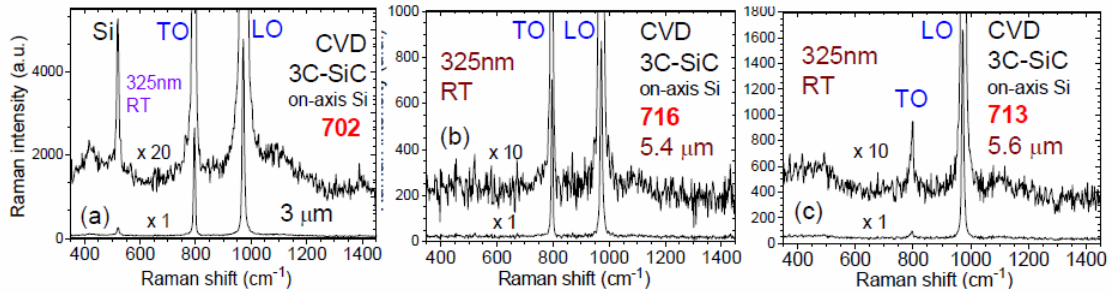

Fig. 2. UV excited Raman spectra, under 325 nm excitation, for three 3C-SiC/Si samples. Due to the shallow penetrating depth of UV 325 nm light, the Si Raman mode is not seen for 3C-SiC films thicker than 5 μm.

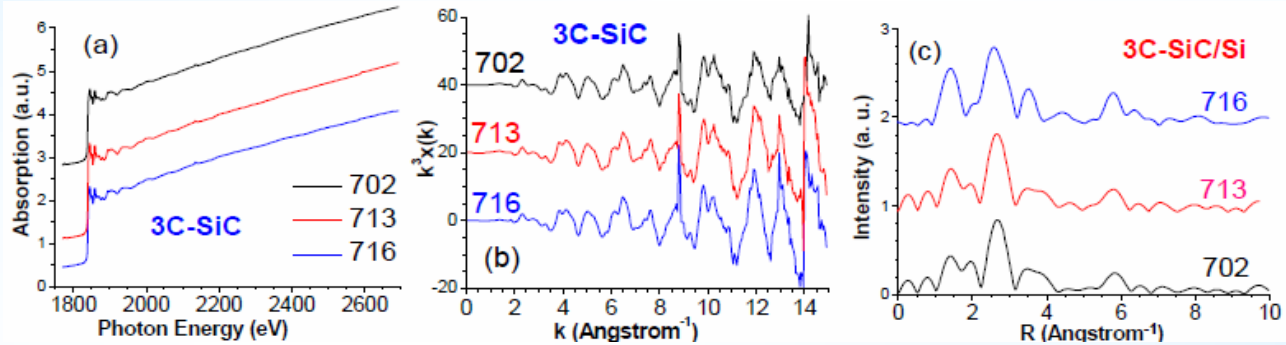

***Fig. 3* XAS ... spectra.**

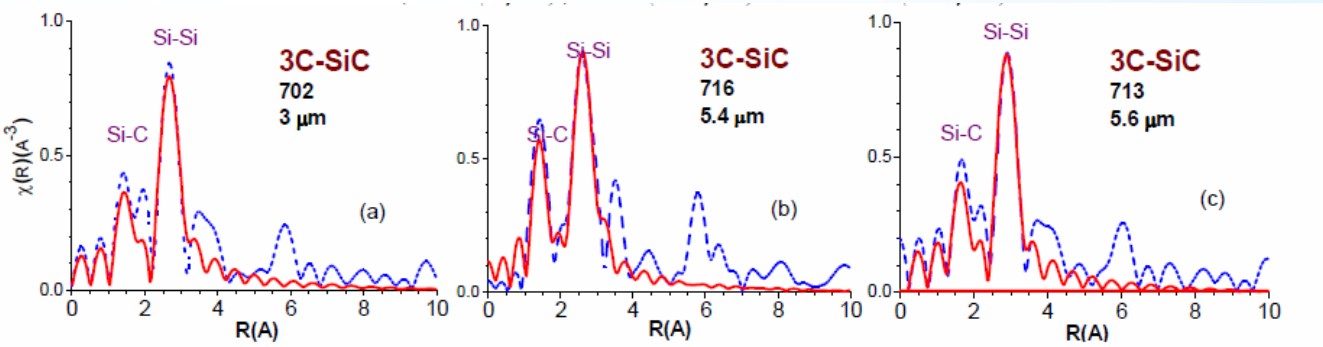

Fig. 4. Simulation fits on Fourier Transform spectra in Fig. 3 (c), for three 3C-SiC/Si samples.

Table 1. Simulation results on the Fourier transform Si K-edge EXAFS spectra {R(Si-C) is the bond length of Si-C, R2(Si-Si) is the bond length of Si-Si.}

Sample	Thickness (μm)	R(Si-C) (Å)	R2(Si-Si) (Å)
C702	3.0	1.87866	3.07046
C716	5.4	1.88270	3.07450
C713	5.6	1.88260	3.07440

4H-SiC wafers studied by X-ray absorption and Raman scattering

Qiang Xu, Hua Yang Sun, Cheng Chen, Ling-Yun Jang, RUSLI, Suwan P. Mendis, Chin Che Tin, Zhi Ren Qiu, Zhengyun Wu, Chee Wee Liu, and Zhe Chuan Feng,

Materials Science & Forum **717-720**, 509-512 (2012). ***{EI}***

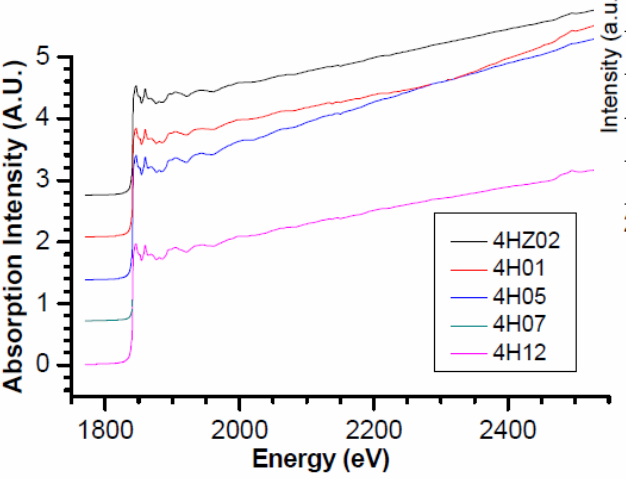

Figure 1. XAS raw data from the Si K-edge for five experimental 4H-SiC samples.

$$I(\omega) \propto \int_0^1 \exp(-q^2L^2/4)\frac{d^3q}{[\omega-\omega(q)]^2+(\Gamma_0/2)^2}$$

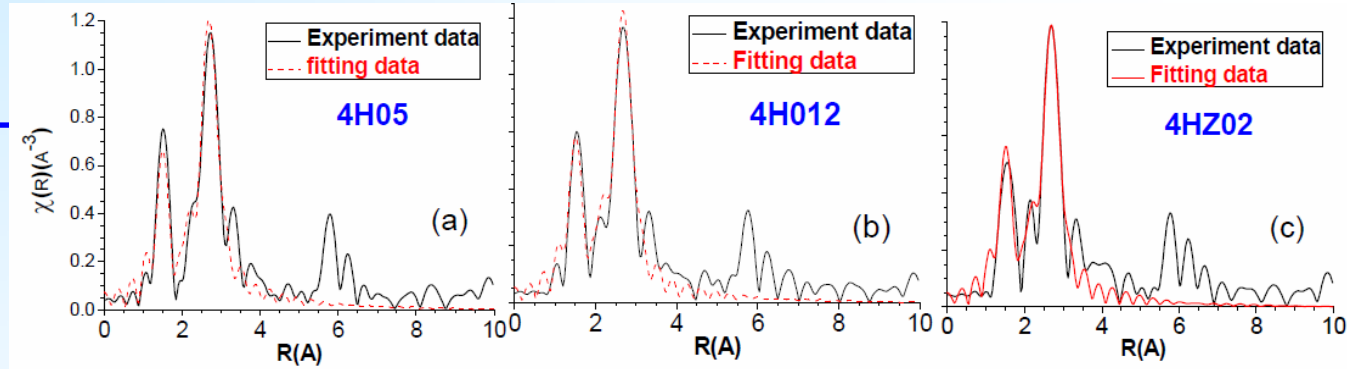

Figure 2. Fourier transformation spectra and fitting results of three 4H-SiC samples studied.

Table 2. EXAFS fitting results of 4H-SiC

Sample	R(Si-C) [Å]	R(Si-Si) [Å]
4H05	1.8968	3.0886
4H012	1.8988	3.0906
4HZ02	1.9047	3.0965

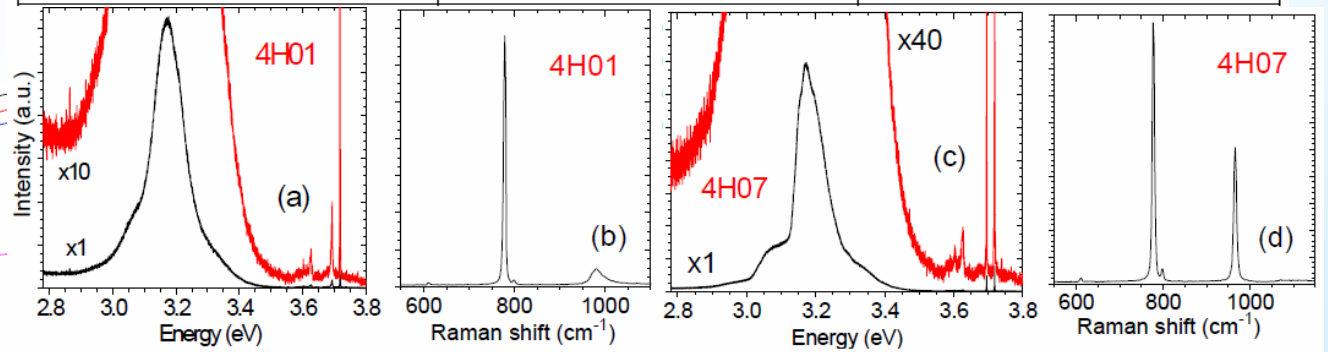

Figure 3. UV (325 nm) excited micro-PL-Raman spectra from two 4H-SiC samples.

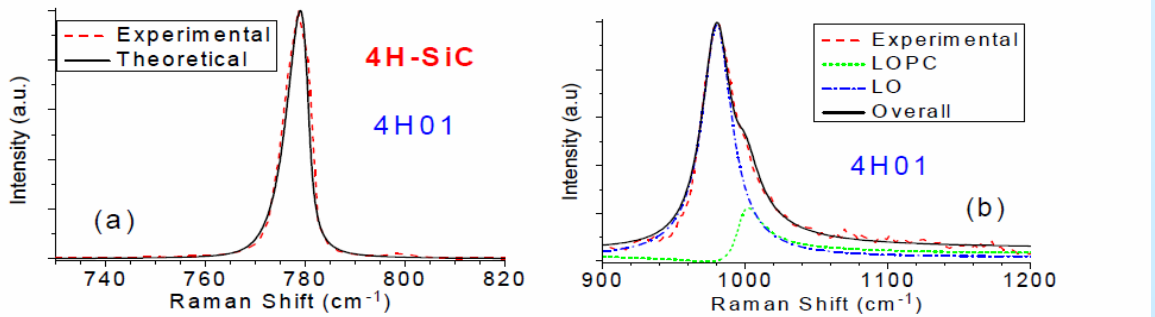

Figure 4. Theoretical fits on 4H-SiC #4H01: (a) spatial correlation model fits on E_2(TO) mode and (b) two mode fits on LO and LOPC phonon modes, respectively.

Rutherford Backscattering and Optical Studies of InAlGaP Materials Grown on GaAs by Metalorganic Chemical Vapor Deposition

Lin Li, Chi-Jing Hong-Liao, Yi Zhe Huang, Cheng Chen, Shude Yao, ZiRong Qiu, H. H Lin, Ian T. Ferguson and Zhe Chuan Feng, SPIE **8484**-34, oral, San Diego, 16 August 2012. ***{SCI}***

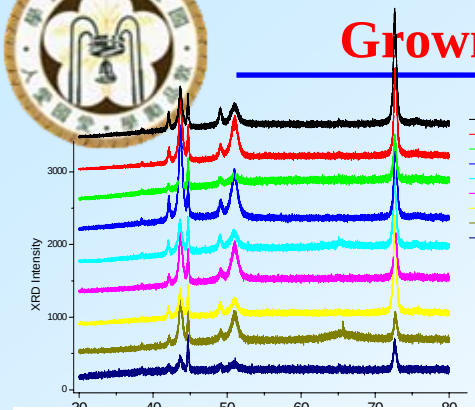

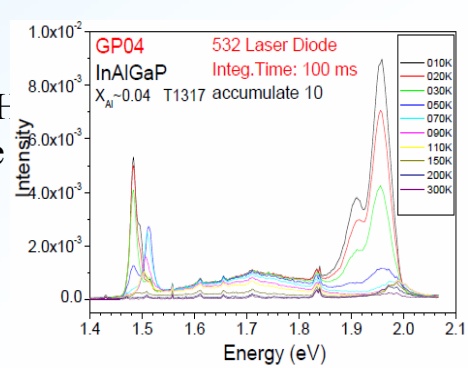

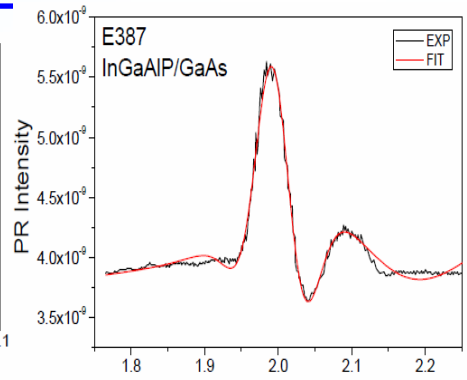

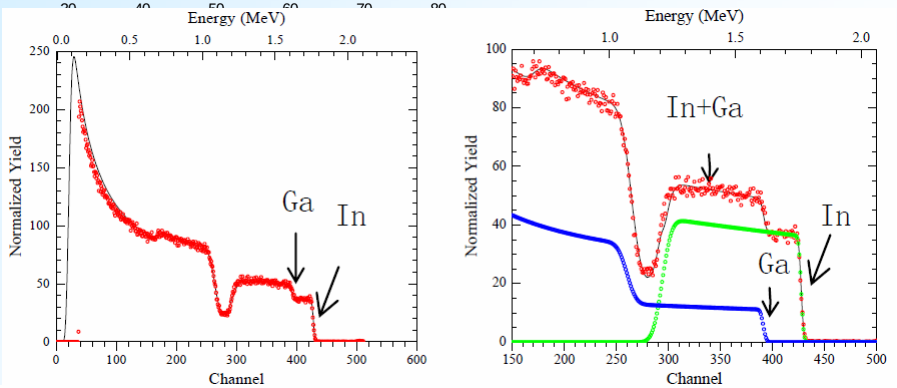

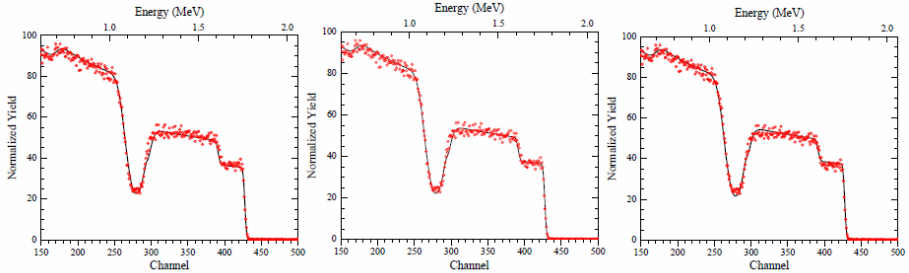

a) $In_{0.485}Ga_{0.365}Al_{0.150}P$ b) $In_{0.470}Ga_{0.380}Al_{0.150}P$ c) $In_{0.500}Ga_{0.350}Al_{0.150}P$

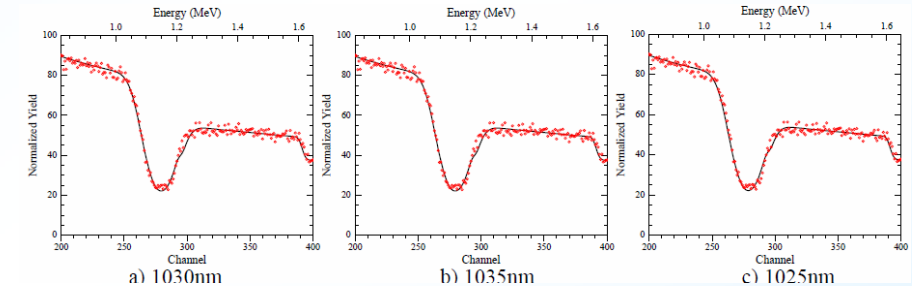

a) 1030nm b) 1035nm c) 1025nm

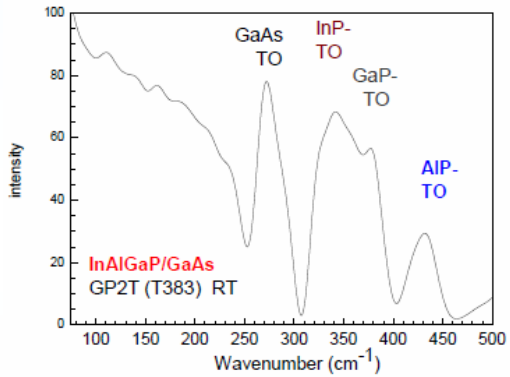

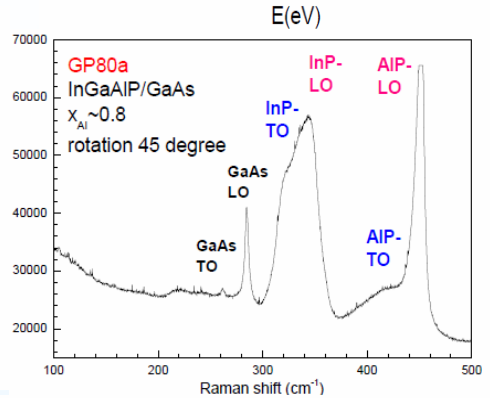

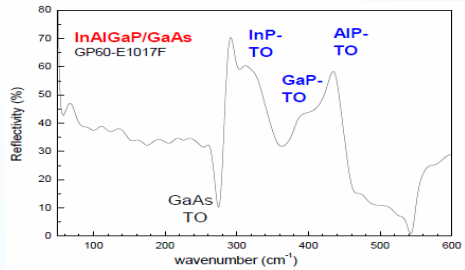

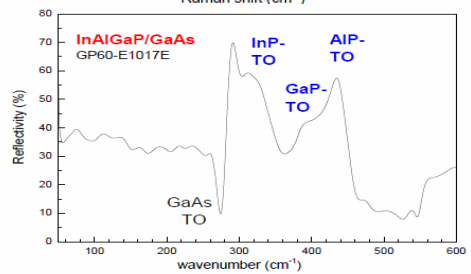

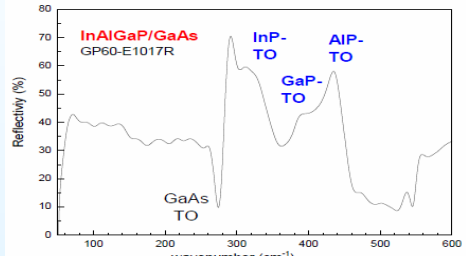

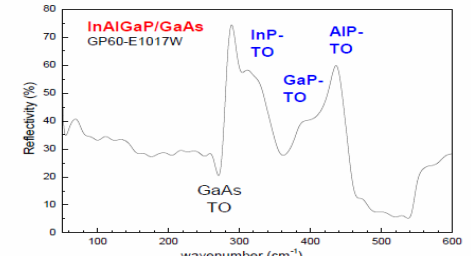

Infrared and X-ray Absorption Studies of CdTe Thin Films

Wenjie Wang, Yu Cheng Yang, Ting-Shan Chan, Peng Chen, Tzuen-Rong Yang, Zhe Chuan Feng, SPIE **8470**-30, poster, San Diego, 13 August 2012.

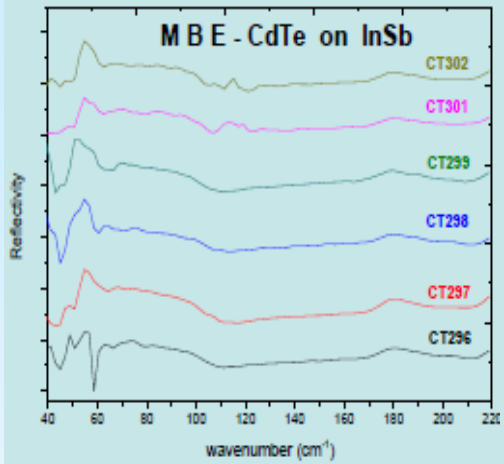

Sample	Ion cleaning		MBE-grown CdTe films
	Time(hr)	Temperature(°C)	Thickness(μm)
296	2.25	RT	1.14
297	0.5	RT	1.25
298	1	RT	1.25
299	1	100	1.31
301	1	230	1.13
302	1	250	1.21

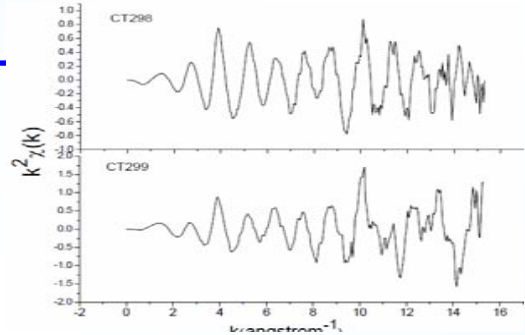

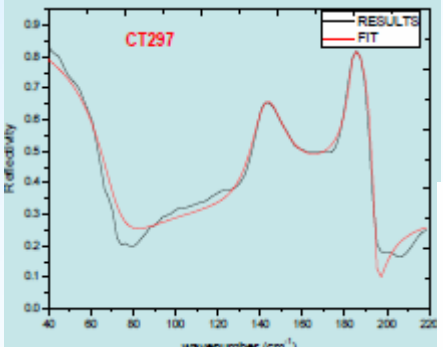

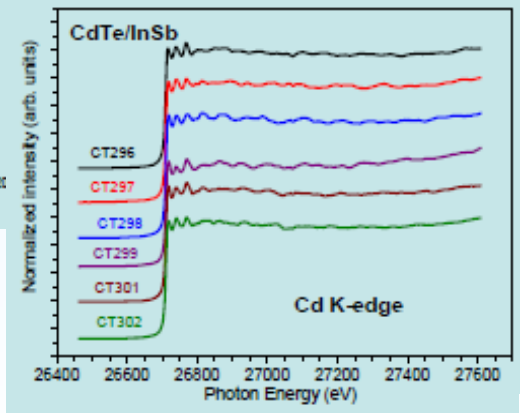

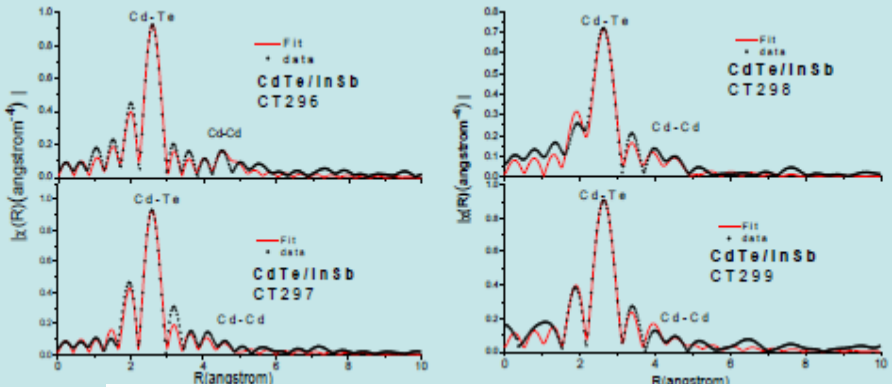

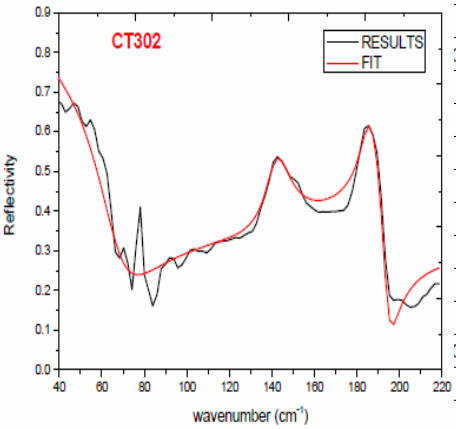

	CT296	CT297	CT298	CT299	CT301	CT302
	CdTe film					
Dielectric constant (infinite)	7.1	7.1	7.1	7.1	7.1	7.1
Oscillator Strength	2.59	3.31468	1.77655	2.62	1.75	1.65
TO Frequency	142.4	142.193	142.2	141	142.5	142
Damping Constant	9.805	8.96596	9.69811	9.442	12.11	9.91
Carrier Concentration (10E18)	0.07256	0.11983	0.23597	0.073	0.0593	0.09421
Mobility (cm2/V.s)	1634.73	2721.55	1609.94	1090.3	733.439	1312.51
Effective Mass / electron's	0.13	0.09	0.11	0.09	0.11	0.11
Thickness (μm)	1.14	1.25	1.25	1.31	1.13	1.21
	InSb substrate					
Dielectric constant (infinite)	15.3	15.3	15.3	15.3	15.3	15.3
Oscillator Strength	1.515	1.71744	0.63764	1.3586	1.535	1.56
TO Frequency	184.3	183.053	185.7	183.2	185.4	184.4
Damping Constant	6.81	2.81253	5.4759	5.51	6.8	6.3
Carrier Concentration (10E18)	0.0131	0.01414	0.00831	0.0147	0.01277	0.01313
Mobility (cm2/V.s)	24007.8	35575	32083.9	20599.7	19430.5	29318.1
Effective Mass / electron's	0.014	0.014	0.0149	0.01483	0.014	0.014

Table 3 The results of the EXAFS data fits for first coordination shell atom around Cd atom.

CdTe/InSb	S_0^2	CN(Cd-Te)	R(Cd-Te) (Å)	σ^2
CT296	0.895	3.58	2.80200	0.00630
CT297	0.850	3.4	2.79933	0.00578
CT298	1.190	4.76	2.82210	0.01051
CT299	0.949	3.796	2.81371	0.00451
CT301	1.200	4.8	2.77818	0.01141
CT302	0.940	3.76	2.81274	0.00659

Table 4 The results of the EXAFS data fits for second coordination shell atom around Cd atom.

CdTe	S_0^2	CN(Cd-Cd)	R(Cd-Cd) (Å)	σ^2
CT296	1.000	12	4.70222	0.02254
CT297	1.000	12	4.68874	0.03727
CT298	1.000	12	4.77759	0.03463
CT299	0.910	10.92	4.53381	0.02964
CT301	1.080	12.96	4.62935	0.04531
CT302	1.020	12.24	4.80179	0.03294

APPLIED PHYSICS LETTERS **101**, 091115 (2012)

Observation of In-related collective spontaneous emission (superfluorescence) in $Cd_{0.8}Zn_{0.2}Te$:In crystal

C. R. Ding,[1,a)] Z. L. Li,[1] Z. R. Qiu,[1,b)] Z. C. Feng,[2,c)] and P. Becla[3]
[1]*State Key Laboratory of Optoelectronic Materials and Technologies and School of Physics and Engineeri Sun Yat-Sen University, Guangzhou 510275, China*
[2]*Insistute of Photonics and Optoelectronics & Department of Electrical Engineering, National Taiwan University, Taipei 106-17, Taiwan*
[3]*Department of Materials Science and Engineering, Massachusetts Institute of Technology, Cambridge, Massachusetts 02139, USA*

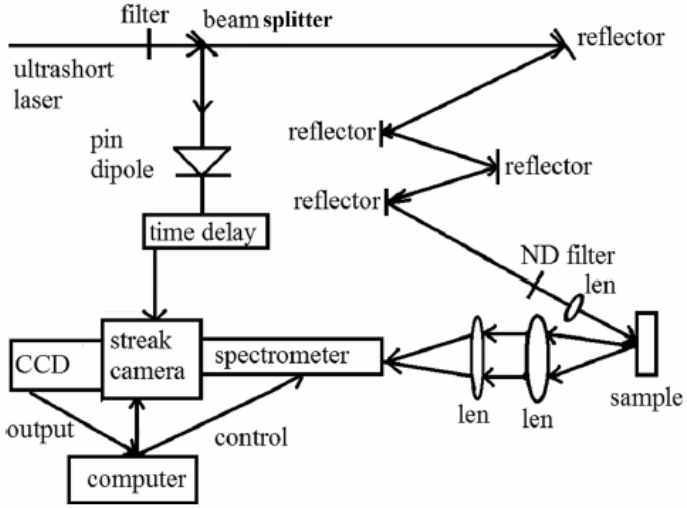

FIG. 1. Schematic diagram of the experimental setup for time-resolved and ime-integrated photoluminescence.

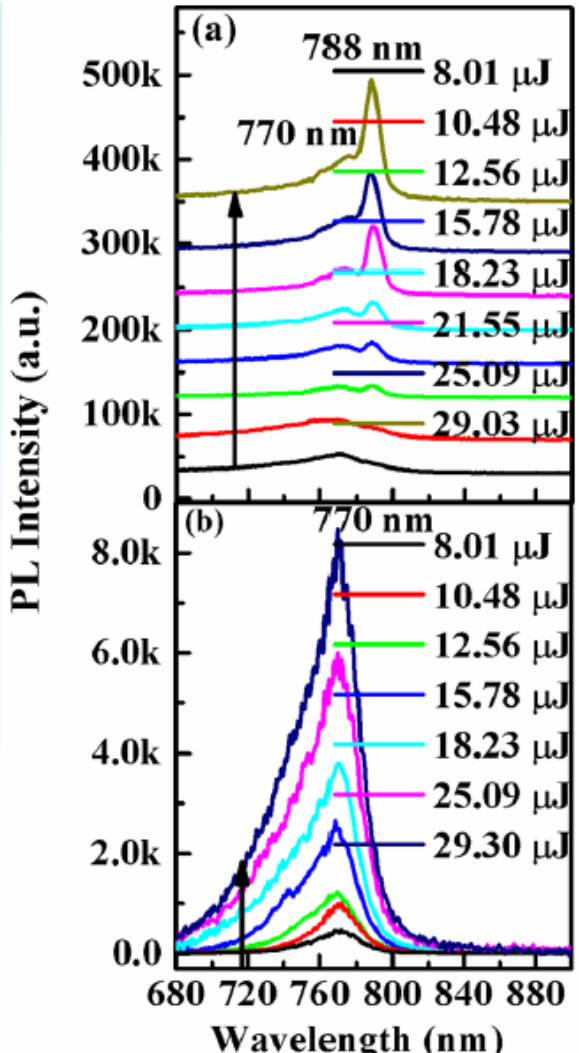

FIG. 2. A typical steady-state fluorescence spectra obtained from intentional indium doped $Cd_{0.8}Zn_{0.2}Te$:In (a) and $Cd_{0.8}Zn_{0.2}Te$ crystals (b). Red and green solid line: fits to spectra with Gauss function curves.

FIG. 3. Pump energy (P) dependent emission spectra from intentional indium doped $Cd_{0.8}Zn_{0.2}Te$:In (a) and $Cd_{0.8}Zn_{0.2}Te$ crystals (b). The arrows show the increase of pump energy.

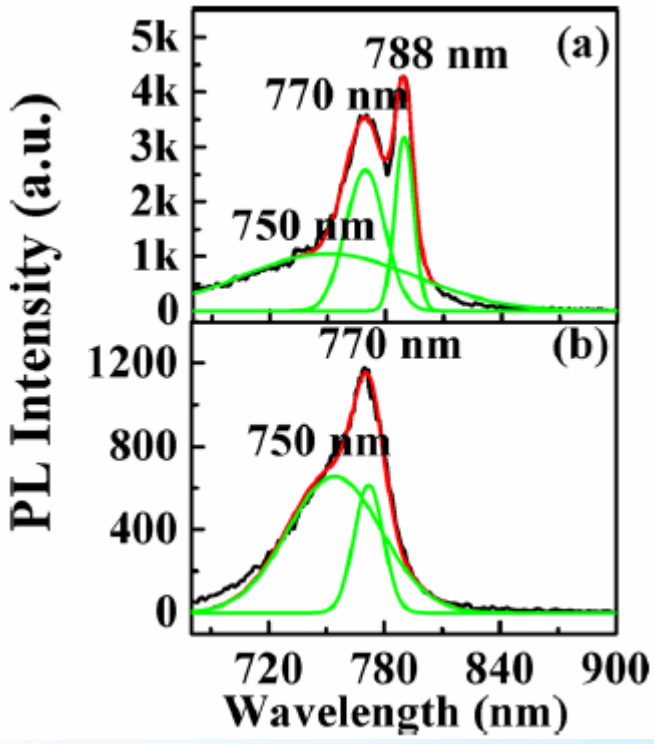

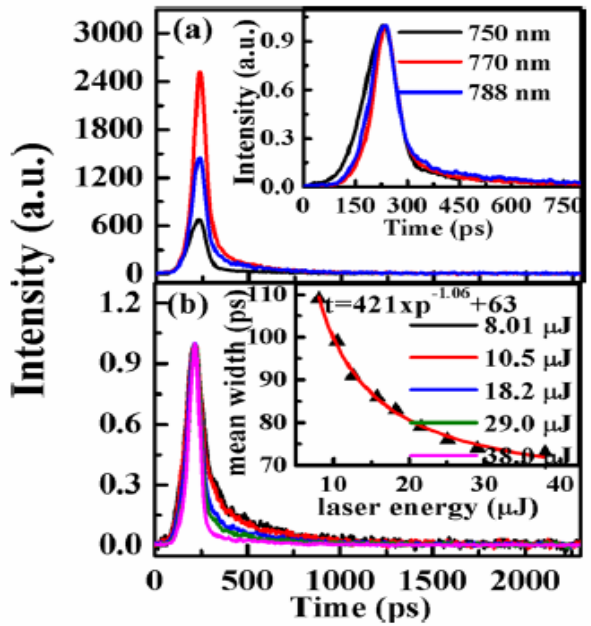

FIG. 5. (a) Decay dynamics processes of the emission at 750 nm (black line), at 770 nm (red line), and at 788 nm (blue line) from $Cd_{0.8}Zn_{0.2}Te$:In crystal at the pump energy of 18.23 μJ. The inset shows normalized decay curves for observing delay of the initial rise. (b) Pump energy dependence of normalized decay curves at the emission of 788 nm. The inset shows pump energy dependence of mean output pulse width. The red solid line represents fits to the data of the form $t \propto P^{-1.11}$ for the mean output pulse width.

Bond lengths and lattice structure of $InP_{0.52}Sb_{0.48}$ grown on GaAs

Chen-Jun Wu, Zhe Chuan Feng, Wen-Ming Chang, Chih-Chung Yang,
and Hao-Hsiung Lin, ***Appl. Phys. Lett***. **101**, 091902 (2012). *{SCI}*

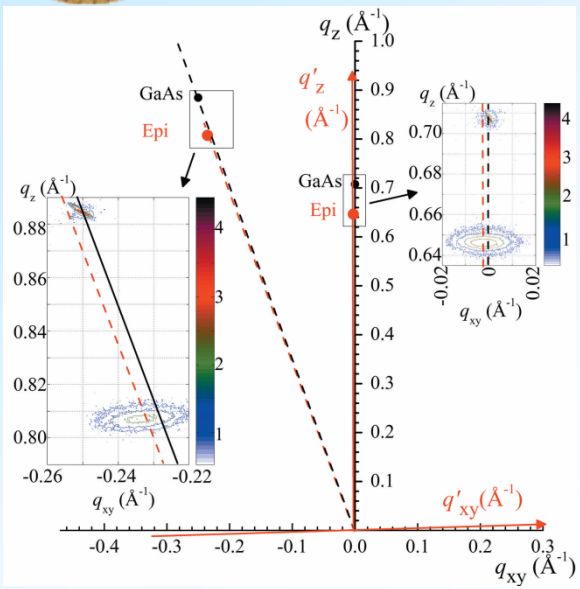

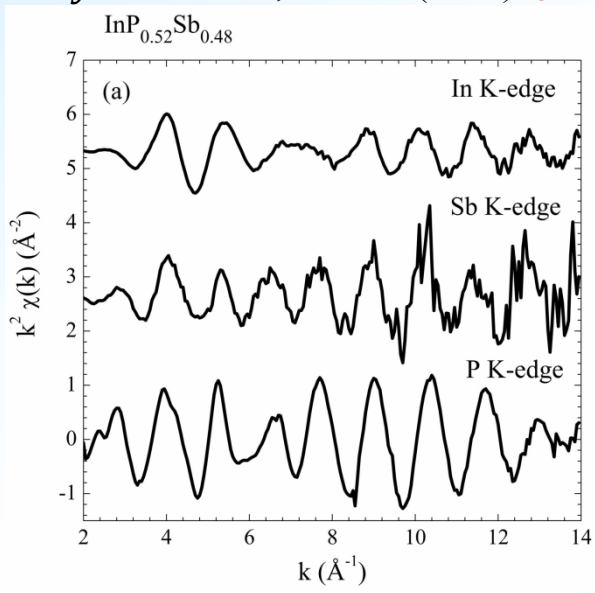

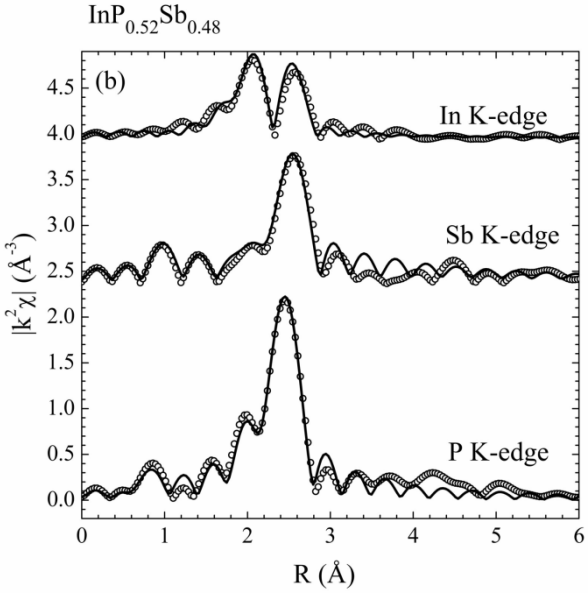

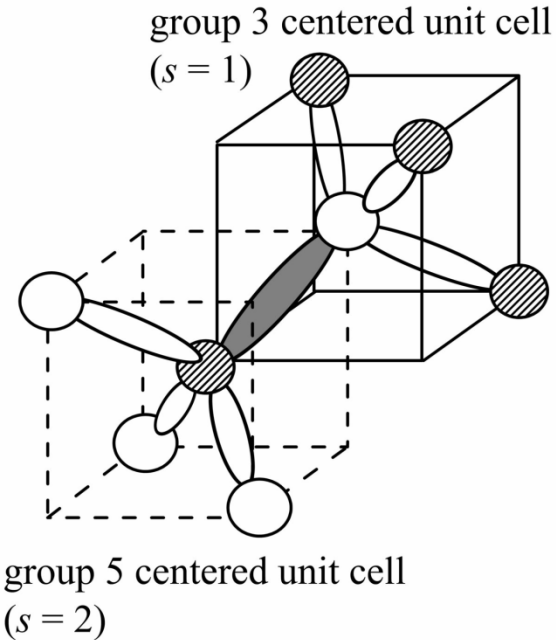

Fig. 1 (color online) Lattice points (0 0 4) and (-1 -1 5) on reciprocal space. The detailed reciprocal space mappings of InPSb sample and substrate are shown in the right and left insets. The vertical lattice constant of the epilayer is 6.187 Å, and the horizontal lattice constant of the epilayer is 6.131 Å.
Fig. 2 The In, Sb and P K-edge (a) extended X-ray absorption fine structure (EXAFS) oscillation and (b) Fourier transformed EXAFS signals of InP0.52Sb0.48 sample. The intensity is weighted by k2. We did not perform the phase correction to the spectra. The best fitted results are represented as the circles in R-space.
Fig. 3 The group-3-centered and group-5-centered unit cells of zincblende structure.
Fig. 4 Distortion energy and conventional elastic strain energy as functions of *az*/*a*xy ratio. The distortion energy was calculated using valence force field model and the strain energy was on the ground of virtual crystal approximation and the elastic constants. The inset shows the calculated bond lengths in InPSb supercells, which are in good agreement with the results determined from EXAFS measurement.

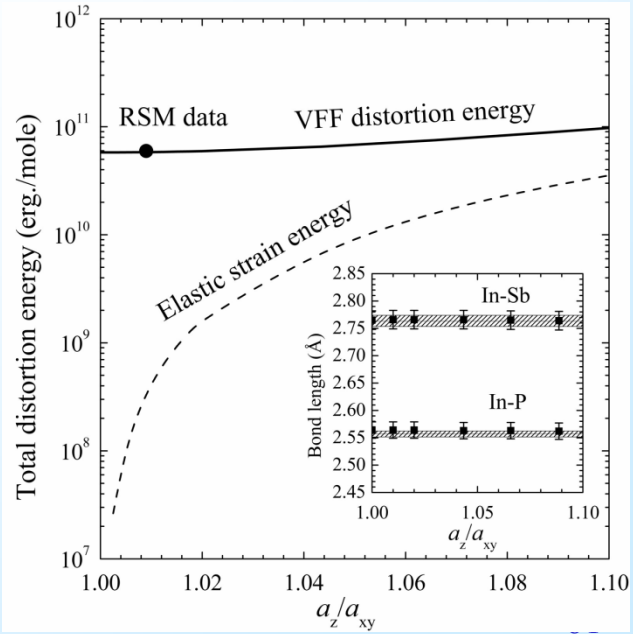

X-Ray Absorption and Raman Studies of GaN Thin Films Grown on Si by Plasma Assisted Molecular Beam Epitaxy

National synchrotron radiation research center (NSRRC)

X-Ray Absorption

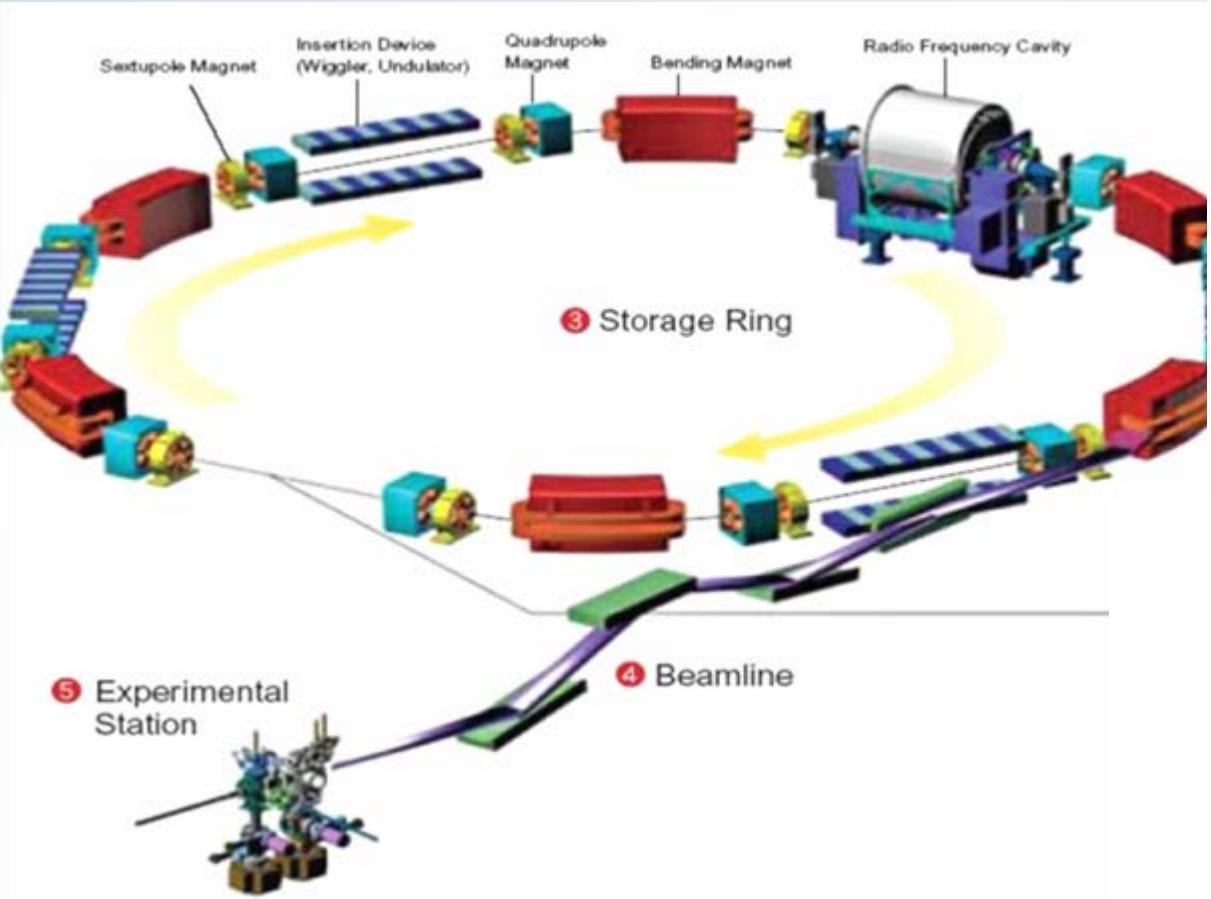

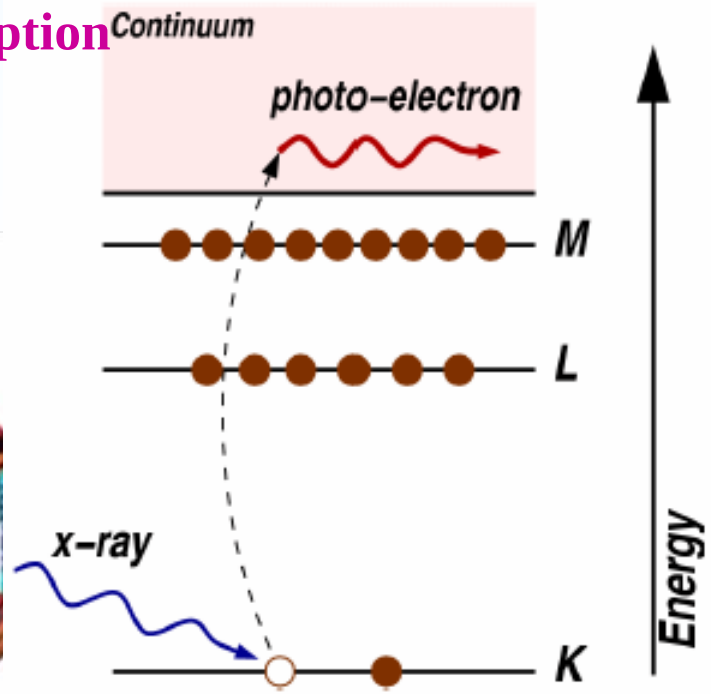

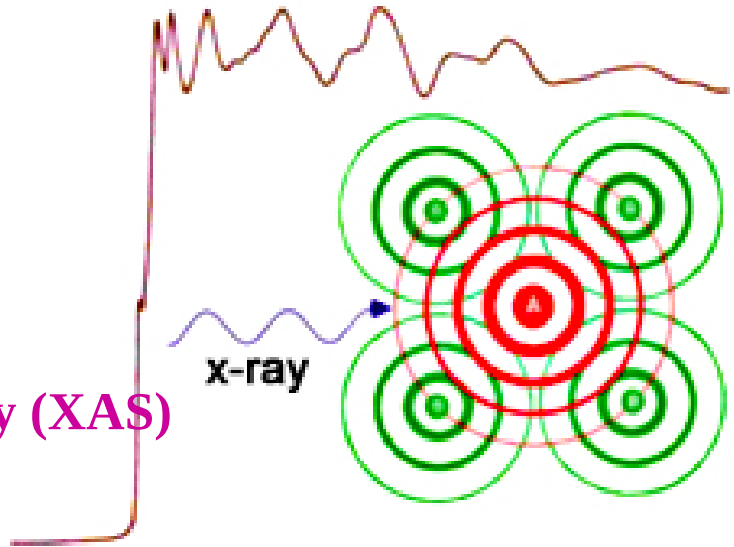

X-ray Absorption Spectroscopy (XAS)

XAFS = NEXAFS + EXAFS

I. XANES (X-ray Absorption Near-Edge Spectroscopy):

The XANES can reflect the electronic properties of the absorbing atom (such as the oxidation state and d-orbital occupancy) and can be utilized a to distinguish different site symmetry.

II. EXAFS (Extended X-ray Absorption Fine-Structure):

EXAFS provides the information of local atomic structure around the absorbing atom, including the type and the number of atoms in specific coordination shell, the interatomic distance, and the structural disorder.

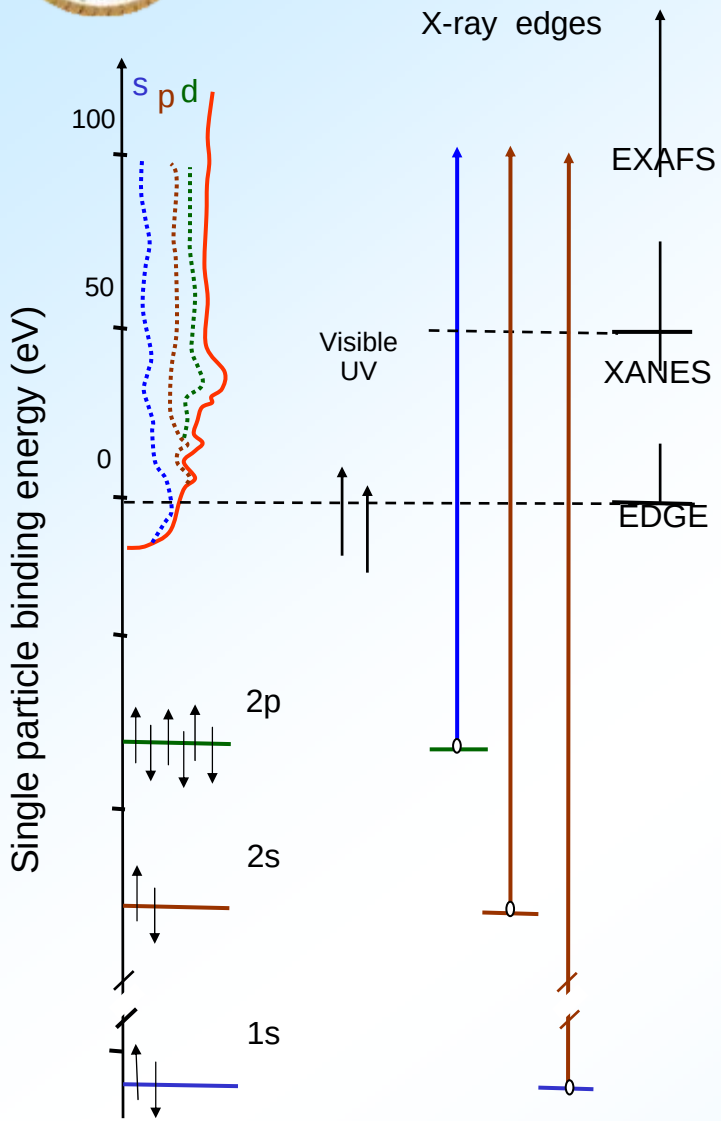

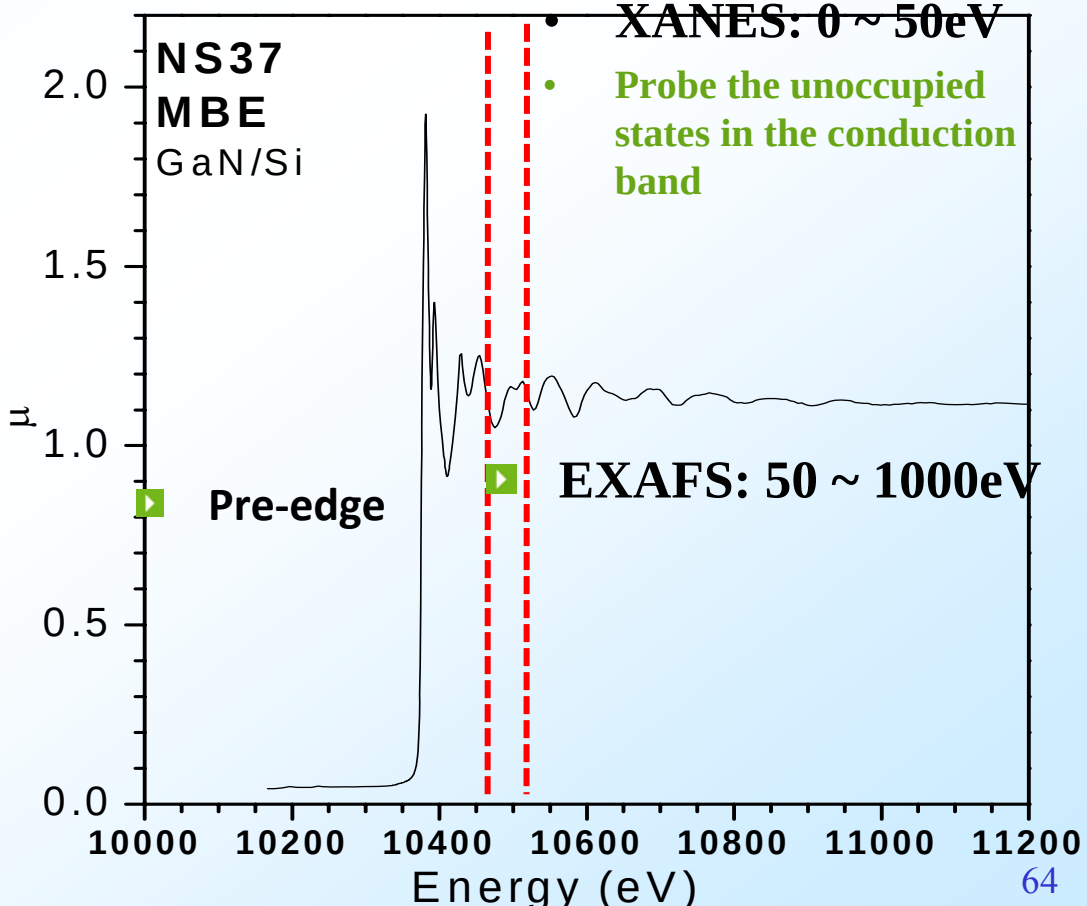

Shape of the crystal structure of GaN

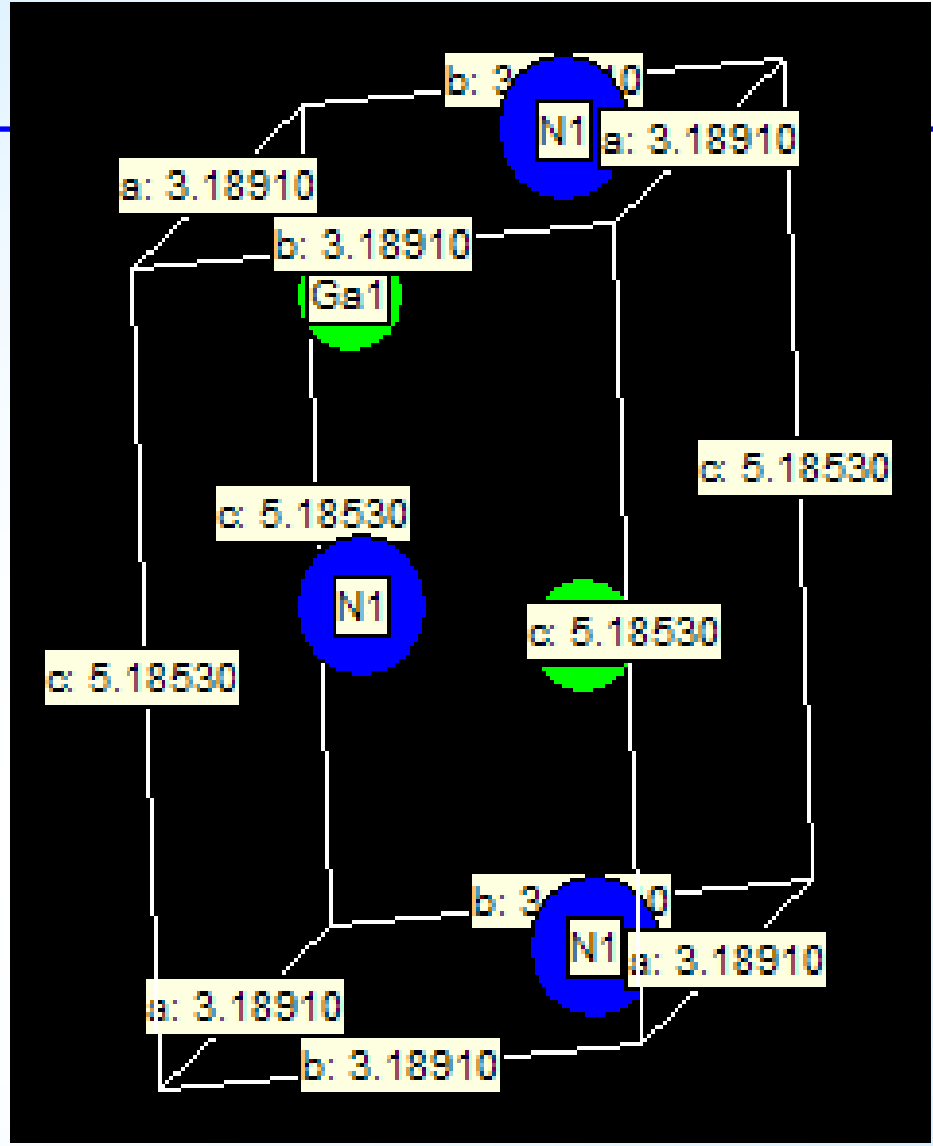

Table 1 The database of GaN

ICSD	Structured	Space Group	Crystal System	(a, b, c)	(α, β, γ)
88948	Ga N	P 63 m c	hexagonal	(3.1891,3.1891,5.1853)	(90,90, 120)

Fourier Transform spectra on

Extended X-ray Absorption Fine-Structure Spectroscopy (EXAFS)

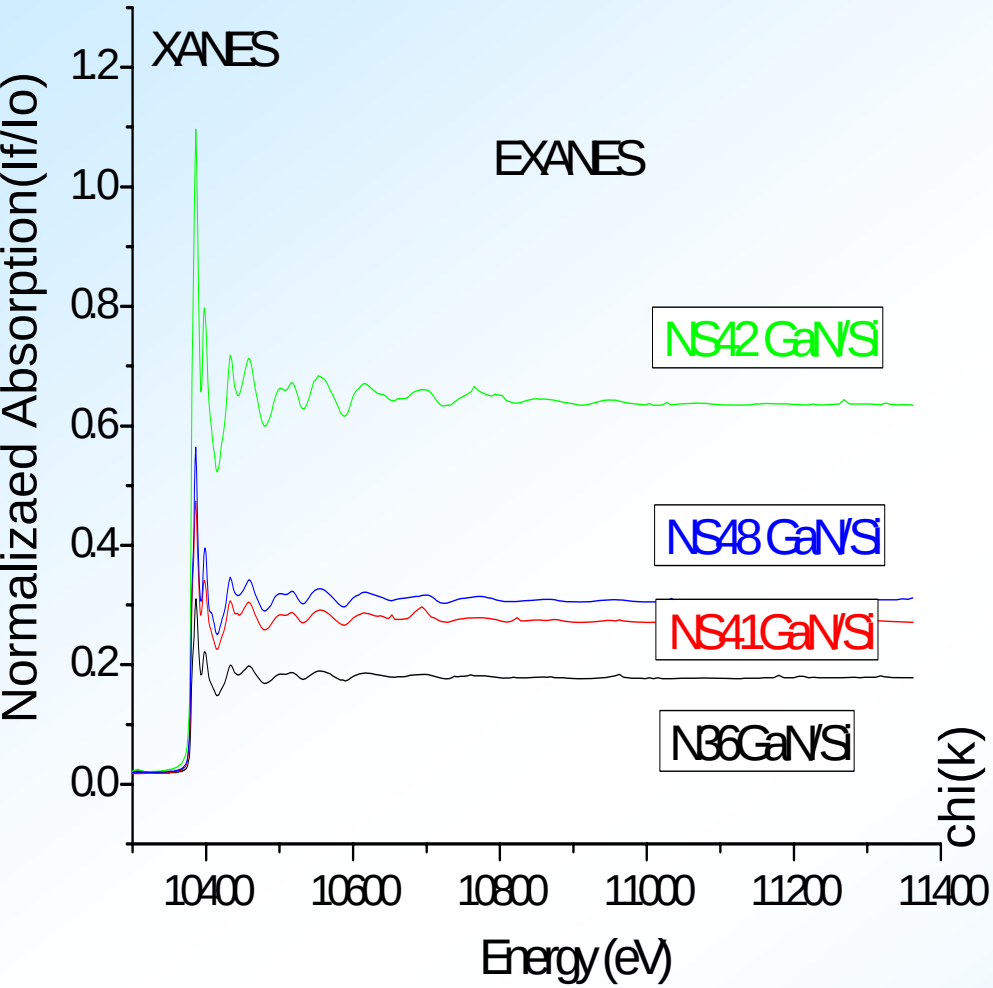

X-ray Absorption Fine-Structure (XAFS)

- Fourier transforms comparison of Ga K-edge EXAFS for GaN/Si

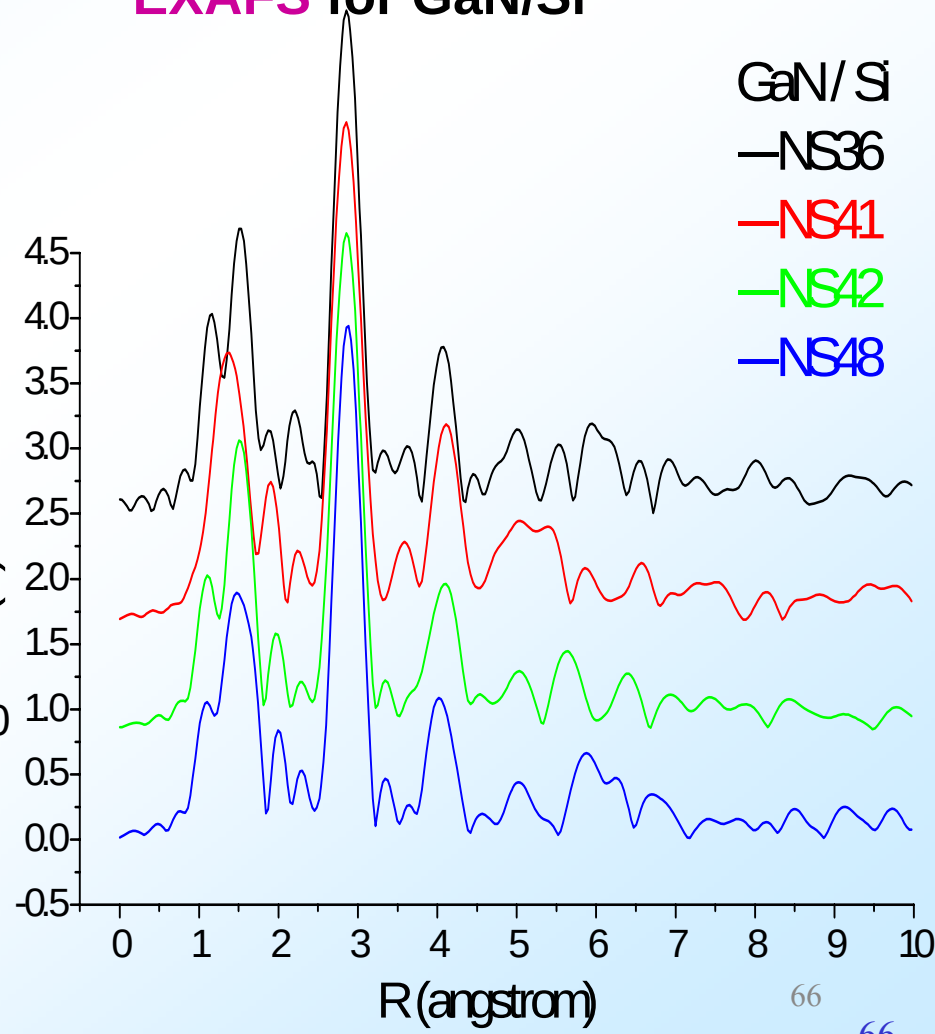

66

Fourier transformed EXAFS spectra around Ga K edge of sample NS42

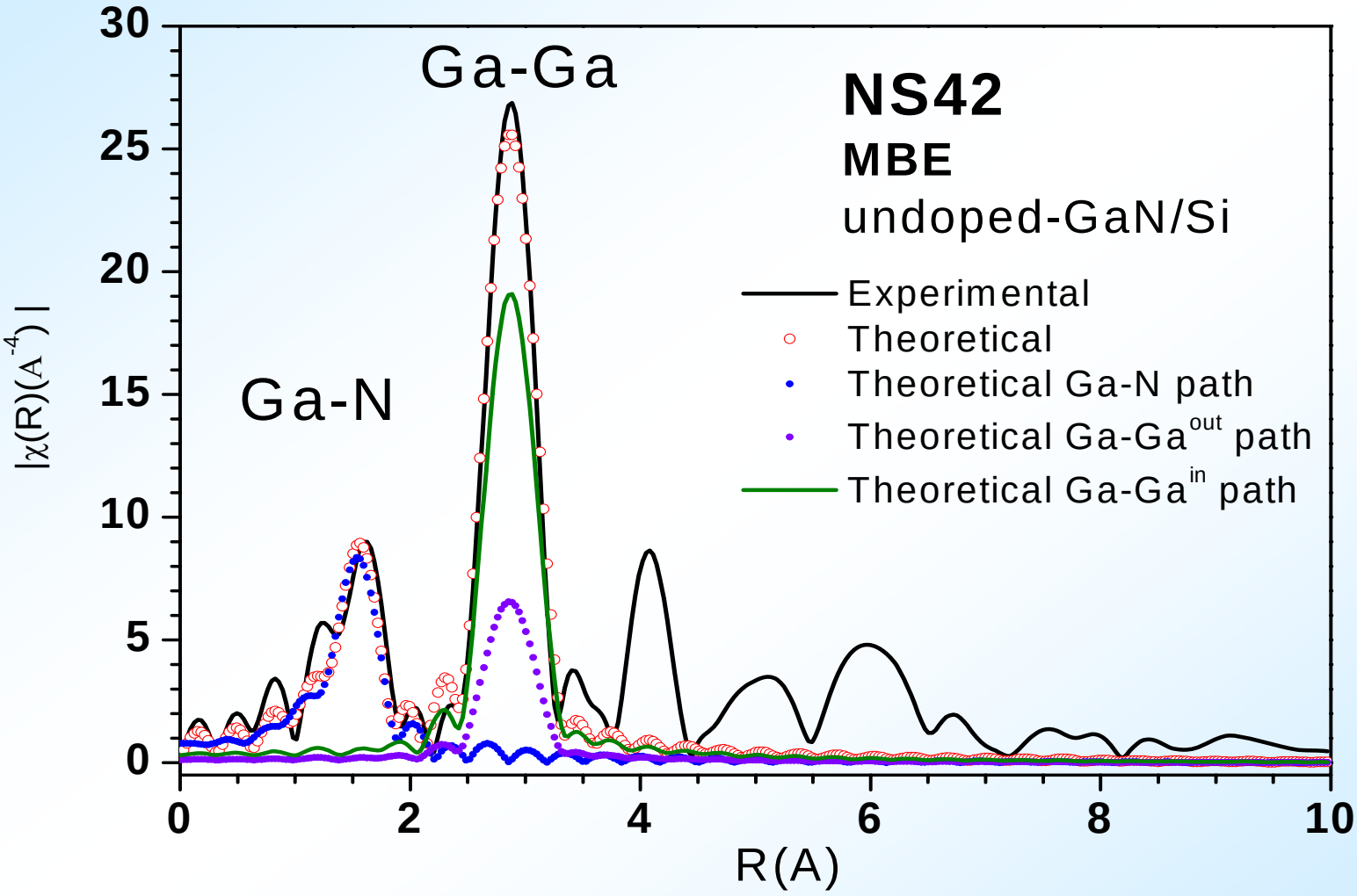

Purple dashed line is the fitting result of the normal incident of X-ray and green line is the fitting result of the grazing incident of the X-ray.

Result & Discussion

Polarization-dependent NEXAFS spectra of Ga K-edge

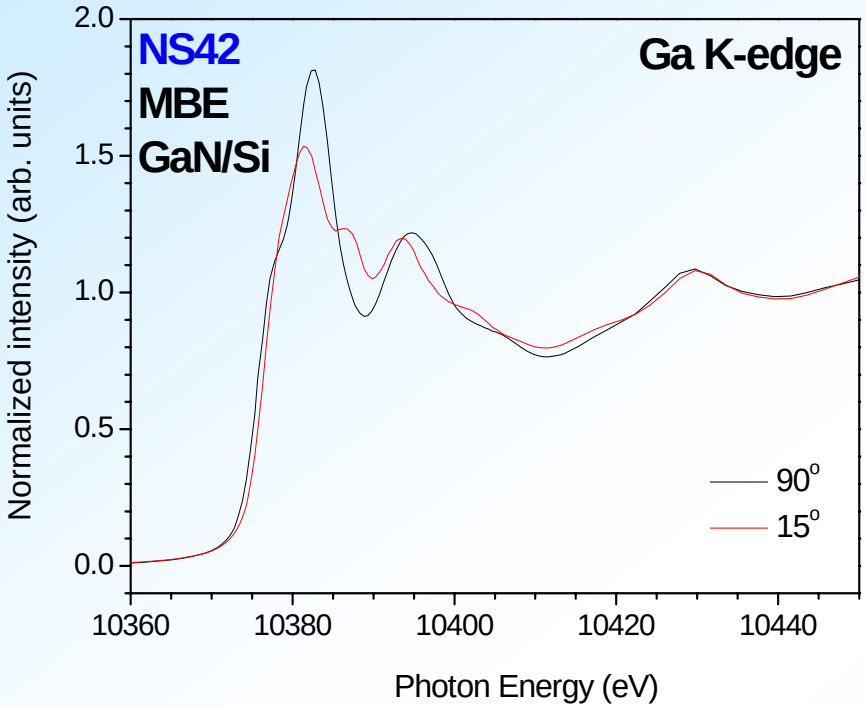

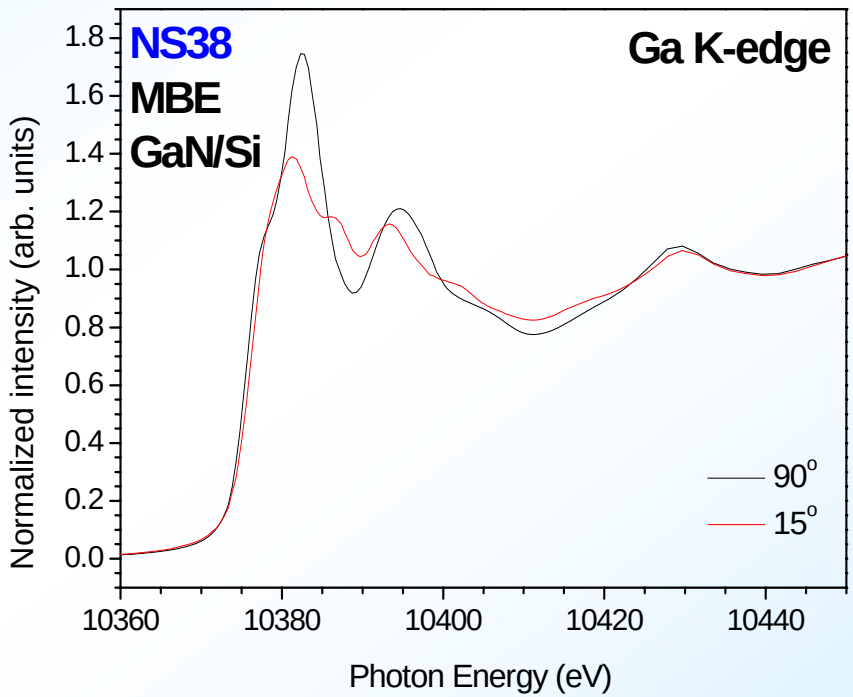

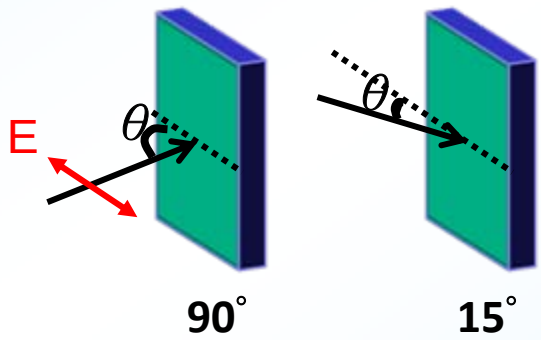

- Ga: $[Ar]3d^{10}4s^24p^1$ N:$1s^22s^2sp^3$
- Ga^{3+} N^{3-}
- Ga K-edge: 4p derived states in the CB
- From polarization-dependent NEXAFS
  ➔anisotropy of p states

Result & Discussion

Polarization-dependent NEXAFS spectra of NS48

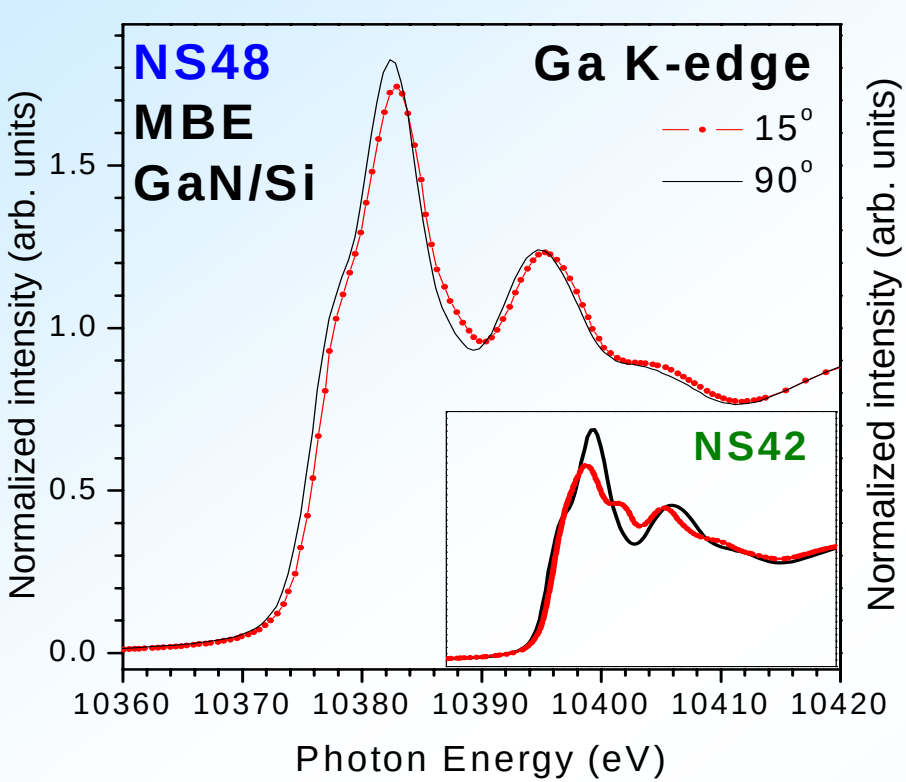

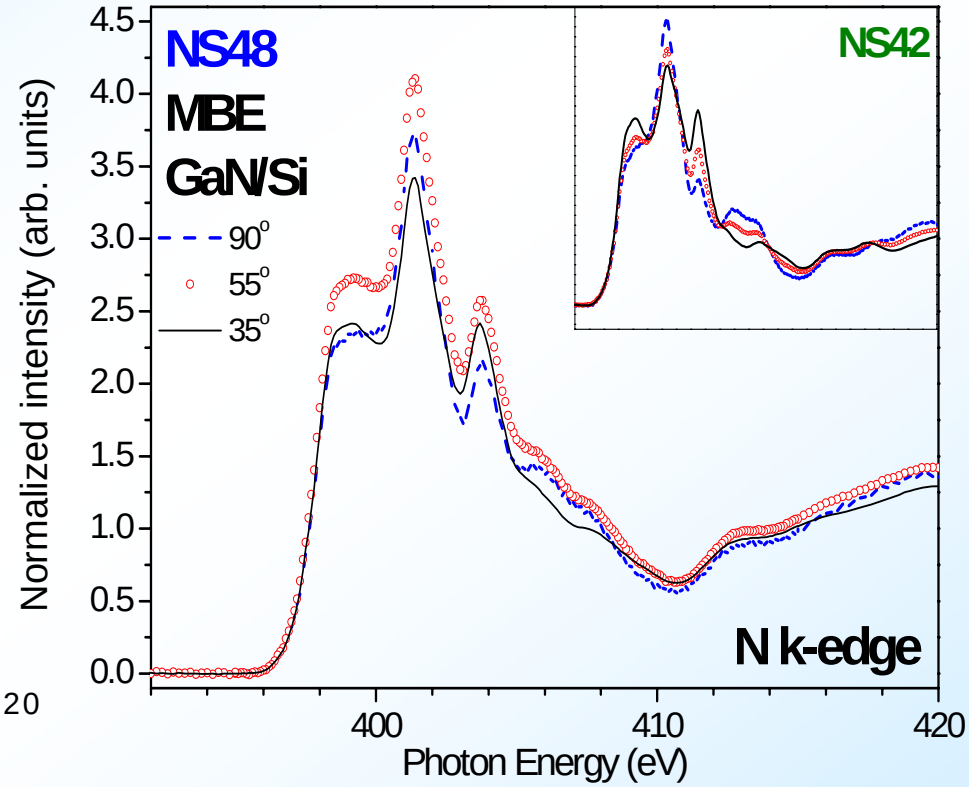

- The local symmetry around the nitrogen and gallium can be seen clearly
- It suggests that there is a high fraction of cubic structure in the GaN layer of sample NS48

Result & Discussion

Polarization-dependent NEXAFS spectra of N K-edge

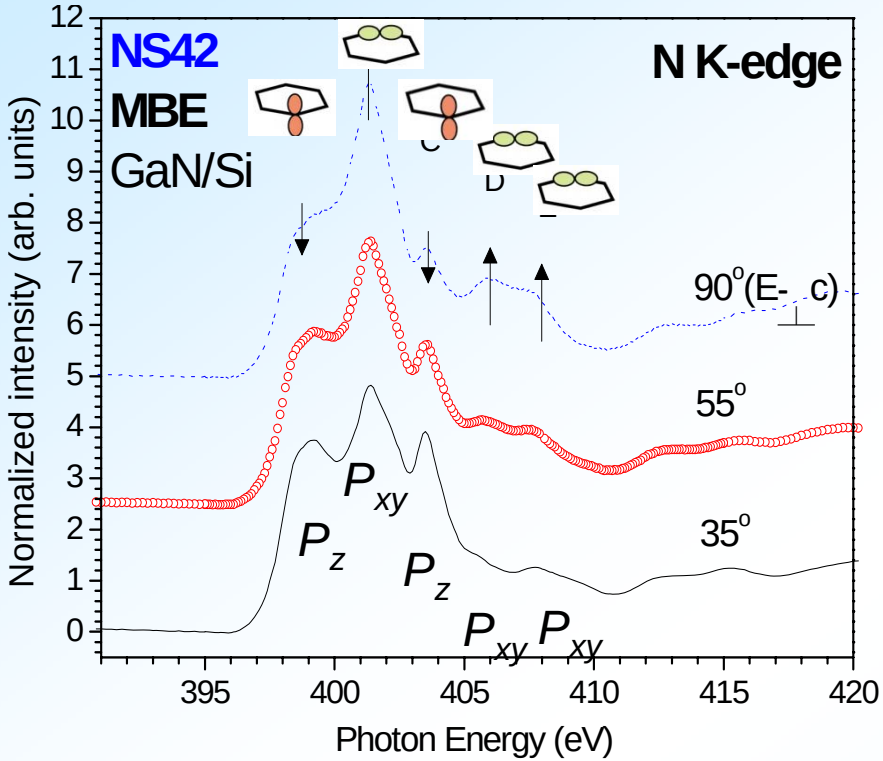

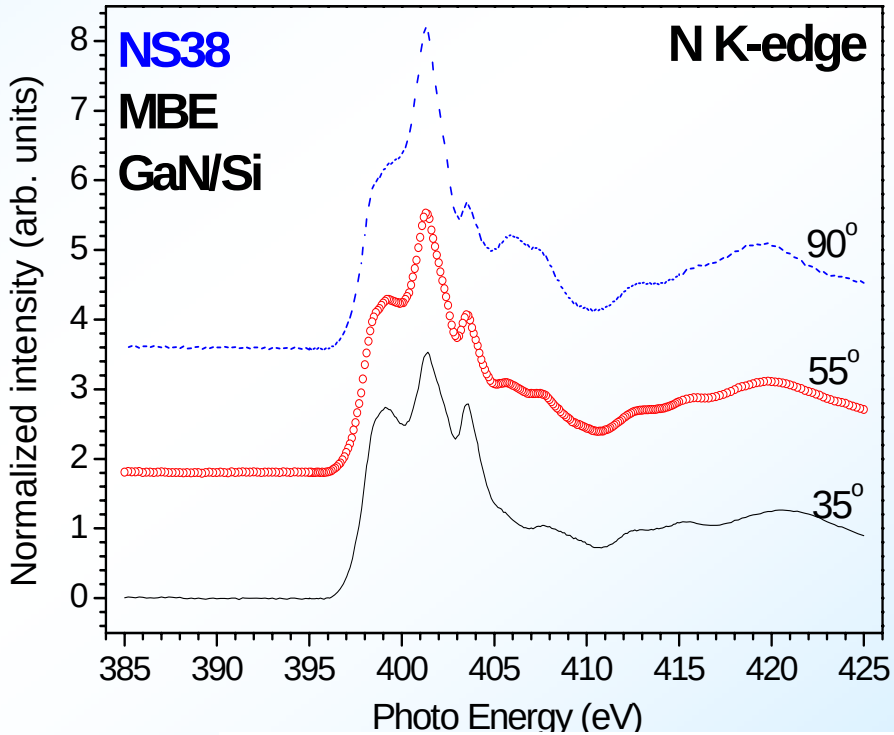

- N K-edge: 2p derived states in the CB
- From polarization-dependent NEXAFS ➔ GaN
- From $\left|\langle f|\mathbf{a}\bullet\mathbf{r}|i\rangle\right|$ in the case of w-GaN

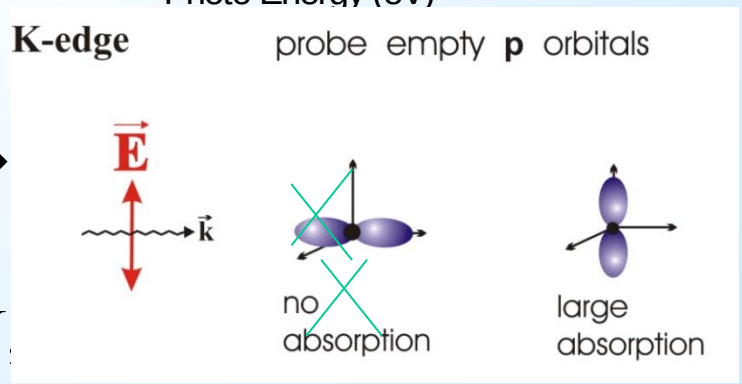

if **E** // **c**, , $1s \rightarrow P_{xy}$ states

Result & Discussion

XRD & UV Raman-PL spectra of NS42, NS38, NS48

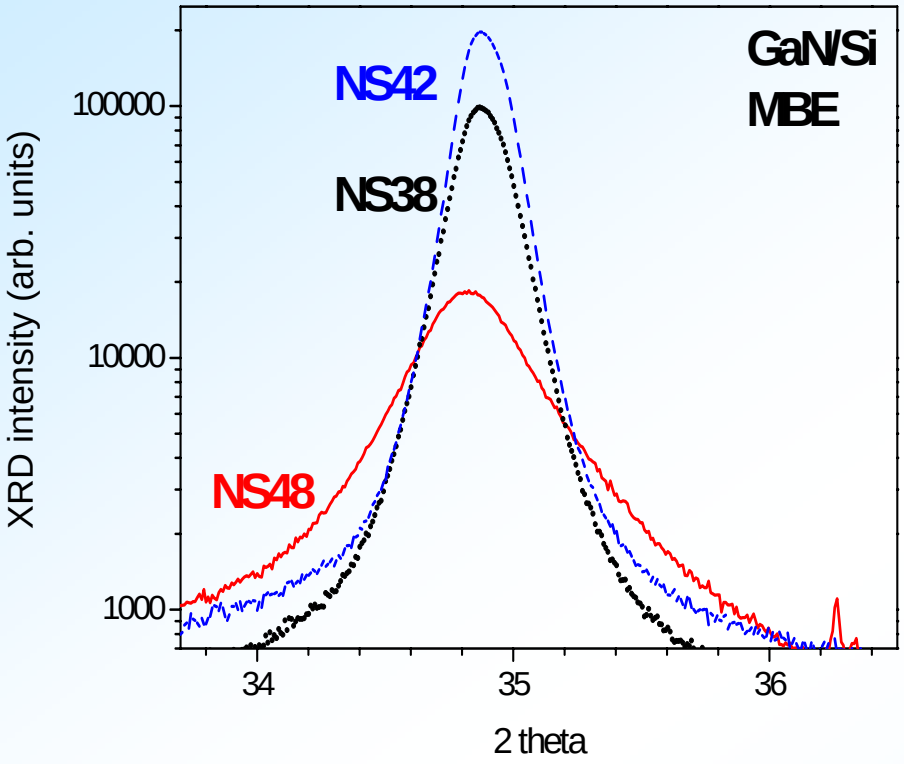

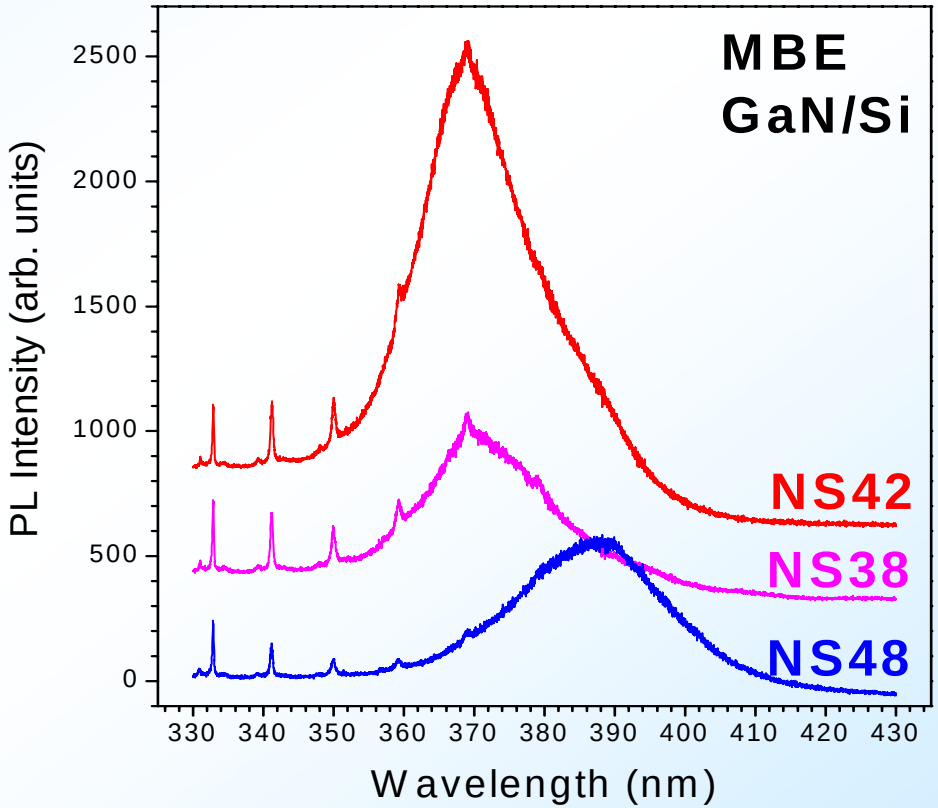

- **From XRD, 34.5°➔(0002) w-GaN , (111) c-GaN**

➔ **The standard XRD is unable to distinguish between the two poly types.**

- c-GaN to have a narrower forbidden gap than the wurtzite polytype➔3.28, 3.30 eV *(Z. Sitar et al. J. Materials Science Letters, **11** 261 (1992))*
- This can be further illustrated the existence of the cubic phase in the GaN layer

Raman Spectroscopy analyses – high E_2 mode and theoretical fit from two undoped-GaN/Si.

from spatial correlation model, the first-order Raman spectrum I(w) :

$$I(\omega) \propto \int \exp(-q^2 L^2/4) \frac{d^3 q}{[\omega - \omega(q)]^2 + (\Gamma_0/2)^2}$$

$$\omega^2(q) = A + \{A^2 - B[1 - \cos(\pi q)]\}^{1/2}$$

$$\omega(q) = A - Bq^2$$

	A	B	L (a)	Γ_o (cm^{-1})	$\omega(E_2)$ (cm^{-1})
NS38	**566.8**	**108.0**	**7.1**	**3.0**	**561.8**
NS42	**567.9**	**110.0**	**8.3**	**4.0**	**563.5**

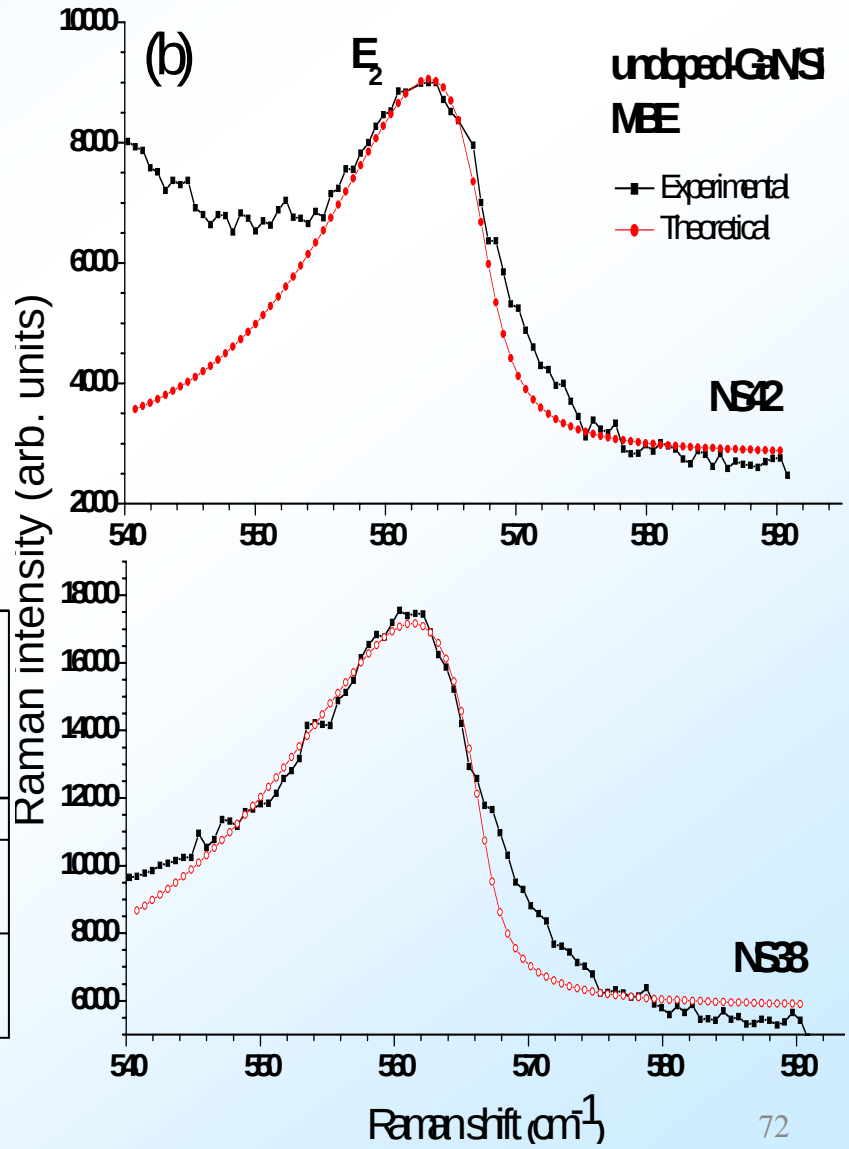

72

Sample	R_{GaN} (Å)	σ^2_{GaN} (Å²)	R^{out}_{GaGa} (Å)	R^{in}_{GaGa} (Å)	σ^2_{GaGa} (Å²)
NS38	**1.93080 (±0.008)**	**0.00124 (±0.0014)**	**3.17215 (±0.002)**	**3.18870 (±0.003)**	**0.00555 (±0.0006)**
NS42	**1.93184 (±0.020)**	**0.00406 (±0.0030)**	**3.17188 (±0.002)**	**3.18491 (±0.005)**	**0.00582 (±0.0010)**
M1044n	1.92629 (±0.016)	0.00248 (±0.0025)	3.17426 (±0.002)	3.17355 (±0.004)	0.00505 (±0.0005)
M1038n	1.93292 (±0.012)	0.00131 (±0.0024)	3.17157 (±0.003)	3.17668 (±0.004)	0.00445 (±0.0007)
M1232n	1.92795 (±0.009)	0.00172 (±0.0017)	3.17064 (±0.003)	3.17709 (±0.002)	0.00445 (±0.0006)
N933n	1.93057 (±0.008)	0.00131 (±0.0017)	3.17128 (±0.003)	3.18250 (±0.002)	0.00445 (±0.0006)

Result & Discussion

	NS38	NS42	M1044n	M1038n	M1232n	N933n
a(Å)	3.18870 (±0.00	3.18491 (±0.00	3.17355 (±0.004)	3.17668 (±0.004)	3.17709 (±0.002)	3.18250 (±0.002)
c(Å)	5.16653 (±0.00 4)	5.16898 (±0.00 5)	5.18412 (±0.004)	5.17497 (±0.005)	5.17236 (±0.004)	5.16949 (±0.004)

NS38 > NS42; M1044n < M1038n < M1232n

$$R_{GaGa}^{in} = a$$

$$R_{GaGa}^{out} = \sqrt{\frac{1}{3}a^2 + \frac{1}{4}c^2}$$

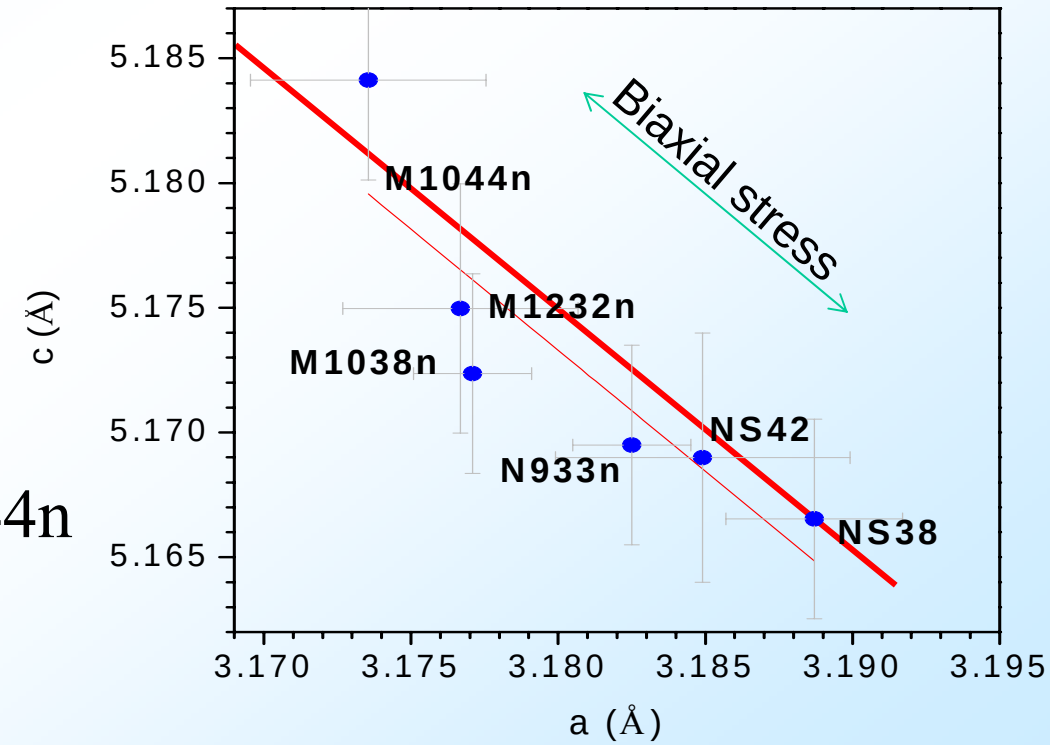

- a: GaN/Si > GaN/sapphire
- a:M1232n>M1038n>M1044n
- Doping concentration:

M1232n>M1038n>M1044n

Conclusion

- We have employed synchrotron radiation (SR) X-ray absorption fine-structure spectroscopy (XAFS) technology to study Ga K-edge absorption and Fourier transform spectra for GaN grown on Si.
- The Ga-N bond lengths and coordination numbers were determined, via analyzing the absorption spectra of the Gallium K-edge of GaN/Si.
- The Ga-Ga distance in GaN of all samples (NS36, NS41, NS42, NS48) are the same.
- But the Ga-N distance from the shortest to the longest: NS41 < NS48 < NS42 < NS36.
- By using the EXAFS fitting program (Artemis and Athena) to analyze these data, obtained fitting results are summarized, and plotted Ga-N bond length and coordination number versus the composition of Gallium.
- Polarization-dependent Ga K-edge & N K-edge XANES spectra can probe the unoccupied *p* states in the CB and prove the isotropic characteristic of *p*-orbital.
- Polarization-dependent XANES spectra for Ga L3-edge indicate that the CB minimum is dominantly Ga s derived states.
- From the result of the polarization-dependent NEXAFS spectra, electrons are transferred from N to Si in the Si:GaN films.
- By combining with XRD, polarization-dependent NEXAFS can be used for the identification of the structure of the examined GaN crystal or other III-Nitride epitaxial films as well.
- Values of the lattice constant of different GaN films can be deduced from EXAFS analysis. Subsequently the strain values were calculated. By combining Raman measurement, the linear coefficient for stress induced shift of Raman frequency can be further obtained.